Epigenetic Control of Centromeric Cid/Cenp-A Levels During Spermatogenesis and Development

Dissertation
zur
Erlangung der naturwissenschaftlichen Doktorwürde
(Dr. sc. nat.)

vorgelegt der
Mathematisch-naturwissenschaftlichen Fakultät
der
Universität Zürich

von
Nitika Taneja Raychaudhuri
aus
Indien

Promotionskomitee
Prof. Dr. Christian F. Lehner (Vorsitz)
Prof. Dr. Gunter Reuter
Dr. Stefan Luschnig

Zürich, 2012

Acknowledgements

I wish to express my deep gratitude to my supervisor Prof. Christian F. Lehner. Saying just 'thank you' would not be enough for the tremendous support and help I have received from him over the years. He taught me the way of scientific thinking and I am extremely thankful for his support to guide my future career.

I am very grateful to the members of Lehner Lab especially Pablo Radermacher, Ariane Blattner, Faina Myachina, Soumya Chaurasia, Peter Lidsky, Björn Handke and to the members of Luschnig Lab for their support, discussions and for the great working atmosphere.

A special thanks goes to Friedricke Althoff who had been a great friend and a great help throughout my PhD.

Last but not least, I would like to thank my both the families for persistently motivating and supporting me.

Dear Arnab, thanks for being there by my side always and building up my confidence in hard times. You are the blissful blessing to my life!

Table of Contents

Appendix I - Centromeric Cid levels inducing meiotic drive

Appendix II - Role of centromeres beyond chromosome segregation during male meiosis

Zusammenfassung

Zentromere sind von größter Wichtigkeit für die richtige Weitergabe der genetischen Information während mitotischer und meiotischer Zellteilungen. Die Identität der Zentromere in Metazoen wird durch epigenetische Mechanismen bestimmt. In Menschen zum Beispiel wurde gezeigt, dass die hochrepetitiven zentromeren DNS-Sequenzen weder genügen noch überhaupt benötigt werden, um das Zentromer zu spezifizieren.

Um die Funktion von Proteinen bei der epigenetischen Markierung und Vererbung der Zentromere zu untersuchen, wäre ein effizientes UAS/GAL4-System sehr nützlich, welches für Analysen in der männlichen Keimbahn in Drosophila nach Gen-Überexpression, Gen-Knockdown oder induzierter Proteindegradation geeignet wäre. Daher wurden neuartige Treiberlinien hergestellt, welche GAL4-Fusionen mit testis-spezifischen Transkriptionsfaktoren exprimieren, in der Hoffnung, dass eine Synergie zwischen den Aktivierungsdomänen von GAL4 und den testis-spezifischen Transkriptionsfaktoren zu einer erhöhten Expression von UASt-Transgenen führen würde. Tatsächlich konnte hierdurch die Effizienz der UASt-Transgene in Spematozyten verbessert werden. Eine der neuen GAL4-Treiberlinien erwies sich bei Experimenten, welche die Funktion von Zentromerproteinen betrafen, als sehr nützlich.

Der Hauptteil dieser Arbeit beschreibt Experimente, welche die Weitergabe des Zentromerproteins Cid und der Zentromeridentität während der männlichen Meiose untersuchen. Meine Ergebnisse zeigten, dass sich die Kontrolle der Beladung der Zentromere mit Cid während der männlichen Meiose von der

Regulation während der mitotischen Zyklen der frühen Embryogenese unterscheidet. Darüber hinaus wurde gezeigt, dass ein starker Mangel an Cid in Spermien zu einem Versagen der paternalen Zentromerfunktion nach der Befruchtung führt. Paternale Chromosomen, denen Cid am Zentromer fehlte, konnten nicht in die gonomere Spindel der ersten Mitose integriert werden, was zu gynogenetisch haploiden Embryonen führte. Weiterhin wurde nach moderater Depletion von Cid in Spermien beobachtet, dass die paternalen Zentromere in der nächsten Generation nicht die normale Cid-Menge zurückerlangen konnten. Daraus folgere ich, dass Cid in Spermien ein essentieller Bestandteil der epigenetischen Markierung der Zentromere ist. Weiterhin übt das in Spermien vorhandene Cid eine quantitative Kontrolle über die Cid-Menge am Zentromer der paternalen Chromosomen während der Entwicklung der nächsten Generation aus.

Summary

Centromeres are of paramount importance for faithful propagation of genetic information during mitotic and meiotic divisions. Centromere identity in metazoans is believed to be specified by epigenetic mechanisms. In humans for example, the highly repetitive centromeric DNA has been shown to be neither sufficient nor required for centromere specification.

In order to study the role of proteins for epigenetic marking and propagation of centromeres, an efficient UAS/GAL4 system for analyses in the male germline of Drosophila after gene overexpression, knock down or induced protein degradation would be very helpful. Therefore, novel driver lines expressing GAL4 fused to testis-specific transcription factors were generated in the hope that a synergism between the activation domains of GAL4 and testis-specific transcription factors might result in enhanced UASt transgene expression. Thereby the efficiency of expression of UASt transgenes in spermatocytes could indeed be improved. One of the novel GAL4 driver lines was very useful for experiments concerning centromere protein function.

The main part of this thesis describes experiments addressing propagation of the centromere protein Cid and of centromere identity during male meiosis. My results revealed that the control of Cid loading onto centromeres during male meiosis is distinct from the regulation observed during the mitotic cycles of early embryogenesis. Moreover, strong Cid depletion in sperm was shown to result in a failure of paternal centromere function after fertilization. Paternal chromosomes lacking centromeric Cid failed to integrate into the gonomeric spindle of the first mitosis, resulting in gynogenetic haploid embryos.

Furthermore, after moderate Cid depletion in sperm, paternal centromeres were found to be unable to re-acquire normal Cid levels in the next generation. Therefore, I conclude that Cid in sperm is an essential component of the epigenetic centromere mark on paternal chromosomes. Moreover, Cid present in sperm centromeres exerts quantitative control over centromeric Cid levels on paternal chromosome throughout development of the next generation.

Background

My experimental thesis work is described in two main chapters. In addition some preliminary studies that I consider to be of potential interest are described in two appendices. The second main chapter of my thesis corresponds to a manuscript that has recently been accepted for publication in the journal PLoS Biology. Therefore, this chapter also contains a separate specific introduction. Similarly, at the start of the first main chapter, I have written an introduction specifically for this chapter. In contrast, the following Background section will cover aspects that are of general importance for all of my experimental work. Although redundancies with the subsequent introductions of the two main chapters were kept low, some overlap could not be avoided.

Centromere

The centromere is a specialized region on each chromosome that recruits the kinetochore machinery (Burrack and Berman, 2012a). The kinetochore serves as a critical structure mediating binding of chromosomes to the spindle microtubules and thus, ensures faithful inheritance of chromosomes during cell division. The kinetochore also functions in engaging the spindle checkpoint in case of erroneous or missing microtubule attachments, leading to a delay in anaphase onset (Khodjakov and Pines, 2010). The intricate centromere-kinetochore machinery thus provides a safeguard mechanism that allows anaphase to proceed only once all the kinetochore pairs are attached in a bipolar manner. This sequence of events is essential to prevent genetic instability at the chromosomal level and the development of chromosomal imbalances (aneuploidy), a phenomenon that is present in about 85% of solid human tumours (Weaver and Cleveland, 2006).

Different organisms have different types of centromeres. Most of the eukaryotes contain 'localised' centromeres, in which centromere formation is restricted to a specific chromosomal locus. On the other hand, in organisms possessing holocentric centromeres such as the nematode *Caenorhabditis elegans*, centromeres extend along the entire chromosome.

The amount of DNA sequences in localised centromeres can evolve rapidly. For example, centromere DNA in the two different yeast species *Saccharomyces cerevisiae* and *Schizosaccharomyces pombe* is of very different length (Pluta et al., 1995). The point centromeres of *S. cerevisiae* span only ~125 bp of DNA and consist of three conserved sequence elements (centromere-determining elements, CDE) that are necessary and sufficient for kinetochore assembly (Fitzgerald-Hayes et al., 1982; Pluta et al., 1995). In contrast the regional centromeres of *S. pombe* span several kilobases of DNA (Clarke, 1998; Pluta et al., 1995).

In general, regional centromeres consist of repetitive sequence with a repeating unit of typically 160–180 bp. Interestingly, the presence of these centromere repeats does not specify the location or the general function of centromeres. The regional centromeres in *Drosophila melanogaster* consist of several islands of complex DNA embedded in large domains of repetitive DNA (Sun et al., 2003). The human centromeres contain a primate-specific satellite family based on a 171 bp repeat known as alpha-satellite repeat (Manuelidis, 1978; Mitchell et al., 1985). Long arrays of tandemly repeated alpha-satellite DNA stretch over mega bases of DNA (Allshire and Karpen, 2008). However a neocentromere has been characterized recently that has been formed in a region completely devoid of alpha-satellite repeats which indicates that these repeats are not required to specify the centromere position (Harrington et al., 1997; Saffery et al., 2000).

Despite the fundamental role of centromeres in all eukaryotes, the repeating sequences found in centromeric DNA have evolved rapidly relative to the rest of the chromosomes.

The key component of the epigenetic mark that specifies the centromere is a variant of histone H3 known as CenH3. CenH3 is named CENP-A in mammals, CID in flies, and Cse4 in budding yeast. CenH3 is localized to all active centromeres regardless of the underlying DNA sequence and is essential for kinetochore formation and chromosome segregation (for review see (Verdaasdonk and Bloom, 2011). Under normal conditions, CenH3 is present exclusively within the centromeric region. The mechanisms of CenH3 targeting to the centromere are not completely understood. Recent research has given exciting clues about mechanisms involved in CENP-A localization. CENP-A is able to bind to any location on the genome as shown by transient expression experiments in different organisms (Heun et al., 2006; Van Hooser et al., 2001). However, CENP-A nucleosomes on non-centromeric DNA are unstable because of their rapid degradation through proteolysis (Moreno-Moreno et al., 2006). In budding yeast, it has been demonstrated that Cse4 located at the centromere is protected from proteolysis (Collins et al., 2004).

The N-terminal domain of CenH3 is highly variable ranging from 20 to 200 amino acids. It has no sequence homology to the N-tail of histone H3. The C-terminal histone-fold domain (HFD) of CenH3, which has been shown to have significant homology to histone H3, shares only 48% identity on average across phylogeny (Torras-Llort et al., 2009). Contrasting patterns of evolution of CenH3 and canonical histone H3 have occurred. Histone H3 contributes to the regulation of many different aspects of chromatin structure and function thus explaining its evolutionary stability. On the other hand, CenH3 only interacts with centromeric DNA that is one of the most rapidly evolving DNA sequences in the genome. This in turn is thought to contribute to rapid adaptive

evolution of CenH3 in both Drosophila and Arabidopsis (Malik and Henikoff, 2001; Talbert et al., 2002).

To recruit CENP-A specifically to centromeres of vertebrates and fungi, a conserved chaperone, called HJURP or Scm3, respectively, plays a crucial role (Camahort et al., 2007; Foltz et al., 2009; Sanchez-Pulido et al., 2009). HJURP selectively recognizes pre-nucleosomal CENP-A from canonical histone H3 and targets it to centromeres (Jansen et al., 2007; Lagana et al., 2010). Both HJURP and Scm3 have been shown to possess CENP-A assembly activities in vitro (Barnhart et al., 2011; Dechassa et al., 2011; Shivaraju and Gerton, 2011). Surprisingly, homologs of these proteins have not been identified in Drosophila, Caenorhabditis, or plants. In *D. melanogaster*, however, Cal1, a novel protein, was identified in a RNAi screen in Drosophila S2 cells (Goshima et al., 2007). Cal1 is found only in Diptera and is essential for CENP-A localization. It interacts with CENP-A in both chromatin and pre-nucleosomal complexes making it a strong candidate for a CENP-A chaperone in this lineage (Mellone et al., 2011).

CenH3 assembles into centromeric chromatin and is retained at centromeres as nucleosomes. The structure of CenH3-containing nucleosomes is a matter of debate. Canonical nucleosomes with histone H3 are octameric $(H3/H4/H2A/H2B)_2$. Human CENP-A can replace histone H3 in nucleosomes that, otherwise, show a canonical histone composition and stoichiometry (Yoda et al., 2000). Affinity purification of CenH3-nucleosomes, both from human and fly cells, is also consistent with the formation of 'canonical' $(CenH3/H4/ H2A/H2B)_2$ octamers (Blower et al., 2002; Foltz et al., 2006). However, on the basis of intra-nucleosomal cross-linking experiments and atomic-force microscopy measurements, an alternative model has been proposed. The model suggests that, in Drosophila, CID nucleosomes exist as (CID/H4/H2A/H2B) tetramers, or 'half-nucleosomes', rather than as octamers (Dalal et al., 2007a; Dalal et al.,

2007b). Recently, cell cycle coupled structural changes of CenH3 nucleosomes have been revealed in human cells and yeast (Bui et al., 2012; Shivaraju et al., 2012). However, a puzzling number of additional variants of CenH3 nucleosome structure and composition such as (hexasome, hemisome, trisome, and reversome) have also been proposed, but they lack substantial experimental evidence (Black and Cleveland, 2011).

The CENP-A containing chromatin is required for the recruitment of all other kinetochore proteins. The study of kinetochore proteins has been difficult for a long time due to low abundance of these proteins and also due to the fact that protein sequences of most kinetochore subunits are evolutionarily highly divergent. The sequences of fungal kinetochore proteins were not sufficient to identify metazoan kinetochore proteins and vice versa in standard BLAST searches, considerably delaying comparative functional studies. The structure and size of kinetochores vary strongly from organism to organism (Przewloka and Glover, 2009). The centromere is occupied throughout the cell cycle by a large multi-subunit complex of proteins, the so-called CCAN (constitutive centromere-associated network) comprised of 16 centromere proteins (CENPs C, H, I, K through U, W, and X) (Foltz et al., 2006; Okada et al., 2006). CENP-C had been proposed to connect CENP-A nucleosomes with CCAN components such as CENP-N (Dunleavy et al., 2009). But recently (Carroll et al., 2010) has shown that CENP-C also binds directly and specifically to CENP-A nucleosomes. Nucleosome binding by CENP-C requires the extreme C terminus of CENP-A and does not compete with CENP-N binding, which suggests that CENP-C and CENP-N recognize distinct structural elements of CENP-A nucleosomes. The absence of the CCAN in *C. elegans* and *D. melanogaster* raises the question how Cenp-C is anchored at the centromere within these species. A direct interaction between Cenp-C and Cid has never been observed. In Drosophila, Cal1 has been shown to directly interact with Cid from its N-terminal and Cenp-C from its C-

terminal region/ domain (Schittenhelm et al., 2010b). Its depletion results in chromosome congression and segregation defects and in a loss of Cid from the centromeres (Erhardt et al., 2008; Goshima et al., 2007; Schittenhelm et al., 2010b). The observation that the centromeric levels of Cal1 are far lower than those of Cid and Cenp-C has indicated that Cal1 does not function as a stable structural centromere component that bridges between Cid and Cenp-C in a 1:1:1 stoichiometry. Moreover, additional evidence supports the proposal that Cal1 functions similar to HJURP/Scm3 as a Cid loading factor (Phansalkar et al., 2012; Schittenhelm et al., 2010b).

Drosophila Spermatogenesis

The Drosophila testis is a long tube with a straight apical tip and a coiled basal end. The different stages of spermatogenesis, from its tip to its basal end are laid out in chronological order, making it easy to discern distinct stages of germ cell development. Male germ line stem cells reside in the germinal proliferation center, at the tip of the testis (White-Cooper, 2004; White-Cooper et al., 2000). The germline proliferation center is composed of a cluster of 12 quiescent somatic cells called the hub. The hub is surrounded by 5-9 germline stem cells (GSCs) and twice as many somatic stem cells (SSCs) that maintain spermatogenesis (Fuller, 1998; Gonczy and Dinardo, 1996; Hardy et al., 1979). The division of GSCs is asymmetric. One of the two daughter cells remains adjacent to the hub and retains stem cell identity (Hardy et al., 1979), whereas the other becomes the gonialblast and is determined to differentiate (Yamashita et al., 2003). In parallel, the SSCs also divide and give rise to two daughter cells, one of which stays closer to the hub and remains an SSC while the other one undergoes differentiation (Hardy et al., 1979). The gonialblast then undertakes four mitotic divisions with incomplete cytokinesis and generates 16 interconnected spermatogonia, while the two somatic cyst cells encapsulate the spermatogonial cluster and grow without further division (Gilboa and Lehmann, 2004; Lin, 2002; Yamashita et al., 2005). Spermatogonial cells then further undergo pre-meiotic S phase and, thus, become primary spermatocytes. The spermatocyte now switches from a program of cell division to one of prolonged phase of growth and expression of spermatocyte-specific genes required in the subsequent meiotic stages (Fig. 1, also see Chapter 2, Fig. 1). During this premeiotic G2 phase, the spermatogonial cell expands approximately 25-fold. In *D. melanogaster,* the primary spermatocyte stage lasts 90 hours (Lindsley and Tokuyasu, 1980). In Drosophila most transcription is shut off upon entry into the meiotic divisions, in

contrast to mammals, where spermatids continue with transcription until chromatin compaction (Monesi, 1965). However, recent evidence in Drosophila has revealed transcription of 24 genes in the mid-elongation spermatids, just before histone to protamine chromatin transition (Barreau et al., 2008).

Meiosis in Drosophila males does not include some characteristic meiotic processes like formation of synaptonemal complexes (Ault et al., 1982; Cooper, 1949) and meiotic recombination (Morgan, 1912). The mature primary spermatocytes undergo two meiotic divisions. In prometaphase I, sister kinetochores appear to form a single microtubule binding surface allowing mono-orientation of the two sister chromatids during meiosis I. The kinetochore changes to a flattened disc and then resolves into a double-disc during late prometaphase II allowing bi-orientation of the sister chromatids during meiosis II (Church and Lin, 1982; Goldstein, 1981). The meiotic divisions give rise to a cyst of 64 haploid onion-stage spermatids. At this stage spermatids contain a "nebenkern", a mitochondrial derivative composed of two giant mitochondria resulting from mitochondrial fusion. The two mitochondria are tightly wrapped around each other in a manner such that transmission electron microscopical images resemble a sliced onion. The onion stage morphology is an excellent indicator of the success of meiotic divisions. For example, when chromosome segregation is irregular then variable abnormally sized nuclei in an onion stage cyst are observed. In contrast, when cytokinesis is irregular then variably sized nebenkerns representing the abnormal amount of mitochondria within an onion stage cyst are observed.

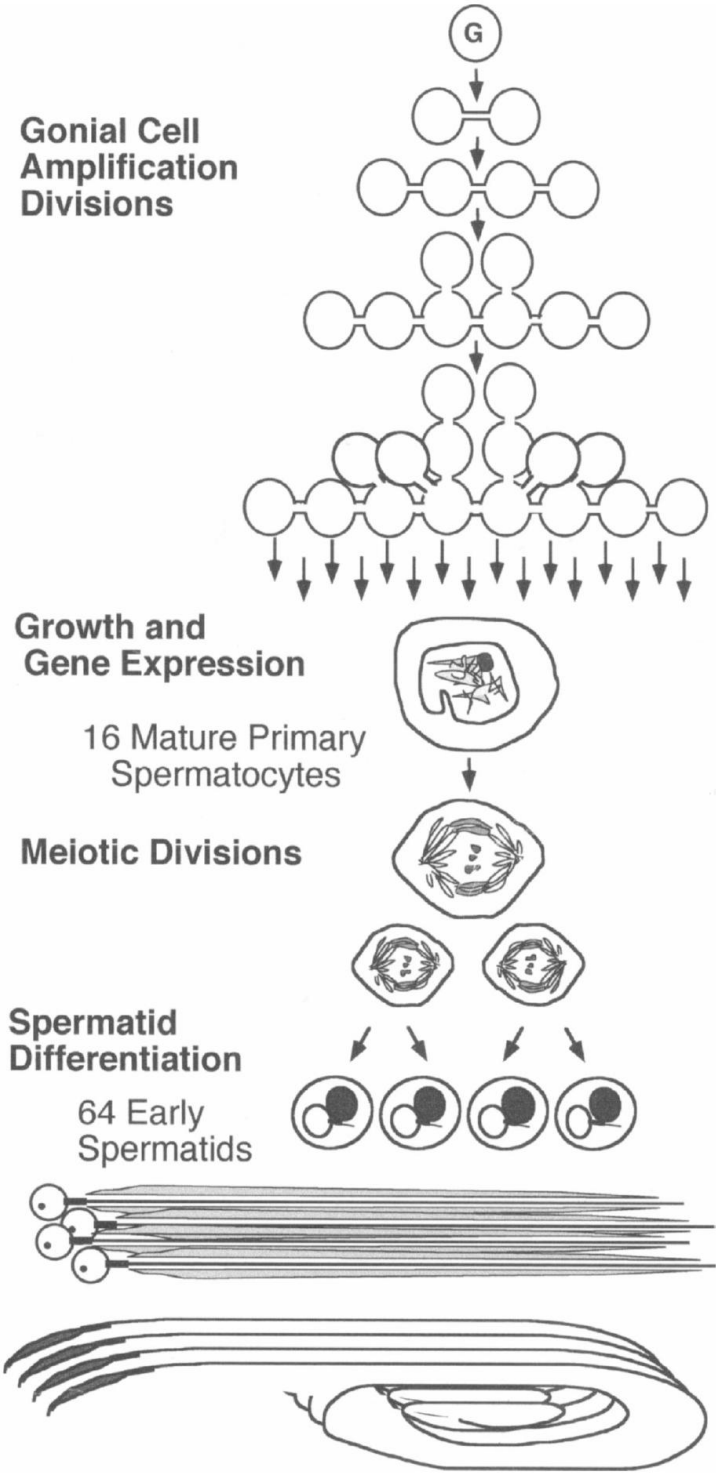

Figure 1. Schematics of spermatogenesis. A spermatogonium (G) undergoes four rounds of mitotic amplification divisions with incomplete cytokinesis. The resulting 16 interconnected cells enter the primary spermatocyte period of growth and gene expression. For simplicity, only one of the 16 primary spermatocytes in a cyst is shown. All 16 primary spermatocytes exit the cell growth and transcription program and enter meiotic divisions, resulting in a cyst of 64 interconnected, onion-stage, haploid, round spermatids. Each spermatid in an onion-stage cyst has the same sized nucleus (white sphere) and the same sized mitochondrial derivative (black sphere). The haploid spermatids remain interconnected and proceed through the dramatic morphological changes of spermiogenesis, eventually, with the production of fully elongated individualized sperms.
Figure adapted from (Fuller, 1998).

Further, sperm maturation involves the conformational change of the chromatin from round to needle shape and the mitochondrial derivatives then elongate along a developing axoneme. During this, the chromatin exchanges histones for protamines and dramatically condenses to a needle-like shape (Rathke et al., 2007). Sperm heads are oriented towards the basal end of the tube, with the tails pushing up the testis towards the apical tip. Since cytokinesis is incomplete during gonial and meiotic divisions, cytoplasmic bridges connect the 64 haploid spermatids with each other. The final phases of spermatogenesis include shedding of cytoplasm into a 'waste bag' (Fabrizio et al., 1998) and individualisation of spermatids (Fuller, 1993). Eventually, mature sperms coil and pass into the seminal vesicle where they acquire motility.

Primary Spermatocytes and Pairing of Homologs

Soon after the gonial mitotic divisions and pre-meiotic S phase, the primary spermatocytes enter the extended so-called 'growth phase' that approximately lasts 3.5 days in *D. melanogaster* (Lindsley and Tokuyasu, 1980). This period is primarily accompanied by certain morphological changes in cell size and chromatin distribution. In general, the stages S1-S6 are distinguished during the spermatocyte growth phase (Cenci et al., 1994). After the primary S1 spermatocyte begins its growth, the nucleus progressively assumes an eccentric position within the cytoplasm and forms a so-called polar spermatocyte stage (Tates, 1971). In young polar spermatocytes (stage S2), the chromatin appears as a compact mass. However, as the polar spermatocytes grow, chromatin subdivides into three masses or clumps that remain closely apposed to the inner nuclear envelope (Cooper, 1965). With nuclear growth, the space between these clumps increases so that in mature spermatocytes most of the karyoplasm is not occupied by the chromatin. The two somatically paired autosomes (2nd and 3rd chromosomes) are represented by the two larger clumps, whereas the third clump with less dense chromatin corresponds to the X and Y chromosome which are associated with the tiny 4th chromosomes which are generally visible as dots (Cenci et al., 1994; Cooper, 1965), also see Chapter 2 Fig.6). At stage S3, Y chromosome loops become apparent. The genes of the three (out of the six) "fertility factors" (kl-5, kl-3 and ks-1) form lampbrush-like loops, a cytological manifestation of their activity (Bonaccorsi et al., 1988). The major characteristic of these Y loops is that several proteins encoded by autosomal genes bind to them. Mutations in these autosomal genes lead to alteration in loop morphology and results in sterility. Some of them also have pleiotropic effects on meiosis and post-meiotic development (Ceprani et al., 2008). The Y loops of mature spermatocytes occupy most of the nucleus and often overlap. Disintegration of the Y

loops starts during stage S6 at the end of the growth phase before the beginning of the first meiotic division. In 1916 Bridges demonstrated that the Y chromosome is not required for viability since flies with X/0 karyotype are vital, phenotypically male but completely sterile individuals (Bridges, 1916). Later, it was shown that the Y chromosome carries genes required only for male fertility.

Lack of the synaptonemal complex and homologous recombination in male Drosophila raises the question how homologous chromosomes can be segregated during meiosis I. Somatic pairing in GSCs is disrupted during gonial mitosis but is required to be re-established in spermatocytes. A mechanism has been proposed by (Vazquez et al., 2002) for the pairing of homologs in primary spermatocytes. According to the model, the heterochromatic associations are responsible for the maintenance of homolog pairing during late G2. In mid-G2, the chromosomes separate into distinct territories, each corresponding to a set of paired homologs. This disrupts non-specific heterochromatic interactions between non-homologous chromosomes while interactions will remain preserved between heterochromatic regions on homologous chromosomes. Territory integrity and resolution have also been shown to depend on condensin II. Two condensin II subunits, Cap-H2 and Cap-D3, are required to promote territory formation. In mutants of either subunit, territory formation fails. Chromatin is dispersed throughout the nucleus during prophase I and condensed bivalents are completely absent during S6-prometaphase I (Hartl et al., 2008). But this does not explain why these territories form in the first place.

In general, chromosomes pair due to the sequence homology between the two homologs. This is consistent with the homolog pairing in autosomes where multiple regions of homology in the euchromatin are sufficient for the initiation of meiotic pairing. But the sex chromosome pair faces a special challenge because the X and Y

chromosomes are essentially devoid of homology except for the nucleolus organizers (NORs). Therefore, their pairing mechanism is distinct than for the autosomes and requires specific sequences from the NORs housing the tandemly repeated rRNA (rRNA) genes. For X–Y homolog pairing at least two proteins are known to be required, Stromalin in Meiosis [SNM; also known as Stromalin-2 (SA-2)] and Modifier of Mdg4 in Meiosis [MNM or Mod(mdg4)56.3]. These proteins persist throughout meiosis I until the homolog separation takes place in anaphase I in male, but are completely absent in female meiosis (Thomas et al., 2005). Thus, these proteins appear to substitute for chiasmata in supporting the association between homologs during male meiosis. The deletion of rDNA locus leads to loss of SNM and MNM localization, thus abolishing the pairing between X and Y. This results in high degree of non-disjunction (Mckee and Karpen, 1990).

SNM and MNM also localize to autosomes, where they have a role in maintaining pairing of autosomal homologs (Thomas et al., 2005). Recruitment of MNM, and perhaps SNM, to autosomes depends on the function of the Teflon (TEF) protein. TEF is required for correct segregation of autosomes but not sex chromosomes (Thomas et al., 2005; Tomkiel et al., 2001). In *tef* mutants pairing between autosomal bivalents is specifically defective with subsequent failure of unpaired autosomes to orient properly in metaphase plate thus resulting in non-disjunction. Conversely, segregation of sex chromosomes is unaffected by *tef* mutation (Tomkiel et al., 2001).

Regulation of Gene Expression in Primary Spermatocytes

Primary spermatocytes transcribe genes required for meiotic and post-meiotic stages (Olivieri and Olivieri, 1965; Schafer et al., 1995). The meiotic arrest genes encode factors that are required for transcriptional activation of most spermatocyte-specific genes (Lin et al., 1996; White-Cooper et al., 1998). In meiotic arrest mutant testes, primary spermatocytes arrested at the end of growth phase, accumulate.

Meiotic arrest genes have been divided into two categories depending on their molecular targets and their specific role in promoting transcription. The *aly*-class, which is constituted of 5 genes: *always early* (*aly*), *cookie monster* (*comr*), *achinthya/vismay* (*achi/vis*), *matotopetli* (*topi*) and *tombola* (*tomb*) (Lin et al., 1996; White-Cooper et al., 1998). Achi/Vis and Topi interact with chromatin by means of sequence-specific DNA-binding activity. Aly and Comr form a complex in the nucleus but only after accumulation of all the other *aly*-class products. This nuclear Aly-Comr complex binds to and stabilizes Tomb. Then they interact with Topi and Achi/Vis and thereby form the Drosophila testis-specific meiotic arrest complex (tMAC) (Beall et al., 2007; Jiang et al., 2007). tMAC seems to be a testis-specific variant of the Drosophila MMB/dREAM complex which appears to correspond to the DRM complex of *C. elegans* (Beall et al., 2007; Korenjak et al., 2004). t-MAC is thought to induce conformational changes in transcriptionally active chromatin, in order to promote high level transcription in spermatocytes. Among the target genes are meiotic control genes like *boule*, *twine* and *Cyclin B*, as well as spermatid differentiation genes such as *fuzzy onions* and *don juan*.

The *can*-class, which includes five meiotic-arrest genes so far (Ayyar et al., 2003; Hiller et al., 2004; Hiller et al., 2001; Jiang and White-Cooper, 2003; Perezgasga et al., 2004; Wang and Mann, 2003; White-Cooper et al., 2000; White-Cooper et al., 1998). These genes encode testis-specific TBP-associated factors (tTAFs). *cannonball* (*can*) encodes a

paralog of dTAF5. *can* is expressed only in male germ cells. *meiosis I arrest* (*mia*) encodes a paralog of dTAF6; *spermatocyte arrest* (*sa*) encodes a paralog of dTAF8; *no hitter* (*nht*) encodes a paralog of dTAF4 and *ryan express* (*rye*) encodes a paralog of dTAF12. As the generally expressed TAF paralogs, tTAFs associate with the transcription factor IID (TFIID). The multisubunit TFIID complex is composed of TATA-binding protein (TBP) and 12-14 other TBP-associated factors (TAFs). TFIID recruitment near the transcriptional start site is thought to, in turn, recruit and/or stabilise PolII binding in the preinitiation complex. *can*-class genes are likely to function by globally sequestering the PRC1 complex (Polycomb Repression Complex), away from active chromatin, and thus, regulating the terminal differentiation of male germ cells (Jiang et al., 2007). tTAFs binding to target promoters reduces Polycomb binding and promotes the recruitment of Trithorax (Trx) complex, an activator complex, with consequent accumulation of H3K4me3, a mark of transcriptional active chromatin (Chen et al., 2005; Hiller et al., 2004; Hiller et al., 2001; Jiang et al., 2007; Kolthur-Seetharam et al., 2008; Metcalf and Wassarman, 2007; Perezgasga et al., 2004; Wright et al., 2006).

The meiotic arrest genes also regulate the transcriptional activation of the spermatocyte specific β2 tubulin (*βTub85D*), which is a major component of the meiotic spindle during spermatogenesis. At the point when spermatocytes enter the growth phase, a switch in expression is initiated from β1 tubulin to the β2 isotype. β1 tubulin is found in mitotically active germ cells and all somatic parts of the testis. β2 tubulin expression reaches its peak in late primary spermatocytes (Buttgereit, 1993). The tubulin isotype switch in the germ line depends on transcriptional control. β1 mRNA and/or protein disappears rapidly during the transition from S1 to S3 spermatocytes. This might be dependent on post-transcriptional control (Buttgereit, 1993). For example, it has been shown that an 18-bp AT-rich element, present in the 5' untranslated regions

of the β2 tubulin mRNA, is responsible for stabilizing β2 about threefold compared to mRNA without the element (Michiels et al., 1993). Mutations in β2 tubulin result in phenotypes of varying severity. For example, mutations in amino acids that characterize the specific β2 isotype disrupt axoneme formation, while mutations in highly conserved amino acids that are common to all β tubulins disrupt microtubule assembly (Fackenthal et al., 1995). In Drosophila spermatogenesis, basal bodies and axonemes utilize the same alpha-tubulin but different β-tubulins. β1 is utilized for the centriole/basal body, and β2 is utilized for the motile sperm tail axoneme.

Thesis objectives

Centromere identity is specified epigenetically in most eukaryotes. Active centromeres contain a centromere-specific histone H3-variant (CenH3). CenH3 is thought to be an important part of the epigenetic mark for the specification of the centromere on the chromosome. How CenH3 is incorporated into centromeres and maintained there during chromosome replication and progression through the cell cycle is therefore the key to understanding this essential epigenetic mechanism.

A major goal of this thesis was to study the loading and propagation of the Drosophila CenH3 (Cid) during male meiosis. Cid loading has previously been characterized during mitotic proliferation, where loading occurs during exit from M phase. As meiosis includes progression through two consecutive M phases without an intervening S phase, Cid loading might have to be regulated differently during meiosis. If new Cid was loaded after each meiotic M phase in amounts precisely equal to the already present centromeric Cid protein, the size of the centromere would be expected to double with each generation unless compensated by periodic reduction. To clarify Cid loading during meiosis, careful quantifications were performed throughout spermatogenesis. Moreover, the hypothesis that pre-existing centromeric Cid protein is required and quantitatively instructive for the amount of new Cid loaded during chromosome replication was addressed. To analyze the role of pre-existing centromeric Cid for loading of new Cid, sperm was generated with experimentally altered Cid levels. Cid in sperm was either reduced to different extent or increased. After fertilization of oocytes with such sperm, the propagation of Cid levels on paternal centromeres was analyzed during development of the next generation.

To achieve the experimental alteration of Cid levels in sperm, various genetic approaches were applied, including the UAS/GAL4 system. Due to poor efficiency of the

conventional UAS/GAL4 system in spermatocytes, the first part of my thesis was focused on improvement of this binary system for use in these cells.

References

Allshire, R.C., and Karpen, G.H. (2008). Epigenetic regulation of centromeric chromatin: old dogs, new tricks? Nat Rev Genet *9*, 923-937.

Ault, J.G., Lin, H.P., and Church, K. (1982). Meiosis in Drosophila melanogaster. IV. The conjunctive mechanism of the XY bivalent. Chromosoma *86*, 309-317.

Ayyar, S., Jiang, J., Collu, A., White-Cooper, H., and White, R.A. (2003). Drosophila TGIF is essential for developmentally regulated transcription in spermatogenesis. Development *130*, 2841-2852.

Barnhart, M.C., Kuich, P.H., Stellfox, M.E., Ward, J.A., Bassett, E.A., Black, B.E., and Foltz, D.R. (2011). HJURP is a CENP-A chromatin assembly factor sufficient to form a functional de novo kinetochore. The Journal of cell biology *194*, 229-243.

Barreau, C., Benson, E., and White-Cooper, H. (2008). Comet and cup genes in Drosophila spermatogenesis: the first demonstration of post-meiotic transcription. Biochem Soc Trans *36*, 540-542.

Beall, E.L., Lewis, P.W., Bell, M., Rocha, M., Jones, D.L., and Botchan, M.R. (2007). Discovery of tMAC: a Drosophila testis-specific meiotic arrest complex paralogous to Myb-Muv B. Genes Dev *21*, 904-919.

Black, B., and Cleveland, D.W. (2011). Epigenetic Centromere Propagation and the Nature of CENP-A Nucleosomes. Cell *144*, 471-479.

Blower, M.D., Sullivan, B.A., and Karpen, G.H. (2002). Conserved organization of centromeric chromatin in flies and humans. Dev Cell *2*, 319-330.

Bonaccorsi, S., Pisano, C., Puoti, F., and Gatti, M. (1988). Y chromosome loops in Drosophila melanogaster. Genetics *120*, 1015-1034.

Bridges, C.B. (1916). Non-disjunction as proof of the chromosome theory of heredity (concluded). Genetics *1*, 107-163.

Bui, M., Dimitriadis, E.K., Hoischen, C., An, E., Quenet, D., Giebe, S., Nita-Lazar, A., Diekmann, S., and Dalal, Y. (2012). Cell-Cycle-Dependent Structural Transitions in the Human CENP-A Nucleosome In Vivo. Cell *150*, 317-326.

Burrack, L.S., and Berman, J. (2012). Flexibility of centromere and kinetochore structures. Trends in genetics : TIG *28*, 204-212.

Buttgereit, D. (1993). Redundant enhancer elements guide beta-1 tubulin gene-expression in apodemes during Drosophila embryogenesis. J Cell Sci *105*, 721-727.

Camahort, R., Li, B., Florens, L., Swanson, S.K., Washburn, M.P., and Gerton, J.L. (2007). Scm3 is essential to recruit the histone H3 variant Cse4 to centromeres and to maintain a functional kinetochore. Molecular Cell *26*, 853-865.

Carroll, C.W., Milks, K.J., and Straight, A.F. (2010). Dual recognition of CENP-A nucleosomes is required for centromere assembly. J Cell Biol *189*, 1143-1155.

Cenci, G., Bonaccorsi, S., Pisano, C., Verni, F., and Gatti, M. (1994). Chromatin and microtubule organization during premeiotic, meiotic and early postmeiotic stages of Drosophila- melanogaster spermatogenesis. J Cell Sci *107*, 3521-3534.

Ceprani, F., Raffa, G.D., Petrucci, R., and Piergentili, R. (2008). Autosomal mutations affecting Y chromosome loops in Drosophila melanogaster. BMC genetics *9*, 32.

Chen, X., Hiller, M., Sancak, Y., and Fuller, M.T. (2005). Tissue-specific TAFs counteract Polycomb to turn on terminal differentiation. Science *310*, 869-872.

Church, K., and Lin, H.P. (1982). Meiosis in Drosophila melanogaster. II. The prometaphase-I kinetochore microtubule bundle and kinetochore orientation in males. The Journal of cell biology *93*, 365-373.

Clark, A.G., Eisen, M.B., Smith, D.R., Bergman, C.M., Oliver, B., Markow, T.A., Kaufman, T.C., Kellis, M., Gelbart, W., Iyer, V.N.*, et al.* (2007). Evolution of genes and genomes on the Drosophila phylogeny. Nature *450*, 203-218.

Clarke, L. (1998). Centromeres: proteins, protein complexes, and repeated domains at centromeres of simple eukaryotes. Current Opinion in Genetics & Development *8*, 212-218.

Collins, K.A., Furuyama, S., and Biggins, S. (2004). Proteolysis contributes to the exclusive centromere localization of the yeast Cse4/CENP-A histone H3 variant. Curr Biol *14*, 1968-1972.

Cooper, K.W. (1949). The cytogenetics of meiosis in Drosophila; mitotic and meiotic autosomal chiasmata without crossing over in the male. Journal of morphology *84*, 81-121.

Cooper, K.W. (1965). Normal spermatogenesis in Drosophila. In Biology of Drosophila (ed M Demerec), 1-61.

Dalal, Y., Furuyama, T., Vermaak, D., and Henikoff, S. (2007a). Structure, dynamics, and evolution of centromeric nucleosomes. Proc Natl Acad Sci U S A.

Dalal, Y., Wang, H., Lindsay, S., and Henikoff, S. (2007b). Tetrameric structure of centromeric nucleosomes in interphase Drosophila cells. PLoS biology *5*, e218.

Dechassa, M.L., Wyns, K., Li, M., Hall, M.A., Wang, M.D., and Luger, K. (2011). Structure and Scm3-mediated assembly of budding yeast centromeric nucleosomes. Nature communications *2*, 313.

Dunleavy, E.M., Roche, D., Tagami, H., Lacoste, N., Ray-Gallet, D., Nakamura, Y., Daigo, Y., Nakatani, Y., and Almouzni-Pettinotti, G. (2009). HJURP is a cell-cycle-dependent maintenance and deposition factor of CENP-A at centromeres. Cell *137*, 485-497.

Erhardt, S., Mellone, B.G., Betts, C.M., Zhang, W., Karpen, G.H., and Straight, A.F. (2008). Genome-wide analysis reveals a cell cycle-dependent mechanism controlling centromere propagation. J Cell Biol *183*, 805-818.

Fabrizio, J.J., Hime, G., Lemmon, S.K., and Bazinet, C. (1998). Genetic dissection of sperm individualization in Drosophila melanogaster. Development *125*, 1833-1843.

Fackenthal, J.D., Hutchens, J.A., Turner, F.R., and Raff, E.C. (1995). Structural-analysis of mutations in the Drosophila beta-2- tubulin isoform reveals regions in the beta-tubulin molecule required for general and for tissue-specific microtubule functions. Genetics *139*, 267-286.

Fitzgerald-Hayes, M., Clarke, L., and Carbon, J. (1982). Nucleotide sequence comparisons and functional analysis of yeast centromere DNAs. Cell *29*, 235-244.

Foltz, D.R., Jansen, L.E., Bailey, A.O., Yates, J.R., 3rd, Bassett, E.A., Wood, S., Black, B.E., and Cleveland, D.W. (2009). Centromere-specific assembly of CENP-a nucleosomes is mediated by HJURP. Cell *137*, 472-484.

Foltz, D.R., Jansen, L.E., Black, B.E., Bailey, A.O., Yates, J.R., 3rd, and Cleveland, D.W. (2006). The human CENP-A centromeric nucleosome-associated complex. Nat Cell Biol *8*, 458-469.

Fuller, M.T. (1993). Spermatogenesis. In The development of Drosophila melanogaster, M. Bate, and A. Martinez Arias, eds. (Cold Spring Harbor, NY, Cold Spring Harbor Laboratory Press), pp. 71-148.

Fuller, M.T. (1998). Genetic control of cell proliferation and differentiation in Drosophila spermatogenesis. Seminars in cell & developmental biology *9*, 433-444.

Gilboa, L., and Lehmann, R. (2004). How different is Venus from Mars? The genetics of germ-line stem cells in Drosophila females and males. Development *131*, 4895-4905.

Goldstein, L.S. (1981). Kinetochore structure and its role in chromosome orientation during the first meiotic division in male D. melanogaster. Cell *25*, 591-602.

Gonczy, P., and Dinardo, S. (1996). The germ line regulates somatic cyst cell proliferation and fate during Drosophila spermatogenesis. Development *122*, 2437-2447.

Goshima, G., Wollman, R., Goodwin, S.S., Zhang, N., Scholey, J.M., Vale, R.D., and Stuurman, N. (2007). Genes required for mitotic spindle assembly in Drosophila S2 cells. Science *316*, 417-421.

Hardy, R.W., Tokuyasu, K.T., Lindsley, D.L., and Garavito, M. (1979). The germinal proliferation center in the testis of Drosophila melanogaster. Journal of ultrastructure research *69*, 180-190.

Harrington, J.J., Vanbokkelen, G., Mays, R.W., Gustashaw, K., and Willard, H.F. (1997). Formation of de novo centromeres and construction of first- generation human artificial microchromosomes. Nat Genet *15*, 345-355.

Hartl, T.A., Sweeney, S.J., Knepler, P.J., and Bosco, G. (2008). Condensin II resolves chromosomal associations to enable anaphase I segregation in Drosophila male meiosis. PLoS Genet *4*, e1000228.

Heun, P., Erhardt, S., Blower, M.D., Weiss, S., Skora, A.D., and Karpen, G.H. (2006). Mislocalization of the Drosophila centromere-specific histone CID promotes formation of functional ectopic kinetochores. Dev Cell *10*, 303-315.

Hiller, M., Chen, X., Pringle, M.J., Suchorolski, M., Sancak, Y., Viswanathan, S., Bolival, B., Lin, T.Y., Marino, S., and Fuller, M.T. (2004). Testis-specific TAF homologs collaborate to control a tissue-specific transcription program. Development *131*, 5297-5308.

Hiller, M.A., Lin, T.Y., Wood, C., and Fuller, M.T. (2001). Developmental regulation of transcription by a tissue-specific TAF homolog. Genes Dev *15*, 1021-1030.

Jansen, L.E., Black, B.E., Foltz, D.R., and Cleveland, D.W. (2007). Propagation of centromeric chromatin requires exit from mitosis. J Cell Biol *176*, 795-805.

Jiang, J., Benson, E., Bausek, N., Doggett, K., and White-Cooper, H. (2007). Tombola, a tesmin/TSO1-family protein, regulates transcriptional activation in the Drosophila male germline and physically interacts with always early. Development *134*, 1549-1559.

Jiang, J., and White-Cooper, H. (2003). Transcriptional activation in Drosophila spermatogenesis involves the mutually dependent function of aly and a novel meiotic arrest gene cookie monster. Development *130*, 563-573.

Khodjakov, A., and Pines, J. (2010). Centromere tension: a divisive issue. Nat Cell Biol *12*, 919-923.

Kolthur-Seetharam, U., Martianov, I., and Davidson, I. (2008). Specialization of the general transcriptional machinery in male germ cells. Cell cycle *7*, 3493-3498.

Korenjak, M., Taylor-Harding, B., Binne, U.K., Satterlee, J.S., Stevaux, O., Aasland, R., White-Cooper, H., Dyson, N., and Brehm, A. (2004). Native E2F/RBF complexes contain Myb-interacting proteins and repress transcription of developmentally controlled E2F target genes. Cell *119*, 181-193.

Lagana, A., Dorn, J.F., De Rop, V., Ladouceur, A.M., Maddox, A.S., and Maddox, P.S. (2010). A small GTPase molecular switch regulates epigenetic centromere maintenance by stabilizing newly incorporated CENP-A. Nature cell biology *12*, 1186-1193.

Lin, H. (2002). The stem-cell niche theory: lessons from flies. Nature reviews Genetics *3*, 931-940.

Lin, T.Y., Viswanathan, S., Wood, C., Wilson, P.G., Wolf, N., and Fuller, M.T. (1996). Coordinate developmental control of the meiotic cell-cycle and spermatid differentiation in Drosophila males. Development *122*, 1331-1341.

Lindsley, D., and Tokuyasu, K.T. (1980). Spermatogenesis. In Genetics and Biology of Drosophila, M. Ashburner, and T.R. Wright, eds. (New York, Academic Press), pp. 225-294.

Malik, H.S., and Henikoff, S. (2001). Adaptive evolution of Cid, a centromere-specific histone in Drosophila. Genetics *157*, 1293-1298.

Manuelidis, L. (1978). Chromosomal localization of complex and simple repeated human DNAs. Chromosoma *66*, 23-32.

Mckee, B.D., and Karpen, G.H. (1990). Drosophila ribosomal-rna genes function as an x-y pairing site during male meiosis. Cell *61*, 61-72.

Mellone, B.G., Grive, K.J., Shteyn, V., Bowers, S.R., Oderberg, I., and Karpen, G.H. (2011). Assembly of Drosophila centromeric chromatin proteins during mitosis. PLoS genetics *7*, e1002068.

Metcalf, C.E., and Wassarman, D.A. (2007). Nucleolar colocalization of TAF1 and testis-specific TAFs during Drosophila spermatogenesis. Developmental dynamics : an official publication of the American Association of Anatomists *236*, 2836-2843.

Michiels, F., Buttgereit, D., and Renkawitzpohl, R. (1993). An 18-bp element in the 5' untranslated region of the Drosophila beta-2 tubulin messenger-rna regulates the messenger-rna level during postmeiotic stages of spermatogenesis. European J Cell Biol *62*, 66-74.

Mitchell, A.R., Gosden, J.R., and Miller, D.A. (1985). A Cloned Sequence, P82h, of the Alphoid Repeated DNA Family Found at the Centromeres of All Human-Chromosomes. Chromosoma *92*, 369-377.

Monesi, V. (1965). Synthetic activities during spermatogenesis in the mouse RNA and protein. Experimental cell research *39*, 197-224.

Moreno-Moreno, O., Torras-Llort, M., and Azorin, F. (2006). Proteolysis restricts localization of CID, the centromere-specific histone H3 variant of Drosophila, to centromeres. Nucleic Acids Res *34*, 6247-6255.

Morgan, T.H. (1912). Special Articles. Science *36*, 718-720.

Okada, M., Cheeseman, I.M., Hori, T., Okawa, K., McLeod, I.X., Yates, J.R., 3rd, Desai, A., and Fukagawa, T. (2006). The CENP-H-I complex is required for the efficient incorporation of newly synthesized CENP-A into centromeres. Nat Cell Biol *8*, 446-457.

Olivieri, G., and Olivieri, A. (1965). Autoradiographic study of nucleic acid synthesis during spermatogenesis in Drosophila melanogaster. Mutat Res *2*, 366-380.

Perezgasga, L., Jiang, J., Bolival, B., Jr., Hiller, M., Benson, E., Fuller, M.T., and White-Cooper, H. (2004). Regulation of transcription of meiotic cell cycle and terminal differentiation genes by the testis-specific Zn-finger protein matotopetli. Development *131*, 1691-1702.

Phansalkar, R., Lapierre, P., and Mellone, B.G. (2012). Evolutionary insights into the role of the essential centromere protein CAL1 in Drosophila. Chromosome Research *20*, 493-504.

Pluta, A.F., Mackay, A.M., Ainsztein, A.M., Goldberg, I.G., and Earnshaw, W.C. (1995). The centromere: hub of chromosomal activities. Science *270*, 1591-1594.

Przewloka, M.R., and Glover, D.M. (2009). The Kinetochore and the Centromere: A Working Long Distance Relationship. Annual Review of Genetics *43*, 439-465.

Rathke, C., Baarends, W.M., Jayaramaiah-Raja, S., Bartkuhn, M., Renkawitz, R., and Renkawitz-Pohl, R. (2007). Transition from a nucleosome-based to a protamine-based chromatin configuration during spermiogenesis in Drosophila. Journal of Cell Science *120*, 1689-1700.

Saffery, R., Irvine, D.V., Griffiths, B., Kalitsis, P., Wordeman, L., and Choo, K.H.A. (2000). Human centromeres and neocentromeres show identical distribution patterns of > 20 functionally important kinetochore-associated proteins. Human Molecular Genetics *9*, 175-185.

Sanchez-Pulido, L., Pidoux, A.L., Ponting, C.P., and Allshire, R.C. (2009). Common ancestry of the CENP-A chaperones Scm3 and HJURP. Cell *137*, 1173-1174.

Schafer, M., Nayernia, K., Engel, W., and Schafer, U. (1995). Translational control in spermatogenesis. Dev Biol *172*, 344-352.

Schittenhelm, R.B., Althoff, F., Heidmann, S., and Lehner, C.F. (2010). Detrimental incorporation of excess Cenp-A/Cid and Cenp-C into Drosophila centromeres is prevented by limiting amounts of the bridging factor Cal1. Journal of Cell Science *123*, 3768-3779.

Shivaraju, M., and Gerton, J.L. (2011). The dynamics of the Cse4 chaperone Scm3. Cell cycle *10*, 3823-3824.

Shivaraju, M., Unruh, J.R., Slaughter, B.D., Mattingly, M., Berman, J., and Gerton, J.L. (2012). Cell-cycle-coupled structural oscillation of centromeric nucleosomes in yeast. Cell *150*, 304-316.

Sun, X., Le, H.D., Wahlstrom, J.M., and Karpen, G.H. (2003). Sequence analysis of a functional Drosophila centromere. Genome research *13*, 182-194.

Talbert, P.B., Masuelli, R., Tyagi, A.P., Comai, L., and Henikoff, S. (2002). Centromeric localization and adaptive evolution of an Arabidopsis histone H3 variant. Plant Cell *14*, 1053-1066.

Tates, A.D. (1971). Cytodifferentiation during spermatogenesis in Drosophila melanogaster: an electron microscope study. . PhD thesis.

Thomas, S.E., Soltani-Bejnood, M., Roth, P., Dorn, R., Logsdon, J.M., Jr., and McKee, B.D. (2005). Identification of two proteins required for conjunction and regular segregation of achiasmate homologs in Drosophila male meiosis. Cell *123*, 555-568.

Tomkiel, J.E., Wakimoto, B.T., and Briscoe, A., Jr. (2001). The teflon gene is required for maintenance of autosomal homolog pairing at meiosis I in male Drosophila melanogaster. Genetics *157*, 273-281.

Torras-Llort, M., Moreno-Moreno, O., and Azorin, F. (2009). Focus on the centre: the role of chromatin on the regulation of centromere identity and function. EMBO J.

Van Hooser, A.A., Ouspenski, II, Gregson, H.C., Starr, D.A., Yen, T.J., Goldberg, M.L., Yokomori, K., Earnshaw, W.C., Sullivan, K.F., and Brinkley, B.R. (2001). Specification of kinetochore-forming chromatin by the histone H3 variant CENP-A. J Cell Sci *114*, 3529-3542.

Vazquez, J., Belmont, A.S., and Sedat, J.W. (2002). The dynamics of homologous chromosome pairing during male Drosophila meiosis. Curr Biol *12*, 1473-1483.

Verdaasdonk, J.S., and Bloom, K. (2011). Centromeres: unique chromatin structures that drive chromosome segregation. Nature Reviews Molecular Cell Biology *12*, 320-332.

Wang, Z., and Mann, R.S. (2003). Requirement for two nearly identical TGIF-related homeobox genes in Drosophila spermatogenesis. Development *130*, 2853-2865.

Weaver, B.A., and Cleveland, D.W. (2006). Does aneuploidy cause cancer? Curr Opin Cell Biol *18*, 658-667.

White-Cooper, H. (2004). Spermatogenesis: analysis of meiosis and morphogenesis. Methods Mol Biol *247*, 45-75.

White-Cooper, H., Leroy, D., MacQueen, A., and Fuller, M.T. (2000). Transcription of meiotic cell cycle and terminal differentiation genes depends on a conserved chromatin associated protein, whose nuclear localisation is regulated. Development *127*, 5463-5473.

White-Cooper, H., Schafer, M.A., Alphey, L.S., and Fuller, M.T. (1998). Transcriptional and post-transcriptional control mechanisms coordinate the onset of spermatid differentiation with meiosis I in Drosophila. Development *125*, 125-134.

Wright, K.J., Marr, M.T., 2nd, and Tjian, R. (2006). TAF4 nucleates a core subcomplex of TFIID and mediates activated transcription from a TATA-less promoter. Proceedings of the National Academy of Sciences of the United States of America *103*, 12347-12352.

Yamashita, Y.M., Fuller, M.T., and Jones, D.L. (2005). Signaling in stem cell niches: lessons from the Drosophila germline. Journal of Cell Science *118*, 665-672.

Yamashita, Y.M., Jones, D.L., and Fuller, M.T. (2003). Orientation of asymmetric stem cell division by the APC tumor suppressor and centrosome. Science *301*, 1547-1550.

Yoda, K., Ando, S., Morishita, S., Houmura, K., Hashimoto, K., Takeyasu, K., and Okazaki, T. (2000). Human centromere protein A (CENP-A) can replace histone H3 in nucleosome reconstitution in vitro. Proceedings of the National Academy of Sciences of the United States of America *97*, 7266-7271.

Chapter 1

Novel GAL4 driver lines for efficient UAS gene expression in spermatocytes

Introduction

The yeast transcription factor GAL4 is widely used in Drosophila for regulated expression of transgenes with the GAL4 binding sequence (UAS; upstream activator sequence) in front of a promoter. The binary GAL4/UAS system is a very useful tool that allows the selective expression of UAS transgenes in a variety of tissue- or stage-specific patterns because a large selection of driver lines expressing GAL4 in specific spatiotemporal patterns in various somatic tissues is available. To improve the GAL4/UAS system various Gal4 variants have been generated. Detailed deletion analyses of GAL4 transcriptional potential in yeast showed that a main part of GAL4 can be deleted without losing its stimulation potential for the transcription of UAS-linked genes (Ma and Ptashne, 1987). A GAL4 minimal domain comprising the N-terminal DNA-binding sequence and the C- terminal transcriptional activation domain (GAL4Δ) are required. Another variant of GAL4 is GAL4-VP16, which is a fusion of a DNA-binding fragment of the yeast activator GAL4 to a highly acidic portion of the herpes simplex virus protein VP16. VP16 activates transcription of early viral genes by using its amino-terminal sequences by attaching to one or more host-encoded proteins that recognise DNA sequences in their promoters. GAL4-VP16 has been shown to activate transcription efficiently in mammalian cells (Sadowski et al., 1988). A comparative analysis of original GAL4, chimerical GAL4-VP16 and the shortened version GAL4Δ for their transcriptional potential has been performed in flies (Viktorinova and Wimmer, 2007). The expression of UAS transgenes was shown to be strongest when expression was driven by GAL4Δ.

Unfortunately, the original GAL4/UAS system does not work efficiently in the germline (Brand and Perrimon, 1993). In the female germline GAL4 was shown to be insufficient for transcriptional activation of UAS transgenes (Rorth, 1998). To overcome this problem, Rorth (1998) developed a modified UAS target gene vector, pUASp, in which the *hsp70* promoter and SV40 terminator of the original vector pUASt were replaced with the P transposase promoter including first intron and the *fs(1)K10* 3' UTR. pUASp-based transgenes were shown to be

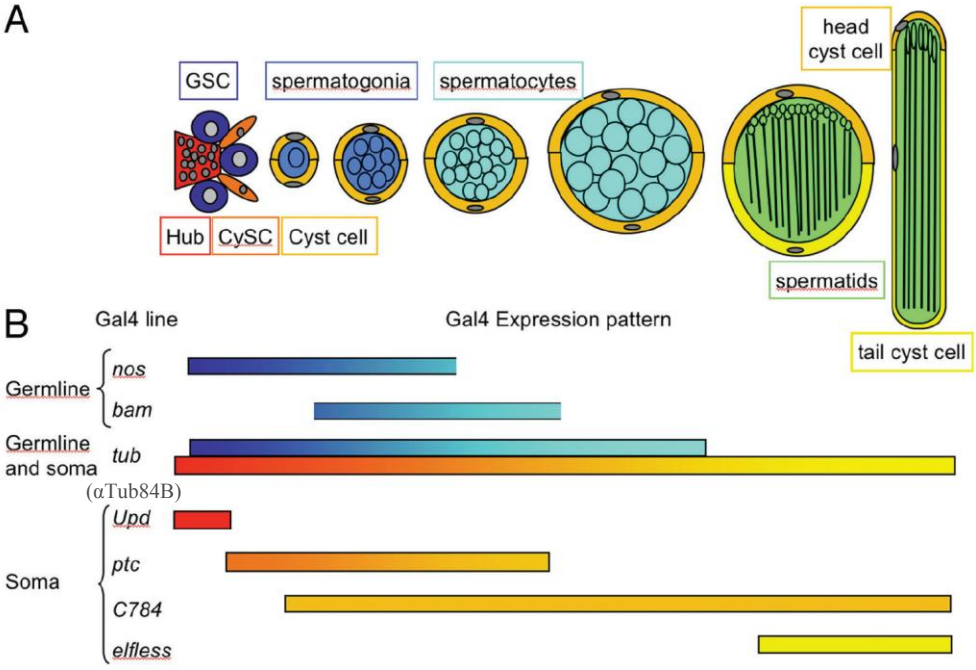

Figure 1. Schematic representation of expression pattern of GAL4 drivers in the testis. (A) Male germline stem cells (GSC, dark blue) and cyst stem cells (CySC, dark orange) contact the hub (red) at testis tip. Spermatogonia (light blue) are encapsulated by cyst cells (light orange) and displaced from the hub. Spermatogonia differentiate into spermatocytes (cyan) which grow extensively before completing meiosis and becoming spermatids (green). Head and tail (yellow) cyst cells are distinguishable associated with elongating spermatids. (B) Different GAL4 driver lines can be used to drive downstream gene expression with spatial and temporal control. The bars indicate the developmental stage and cell type specificity of the expression of Gal4 in particular lines.
Figure adapted from (White-Cooper, 2012).

functional in the female germline. In the male germline both pUASt and pUASp transgenes have been used successfully but only during the early stages (GSCs and spermatogonia). However, in spermatocytes, the efficiency of the available GAL4 tools has been observed to be poor (Fig. 1). Few GAL4 lines have been reported to drive expression of UASt transgenes in the male germ line during the spermatocyte stages (Fig.1; see also (Arya et al., 2006; Baker and Fuller, 2007; Franklin-Dumont et al., 2007; Hrdlicka et al., 2002)). But these GAL4 driver lines do not appear to drive strong expression as required for efficient RNAi in spermatocytes (Kränzlin, 2008).

The poor efficiency of the GAL4/UAS system in spermatocytes might reflect an inefficient interaction between the activation domain of GAL4 and testis-specific transcription factors (TFs) (Fig. 2b). In contrast, GAL4 co-operates effectively with the the transcription machinery in somatic cells (Fig. 2a). The fact that testis express testis-specific TAFs (tTAFs) and thus have a testis-specific TFIID complex instead of canonical TFIID is clearly consistent with this speculation.

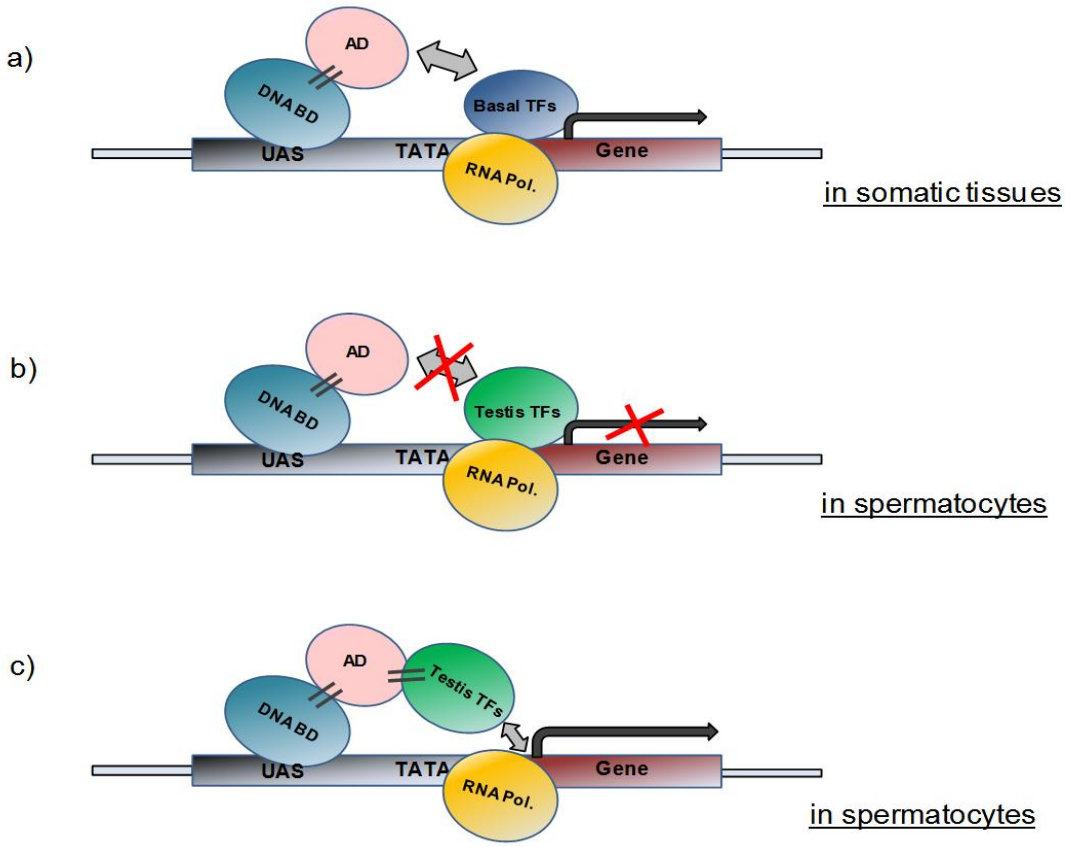

Figure 2. (a) A diagrammatic representation of conventional GAL4/UAS system in somatic tissues. (b) Hypothetical explanation for inefficiency of the conventional GAL4/UAS system in spermatocytes and (c) deduced strategy for improvement in spermatocytes (BD: GAL4 DNA binding domain, AD: GAL4 activation domain, TFs: Transcription factors, '// 'indicates protein fusion).

According to this speculation, a better efficiency might result from expression of GAL4 fused to testis-specific TFs (Fig. 2c). As a higher efficiency of the GAL4/UAS system would provide invaluable support for analysis of spermatogenic processes (including meiosis), this strategy was experimentally evaluated.

Results and Discussion

Initially, three spermatocyte-specific genes (*spermatocyte arrest (sa)*, *tombola (tomb)*, *matotopetli (topi)*) (Hiller et al., 2001; Jiang et al., 2007; Michiels et al., 1989) were used for the generation of novel GAL4 driver lines (Kränzlin, 2008). These genes were used because they have been very well characterized. Also, it has been demonstrated previously that the function of these proteins does not get abolished upon fusion with heterologous protein domains such as GFP (Chen et al., 2005).

In the first set of transgene constructs, fusions between GAL4Δ and testis-specific transcription factors were generated. GAL4Δ was selected for fusion because it was shown to be efficient in driving UAS transgene in fly head extracts (Viktorinova and Wimmer, 2007). These constructs were generated using a recombinant P element vector (CaspeR4) and fly lines were derived by random P element integration into the fly genome. This was followed by an initial evaluation of the novel drivers by crossing with UASt-2xGFP III and analyzing the GFP signal intensity in testis. In comparison with *sa* and *tomb*, the most efficient expression of GFP was observed with the cis regulatory region of *topi* (Kränzlin, 2008).

To further improve the efficiency of the driver lines, additional constructs were generated in this study. The efficiency obtained with the cis regulatory region of *βTub85D* instead of the *topi* control region was analyzed. Based on FlyBase data, the level of expression of *βTub85D* is far higher than that of *topi*. Therefore, the *βTub85D* regulatory region was expected to result in stronger expression of the GAL4 variant and hence better efficiency of UAS transgene activation. These

constructs were inserted into newly developed att vectors (Bischof et al., 2007) allowing site-specific integration of transgenes with the phiC31 system. This allowed comparisons of transgenes inserted at the same chromosomal location thereby eliminating any potential interference by transgene insertion position effects.

As illustrated in Fig.3, the analysis of UASt-2xGFP expression revealed that *topi-GAL4Δ-topi* drives stronger expression than *βTub85D-GAL4Δ-topi* contrary to the expectations (see also Table 1).

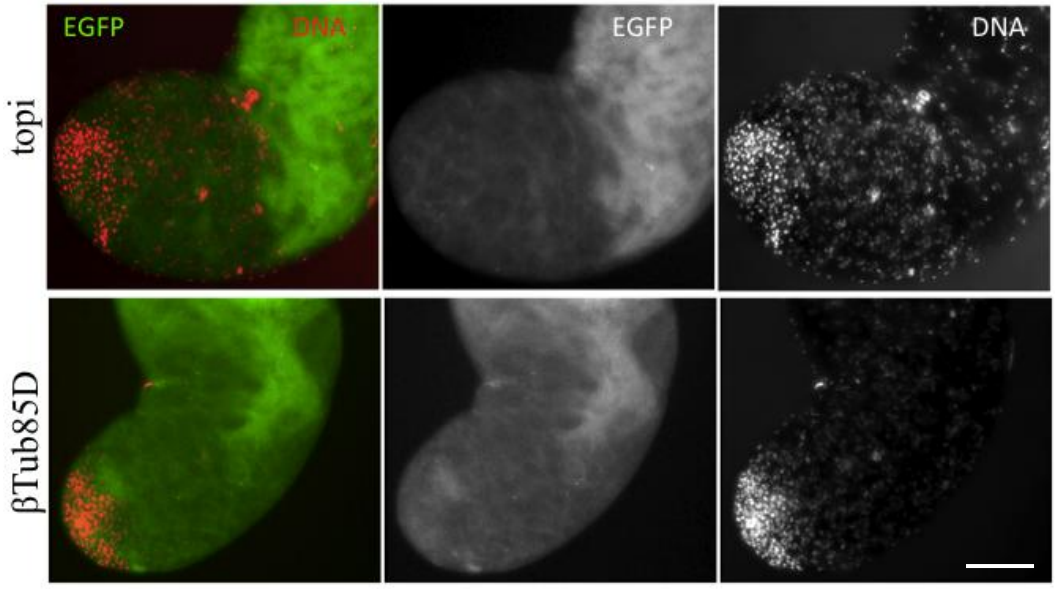

Figure 3. Comparison between the *topi* and *βTub85D* regulatory region.
The upper panel shows testis from a male where *topi-GAL4Δ-topi* is driving UASt-2xGFP expression. The lower panel shows testis from a male where *βTub85D-GAL4Δ-topi* is driving UASt-2xGFP expression. Scale bar = 10μm.

The unexpected poor activity of the *βTub85D* regulatory region has recently also been noted in a review (White-Cooper, 2012). The likely reason for poor efficiency of the corresponding driver line could be due to the timing of expression of GAL4 relative to the shut-down of transcription that occurs in

maturing primary spermatocytes. There is probably insufficient time for GAL4 to accumulate to levels required for driving target gene expression.

Table1: Efficiency of GFP expression driven by various Gal4 drivers.

Construct name	Vector[c]	regulatory region	coding region (testis TF)	GAL4 version[d]	position[e]	efficiency
sa-GAL4Δ[a]	C4	sa	sa	Δ	C	-
tomb-GAL4Δ[a]	C4	tomb	tomb	Δ	N	-
topi-GAL4Δ[a]	C4	topi	topi	Δ	N	+(+)
topi-GAL4Δ-topi[b]	att	topi	topi	Δ	N	+(+)
βTub85D-GAL4Δ-topi[b]	att	βTub85D	topi	Δ	N	+
topi-GAL4(FL)-topi[b]	att	topi	topi	FL	N	+
topi-GAL4-VP16-topi[b]	att	topi	topi	VP16	N	++
topi-GAL4-VP16[b]	att	topi	none	VP16	-	-

a) (Kränzlin, 2008)
b) this study
c) Transgene vector, C4: CaspeR4 (Thummel and Pirrotta, 1992), att: attB (Bischof et al., 2007)
d) GAL4 version. Δ: GAL4 a.a. 1-147 (DNA binding domain), a.a.768-881(activation domain); FL: GAL4 a.a. 1-881; VP16: VP16 a.a. 413-490 (activation domain).
e) The position of fusion is indicated with 'N' denoting insertion of GAL4 version before N-terminus of testis TF and 'C' after C-terminus of testis TF.

To further improve the efficiency of driver lines, different GAL4 versions were compared in the context of *topi* fusion genes. An additional set of att constructs were generated using GAL4(FL), GAL4Δ and GAL4-VP16. The efficiency of these driver lines was analyzed using *UASt-2xGFP*. Undoubtedly, the expression driven by *topi-Gal4-VP16-topi* was found to be strongest (Fig.4, see also Table 1).

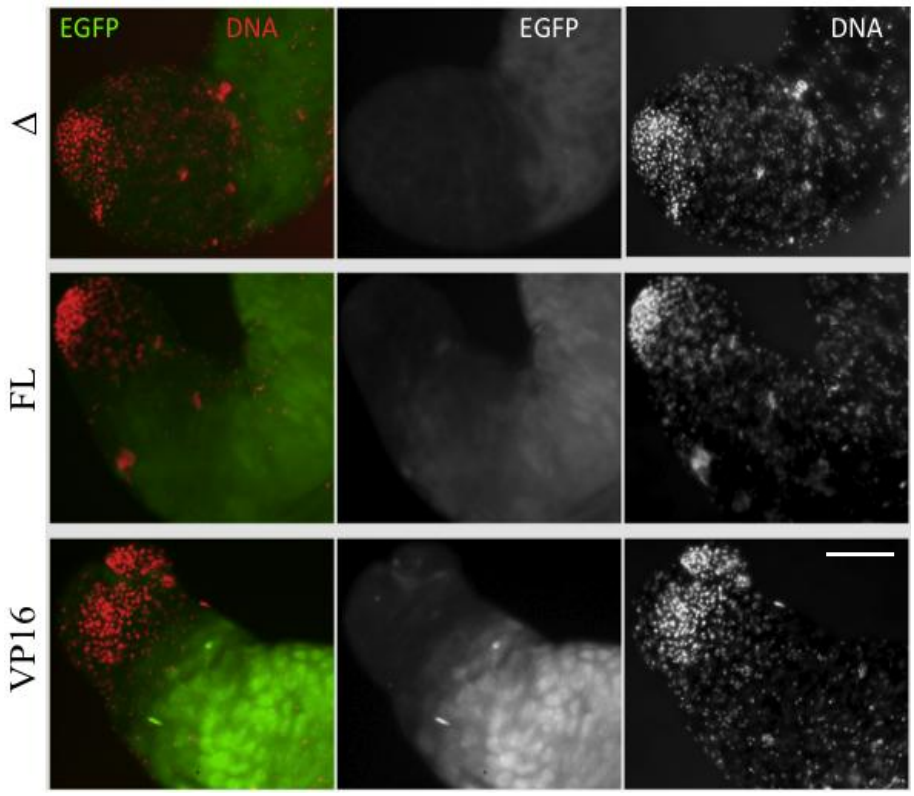

Figure 4. Comparison of different GAL4 variants.
The uppermost panel shows UASt-2xGFP expression driven by *topi-GAL4Δ-topi*, the middle panel shows *UASt-2xGFP* expression driven by *topi-GAL4FL-topi* and the lower panel shows *UASt-2xGFP* expression driven by *topi-GAL4-VP16-topi*. Clearly, the expression was driven strongest in case of GAL4 fused with VP16. Identical settings were used for image acquisition on the widefield microscope. Scale bar = 10µm.

Finally, to test whether fusion with Topi indeed improves the efficiency of GAL4-VP16, a construct was generated, *topi-GAL4-VP16-3'UTR topi* (minus Topi). The expression of *UASt-2xGFP* was found to be higher in case of the GAL4-VP16 fused to Topi compared to GAL4-VP16 that was not fused to Topi (Fig. 5, see also Table 1).

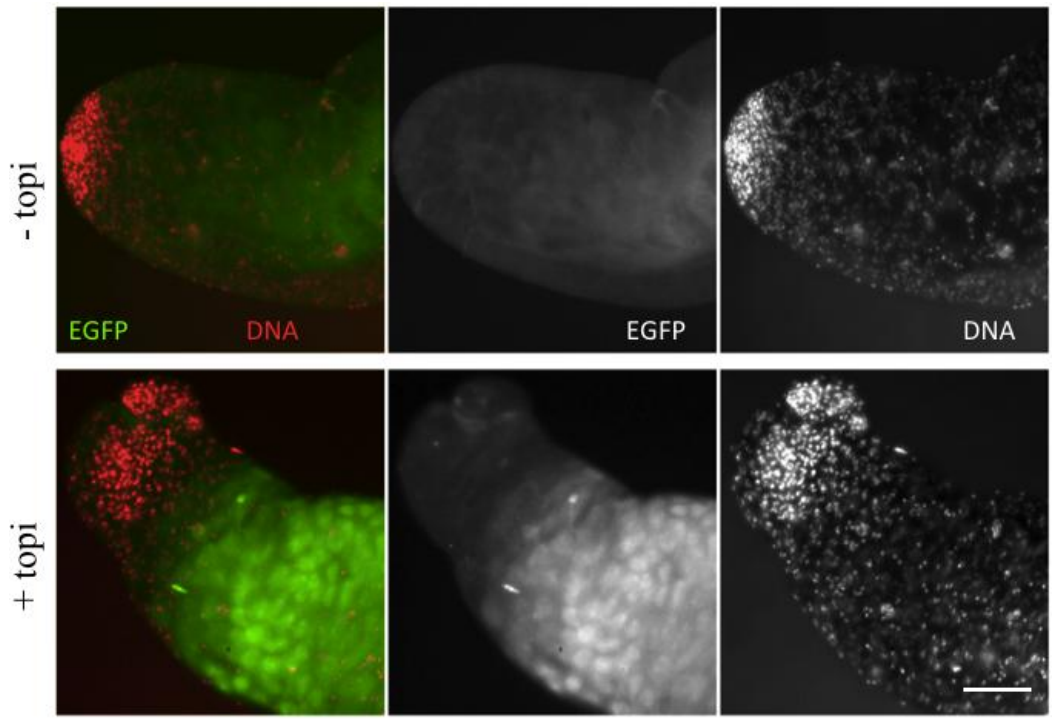

Figure 5. The Topi-GAL4-VP16 fusion protein is more efficient than GAL4-VP16 alone.
The upper panel shows UASt-2xGFP expression driven by *topi-GAL4-VP16-3'UTR-topi* in testis. The lower panel shows UASt-2xGFP expression driven by *topi-GAL4-VP16-topi* in testis. Identical settings were used for image acquisition on the widefield microscope. Scale bar = 10µm.

To test whether the UAS target gene expression efficiency could be further improved, different GAL4 transgenes were combined. It was also shown by (Noguchi and Miller, 2003) that the combination of different drivers enhances transcriptional activation of the UAS target genes. *bam-GAL4-VP16* (Fig. 1, see also (Chen, 2003 #6015)) alone resulted in strong expression in spermatogonia and early spermatocytes whereas *topi-GAL4-VP16-topi* alone resulted in weaker expression in later stages. The combination of *bam-GAL4-VP16* and *topi-GAL4-VP16-topi* resulted in expression in almost the whole testis except in stem cells and hub region (Fig. 6).

Apart from scoring *UAS-2xGFP* expression to evaluate driver line efficiencies, additional confirmation was sought in experiments using *UASt-Spc105^{RNAi}* and analyzing effects of its expression on male fertility (Fig. 7a). Spc105 is an essential kinetochore protein. Moreover, Spc105 knockdown has been shown to be feasible in spermatocytes and results in a clear reduction of male fertility when driven by *bam-GAL4-VP16* (Kränzlin, 2008). Expression of *UASt-Spc105^{RNAi}* by *topi-GAL4-VP16-topi* alone had no effect on male fertility. Even the combination of *bam-GAL4-VP16* and *topi-GAL4-VP16-topi* did not result in greater sterility than *bam-GAL4-VP16* alone.

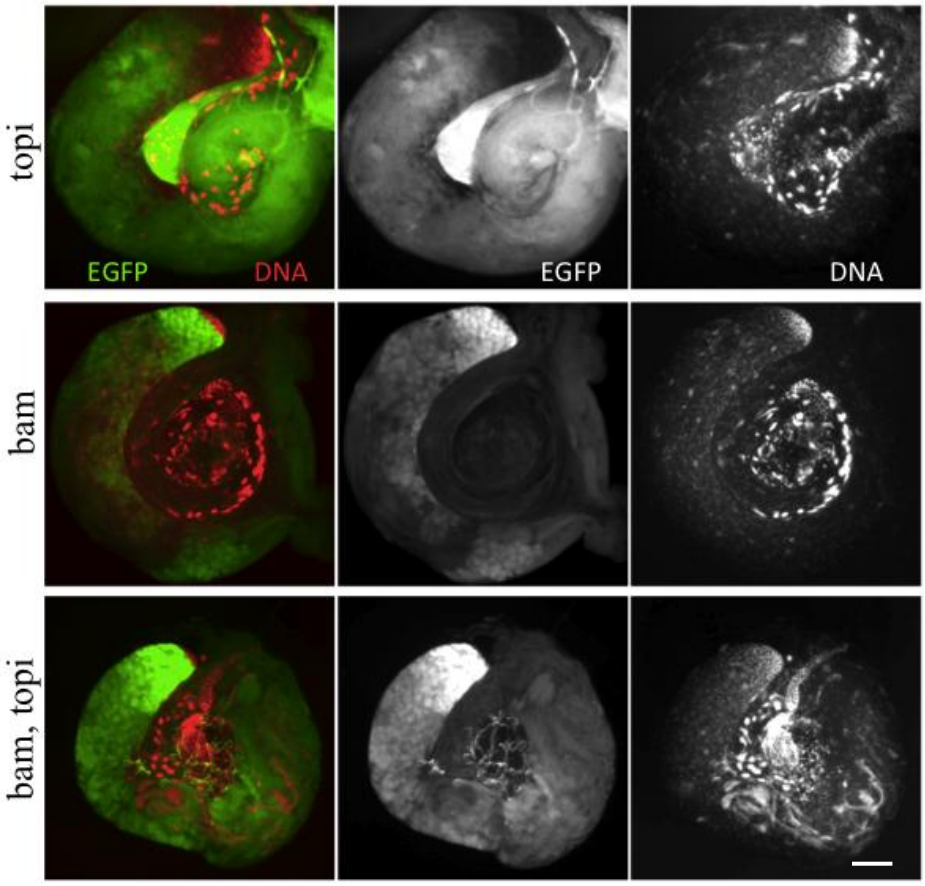

Figure 6. The combination of *bam-GAL4-VP16* and *topi-GAL4-VP16* enhances UASt-GFP expression level.
The uppermost panel shows UASt-2xGFP expression driven by *topi-GAL4-VP16-topi* alone, the middle panel shows UASt-2xGFP expression driven by *bam-GAL4-VP16* alone and the lower panel shows *UASt-2xGFP* expression driven by combination of *bam-GAL4-VP16* and *topi-GAL4-VP16-topi*. Scale bar = 5µm.

The failure of observing a stronger effect with the combination might reflect the fact that *bam-GAL4-VP16* alone already results in complete knock-down. Therefore, *UASt-Cenp-C^{RNAi}* was also used for comparable experiments. In a previous experiment, *bam-GAL4-VP16* in combination with *UASt-Cenp-C^{RNAi}* had resulted in only partial reduction of fertility (Kränzlin, 2008). It is conceivable therefore that stronger *UASt-Cenp-C^{RNAi}* expression might lead to stronger knock-down and accordingly stronger fertility defects. But also in these experiments, the combination of a GAL4 drivers (*bam-GAL4-VP16* and *topi-GAL4-VP16-topi)* was not observed to result in stronger fertility reduction than *bam-GAL4-VP16* alone (Fig. 7b).

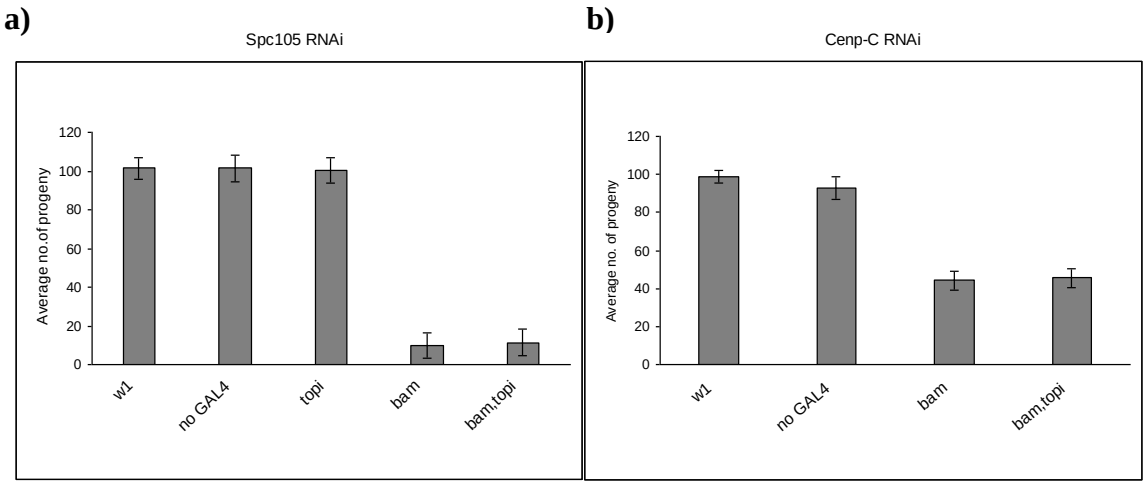

Figure 7. Evaluation of driver lines using male fertility assays.
10 single males (0-3 days old) were crossed to 4 *w¹* virgin females. a) Fertility was measured using *UASt-Spc105^{RNAi}* driven by various GAL4 transgenes. b) Fertility was measured using *UASt-Cenp-C^{RNAi}* driven by various GAL4 transgenes.

For the interpretation of experiments involving the GAL4/UAS system, a precise characterization of the expression pattern of the used GAL4 driver lines is crucial. Therefore, it was analyzed whether *bam-GAL4-VP16* and *topi-GAL4-VP16-topi* are expressed not just in the germline but also in cyst cells. Cyst cells with characteristically flattened nuclei and spermatocytes can be identified based on

DNA staining. For these experiments a *UASt-Cid-EGFP* transgene was used because this led to higher detection sensitivity than with *UASt-2xGFP*, which was

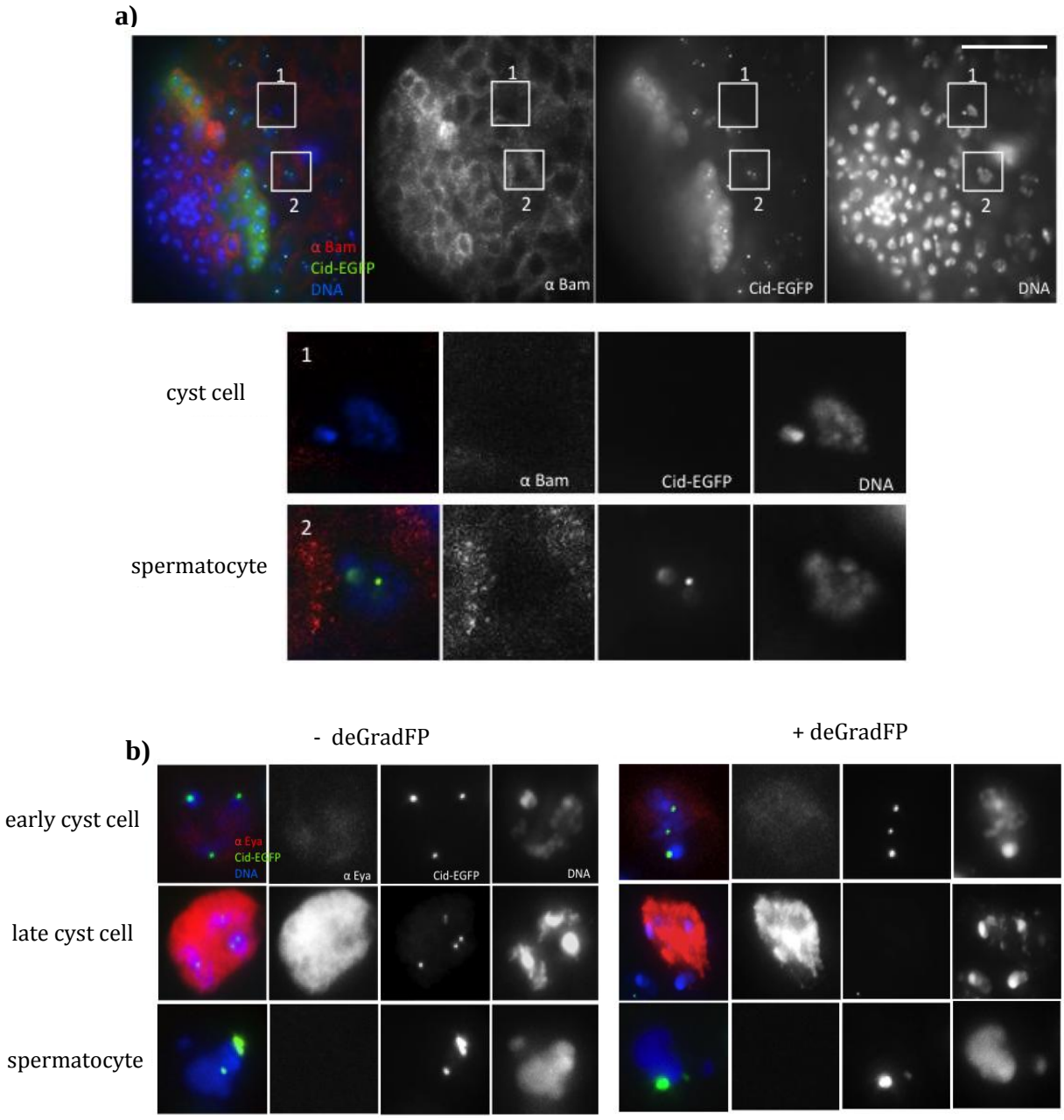

Figure 8. Expression of drivers in cyst cells
a) UAS-Cid-EGFP expression driven by *bam-GAL4-VP16* shows Cid-EGFP signals in the last gonial mitotic division, in early spermatocytes but not in cyst cells. Immunostaining with M α bam antibody shows that Bam expresses in spermatogonial cells and early spermatocytes but not in cyst cells (inset1: cyst cell, inset2: early spermatocyte). b) During spermatogenesis a GFP-specific ubiquitin ligase was either expressed *(+ deGrad cid-EGFP*) or not expressed (- *deGrad cid-EGFP*) by *topi-GAL4-VP16-topi* in males producing only Cid-EGFP instead of normal Cid. Analysis of – and + *deGrad cid-EGFP* reveals the presence of Cid-EGFP signals in (lightly stained Eya-positive) early cyst cells but Cid-EGFP signals are completely abolished in (densely stained Eya-positive) late cyst cells in *+ deGrad cid-EGFP* testis indicating that *topi-GAL4-VP16-topi* drives the expression in these cells. Scale bar = 10μm.

used in the initial experiments. Cid-EGFP is localized to centromeres. The spatial concentration on centromeres makes the resulting dot-like signals readily detectable. In contrast, equal amounts of non-localizing GFP distributed diffusely throughout the cells are far more difficult to detect microscopically. The increased detection sensitivity provided by *UASt-Cid-EGFP* should facilitate an identification of cells where GAL4 drivers are expressed. In combination with *bam-GAL4-VP16,* Cid-EGFP signals could be seen in early spermatocytes but not in somatic cyst cells. These observations are in agreement with published descriptions of *bam* expression (Chen and McKearin, 2003; Insco et al., 2009), which is known to occur in the germline but has never been reported to occur in cyst cells. For further confirmation, double labeling with an antibody against Bam was performed. As shown in (Fig. 8a), anti-Bam staining was clearly present in early spermatocytes but absent in cyst cells. This observation further suggests that *bam-GAL4-VP16* drives expression in spermatocytes but not in cyst cells.

To characterize if *topi-GAL4-VP16-topi* drives expression in cyst cells, a different assay was applied. In these experiments, UASt-NSlmb-vhh-GFP4 (Caussinus et al., 2012) was expressed in a gCid-EGFP background. NSlmb-vhhGFP4 (deGradFP) is a GFP-specific recombinant ubiquitin ligase, which results in a proteasomal degradation of GFP fusion proteins. Testes were immunostained with anti-Eya to identify somatic cyst cells. Eya is an established marker for late cyst cells (Hempel and Oliver, 2007; Papagiannouli and Mechler, 2009). After *topi-GAL4-VP16-topi* driven *UASt-NSlmb-vhh-GFP4* expression in the gCid-EGFP background, Cid-EGFP signals were no longer observed in late spermatocytes and later stages while these stages clearly displayed signals in the gCid-EGFP

background when *topi-GAL4-VP16-topi* or *UASt-NSlmb-vhh-GFP4* were not present. Similarly, early somatic cyst cells (lightly stained with Eya) showed Cid-EGFP on centromeres whereas late somatic cyst cells (densely stained with Eya) were devoid of Cid-EGFP signals on centromeres but only when *topi-GAL4-VP16-topi* and *UASt-NSlmb-vhh-GFP4* were present in the gCid-EGFP background, (Fig. 8b). This suggests that topi-GAL4-VP16 drives expression not only in late spermatocytes but also in late somatic cyst cells.

In summary, the findings obtained in this study might allow a screening for components involved in the spermatogenic processes (including meiosis) at least with a moderate efficiency. Furthermore, to improve this system, a *chiffon* regulatory region might be helpful in driving the expression specifically in early spermatocytes. A recent publication (Bunt et al., 2012) has demonstrated new Gal4 enhancer trap lines for Drosophila spermatocytes. Amongst the various lines, *chif*-Gal4 has been shown to drive the expression of UAS transgene specifically in early spermatocytes along with the somatic cyst cells of the testis. Perhaps, this regulatory region in fusion with testis-TF and GAL4-VP16 variant, along with the combination of above described Gal4 lines might result in a better efficiency in expressing UAS transgenes especially for screening purposes.

Materials & Methods

Drosophila Genetics

Lines with the transgene insertions: *P(w+, attP-βTub85D-GAL4Δ-topi)III, P(w+, attP-gtopi-GAL4Δ-topi)III, P(w+, attP-gtopi-GAL4-FL-topi)III, P(w+ ,attP-gtopi-GAL4-VP16-topi)III, P(w+, attP-gtopi-GAL4-VP16-3'UTR-topi)III* were obtained by PhiC31-mediated germline transformation of *ΦX-86Fb* flies (Bischof et al., 2007) with the constructs described below.

P(w+,UASt-NSlmb-vhh-GFP4) III (Caussinus et al., 2012), *P(w+,bamP-GAL4-VP16)III* (Chen and McKearin, 2003) were kindly provided by E. Caussinus and D. McKearin.

To enhance the expression levels throughout meiosis, the combination of different GAL4 lines was created by meiotic recombination: *P(w+,bamP-GAL4-VP16), P(w+, gtopi-GAL4-VP16-topi)III.*

P(w+, pUASt-2xGFP)III was used for expression analysis experiments of different driver lines. Lines of RNAi, *P(w+, Spc105-RNAi^{GD7306})v44594* and *P(w+, Cenp-C-RNAi^{GD10208})v33790* were provided by the Vienna Drosophila RNAi Center (VDRC).

cid^{T12-1} and *cid^{T22-4}* (Blower et al., 2006) carry premature stop codons. *cid^{G5950}* (Bloomington Drosophila Stock Center #29695) has a P element insertion within the coding sequence. The transgene *P(w+, gcid-EGFP-cid)III.2* (Schuh et al., 2007), has been shown to complement recessive lethal mutations in the corresponding endogenous loci, demonstrating the functionality of the encoded fluorescently tagged centromere.

For DeGrad Cid-EGFP experiments (Fig. 8b), males were generated with the genotype, *w*; cid^{T12-1}/cid^{G5950}, P(w+, gcid-EGFP-cid)II.1; P(w+, UASt-NSlmb-vhhGFP4)III/P(w+, topi-GAL4-VP16-topi)III , P(w+, gcid-EGFP-cid)III.2* by standard crossing schemes. In parallel, males for control experiments were generated with the genotype, *w*; cid^{T12-1}/cid^{G5950}, P(w+, gcid-EGFP-cid)II.1; +/P(w+, topi-GAL4-VP16-topi)III, P(w+, gcid-EGFP-cid)III.2*.

Plasmid Construction

pattB-βTub85D-GAL4Δ-topi

In this construct, the cis-regulatory sequences of the testis-specific gene *βTub85D* control the production of a GAL4Δ-Topi fusion protein.

A topi fragment containing the complete coding region and additional 3' UTR sequences was amplified with NT5 (5´-AGGCGGGTACCATGAAAGTC AAAGTTTCGGG-3´) and NT6 (5´-TAACTCTAGACGCTATCTTGCCGCTTTATTT-3´), which introduced Acc65I and XbaI site respectively. After digestion with Acc65I and XbaI, the PCR fragment was ligated into the two corresponding sites in *pattB* vector (Bischof et al., 2007) and resulting into the cloning intermediate 1: *pattB-topi*. Thereafter, a GAL4Δ fragment was amplified with NT3 (5´-CATGAGCGGCCGCATGAAGCTACTGTCTTCTATC-3´) and NT4 (5´-CATCGG GTACCCTCTTTTTTTGGGTTTGGTG-3´), which introduced NotI and Acc65I site respectively. Ligation of the product and cloning intermediate 1 after digestion with Acc65I and NotI respectively resulted into the cloning intermediate 2: *pattB-GAL4Δ-topi*. Finally, a *βtub85D* fragment containing the cis-regulatory region and 5'UTR sequences was amplified with NT7 (5´-GCCTGCGG CCGCTATCCGTACAGCCAGCTGTG-3´) and NT8 (5´-CAATGCGGCCGCTTTGATAGT AAAGTTAGGGCCC-3´), which introduced Not I site. PCR product and cloning intermediate 2 were digested with NotI and ligated, finally resulting into *pattB-βTub85D-GAL4Δ-topi*

pattB-gtopi-GAL4Δ-topi

In this construct, the cis-regulatory sequences of the spermatocyte-specific gene *topi* control the production of a GAL4Δ-Topi fusion protein.

A topi fragment with an upstream cis-regulatory region and 5'UTR sequences was amplified with NT1 (5´- GCTTGGCGGCCGCCTCGCAGATCGAATGTCTTG-3´) and NT2 (5´- GCTTCGCGGCCGCTTTCATGGCGCTAGTCCG-3´), which introduced NotI sites. Cutting with NotI and thereby ligating of PCR product and cloning intermediate 2 resulted into *pattB-gtopi-GAL4Δ-topi*.

pattB-gtopi-GAL4-FL-topi

In this construct, the cis-regulatory sequences of the spermatocyte-specific gene *topi* control the production of a GAL4-FL-Topi fusion protein.

A GAL4 (FL) fragment was amplified with NT3 (5′-CATGAGCGGCCGCAT GAAGCTACTGTCTTCTATC-3′) and NT4 (5′-CATCGGGTACCCTCTTTTTTTGGGT TTGGTG-3′), which introduced NotI and Acc65I restriction sites. Ligation of the product and cloning intermediate 1 after digestion with Acc65I and NotI respectively resulted into the cloning intermediate 3: *pattB-GAL4FL-topi*. Finally, a topi fragment with an upstream cis-regulatory region and 5'UTR sequences was amplified with NT1 (5′- GCTTGGCGGCCGCCTCGCAGATCGAATGTCTTG-3′) and NT2 (5′- GCTTCGCGGCCGCTTTCATGGCGCTAGTCCG-3′), which introduced NotI sites. Cutting with NotI and thereby ligating of PCR product and cloning intermediate 3 resulted into *pattB-gtopi-GAL4FL-topi*.

pattB-gtopi-GAL4-VP16-topi

In this construct, the cis-regulatory sequences of the spermatocyte-specific gene *topi* control the production of a GAL4-VP16-Topi fusion protein.

A topi fragment with upstream cis-regulatory region and 5'UTR sequences was amplified with NT15 (5′-CTTGGGATCCCTCGCAGATCGAATGTCTTG-3′) and NT16 (5′-CTTC AGATCTTTTCATGGCGCTAGTCCGAT-3′), which introduced BglII and BamHI site respectively. Ligation of the product and pattB vector (Bischof et al., 2007) after digestion with BglII and BamHI respectively resulted into the cloning intermediate 4: *pattB-gtopi*. Thereafter a GAL4-VP16 fragment was amplified using a template *bamP-GAL4-VP16* plasmid (kindly provided by D. McKearin) with NT17 (5′-CGACCAGATCT ATGAAGCTACTGTCTTCTATCG-3′) and NT19 (5′-GTTTAGCGGCCGCCCCACCGTACTCGTCAATTC-3′), which introduced BglII and NotI restriction sites respectively. Ligation of the PCR product and cloning intermediate 4 after digestion with Acc65I and NotI respectively resulted into the cloning intermediate 5: *pattB-gtopi-GAL4-VP16*. Finally, a topi fragment containing the complete coding region and additional 3' UTR sequences was amplified with NT20 (5′-AAGAGGCGGCCGCGATGAAAGTCAAAGTTTCGGG-3′) and NT21 (5′-AATTCGCGGCCGCCGCTATCTTGCCGCTTTATTT-3′), which introduced

NotI site. Cutting with NotI and thereby ligating of PCR product and cloning intermediate 5 resulted into *pattB-gtopi-GAL4VP16-topi*.

pattB-gtopi-GAL4-VP16-3'UTR topi

In this construct, the cis-regulatory sequences of the spermatocyte-specific gene *topi)* control the production of a Gal4-VP16 protein.

A Gal4VP16 fragment was amplified using a template bamP-GAL4-VP16 plasmid (kindly provided by D. McKearin) with NT17 (5´-CGACCAGATCTATGAAGCTACTG TCTTCTATCG-3´) and NT18 (5´- GTTTAGCGGCCGCCTACCCACCGTACTCGTCA-3´), which introduced BglII and NotI restriction sites respectively and a stop codon. Ligation of the PCR product and cloning intermediate 4 after digestion with Acc65I and NotI respectively resulted into the cloning intermediate 6: *pattB-gtopi-Gal4-VP16(Soufir et al.)*. PCR1 was performed to amplify 3'UTR sequence of topi with NT34 (5´-ACGAGTACGGTGGGTAGAAATCATATTCAAATTCGAAT -3´) and pattB-Rev (5´- ATGGACCAGATGGGTGAGG -3´) by using *pattB-topi-Gal4-VP16-topi* plasmid as a template. PCR2 was performed to amplify GAL4-VP16 using OZH-89 (5´- TTCAGTTGATTCTCAGGTCATTT-3´) in combination with NT35 (5´-TTCGAATTTGAATATGATTTCTACCCACCGTACTCGT-3´) using cloning intermediate 6 as a template. PCR3 was performed by using PCR1 and PCR2 mixture as a template, using OZH-89 (5´- TTCAGTTGATTCTCAGGTCATTT-3´) and pattB-Rev. (5´- ATGGACCAGATGGGTGAGG -3´) primers. Ligation of the PCR product and cloning intermediate 6 after digestion with BglII and NotI respectively resulted into *pattB-gtopi-Gal4-VP16-3'UTR topi*.

pUASt-Cid-EGFP

Construct for ectopic expression of Cid with internal EGFP tag by UAS/Gal4 system.

pUASt construct containing coding region of cid with an internal EGFP insertion. This region was amplified with NT41 and NT42 (template: *pCaSpeR4-gCGC)*, digested with *Not* I / *Xba* I and inserted into MCS of *pUASt* vector digested with *Not* I / *Xba* I.

A coding sequence of Cid with an internal EGFP insertion was amplified by using *pCaSpeR4-gcid-EGFP-cid* (Schuh 2007) as a template in combination with the primers NT41 (5´-CTTTAA GCGGCCGC TTAAGCAAATACCGAAAATTTG-3´) and NT42 (5´-GCAAATCTAGAAACTAAGCCTAAACTTCTCTTTTGG-3´), which introduced NotI and XbaI restriction sites respectively. Ligation of the PCR product and pUASt vector after digestion with BglII and NotI respectively resulted into *pUASt-Cid-EGFP*.

Whole mount testis preparation

Flies were anesthetized and dissected under the binocular with two forceps in a testis buffer (183 mM KCl, 47 mM NaCl, 10 mM Tris-HCl, pH 6.8). Testes were isolated by cutting posterior to the seminal vesicle with a hypodermic needle (Terumo Neolus 27G, 0.4x20 mm). Testes were then separated from the accessory glands. 5-10 flies were dissected in a droplet of testis buffer and testes were then transferred to a droplet of 4% paraformaldehyde (in phosphate buffered saline (PBS) on a depression slide for fixation. After 10 min of fixation at room temperature, the fixative was carefully removed with a syringe under the binocular. A droplet of Hoechst staining solution (1 µg/ml Hoechst 33258 in 1x PBS) was added for 10 min (covered from light). The staining solution was then removed with a syringe and testes were washed in a droplet of PBS. Testes were finally transferred into a droplet of mounting media (Vectashield H-1000, Vector Laboratories, Inc.) on a new slide and carefully (to avoid strong squashing of the testes) covered with a coverslip.

Squashed Testis Preparation

Testis squash preparations were made, fixed and stained essentially as described (Gunsalus and Goldberg, 1995) with the following modifications. After dissection in testis buffer (183 mM KCl, 47 mM NaCl, 10 mM Tris-HCl, pH 6.8), testes were transferred to a 5 µl drop of phosphate buffered saline (PBS) on a poly-L-lysine-treated slide and cut open to spill the contents. The sample was squashed very gently after addition of 15 µl of 4% formaldehyde in PBS under a 22 x 22 mm siliconized cover slip. Fixation was continued for 6 minutes.

For immunolabeling, hybridoma supernatant containing mouse monoclonal antibody eya10H6 (eyes absent) and bam (bag of marbles) were kindly provided by the Developmental Studies Hybridoma Bank developed under the auspices of the NICHD and maintained by The University of Iowa, Department of Biology, Iowa City, IA 52242 was diluted 1:100 and 1:10, respectively. Secondary antibody was Alexa568-conjugated goat antibody against mouse IgG.

Fertility tests

Ten single males were crossed with 4 w^1 virgin females. After one day the flies were transferred to a new vial. The first vial was discarded. The flies were transferred from vial (2) to vial (3) after 3 days. The average number of F1 progeny of vial (2) was counted at 8^{th} day after hatching of progenies.

References

Arya, G.H., Lodico, M.J., Ahmad, O.I., Amin, R., and Tomkiel, J.E. (2006). Molecular characterization of teflon, a gene required for meiotic autosome segregation in male Drosophila melanogaster. Genetics *174*, 125-134.

Baker, C.C., and Fuller, M.T. (2007). Translational control of meiotic cell cycle progression and spermatid differentiation in male germ cells by a novel eIF4G homolog. Development *134*, 2863-2869.

Bischof, J., Maeda, R.K., Hediger, M., Karch, F., and Basler, K. (2007). An optimized transgenesis system for Drosophila using germ-line-specific phiC31 integrases. Proc Natl Acad Sci U S A *104*, 3312-3317.

Blower, M.D., Daigle, T., Kaufman, T., and Karpen, G.H. (2006). Drosophila CENP-A mutations cause a BubR1-dependent early mitotic delay without normal localization of kinetochore components. PLoS Genet *2*, e110.

Brand, A.H., and Perrimon, N. (1993). Targeted gene expression as a means of altering cell fates and generating dominant phenotypes. Development *118*, 401-415.

Bunt, S.M., Monk, A.C., Siddall, N.A., Johnston, N.L., and Hime, G.R. (2012). GAL4 enhancer traps that can be used to drive gene expression in developing Drosophila spermatocytes. Genesis.

Caussinus, E., Kanca, O., and Affolter, M. (2012). Fluorescent fusion protein knockout mediated by anti-GFP nanobody. Nature structural & molecular biology *19*, 117-121.

Chen, D., and McKearin, D.M. (2003). A discrete transcriptional silencer in the bam gene determines asymmetric division of the Drosophila germline stem cell. Development *130*, 1159-1170.

Chen, X., Hiller, M., Sancak, Y., and Fuller, M.T. (2005). Tissue-specific TAFs counteract Polycomb to turn on terminal differentiation. Science *310*, 869-872.

Franklin-Dumont, T.M., Chatterjee, C., Wasserman, S.A., and Dinardo, S. (2007). A novel eIF4G homolog, Off-schedule, couples translational control to meiosis and differentiation in Drosophila spermatocytes. Development *134*, 2851-2861.

Gunsalus, K., and Goldberg, M. (1995). Drosophila cofilin is required during embryogenesis and oogenesis. Mol Biol Cell *6*, 135.

Hempel, L.U., and Oliver, B. (2007). Sex-specific DoublesexM expression in subsets of Drosophila somatic gonad cells. BMC developmental biology *7*, 113.

Hiller, M.A., Lin, T.Y., Wood, C., and Fuller, M.T. (2001). Developmental regulation of transcription by a tissue-specific TAF homolog. Genes Dev *15*, 1021-1030.

Hrdlicka, L., Gibson, M., Kiger, A., Micchelli, C., Schober, M., Schock, F., and Perrimon, N. (2002). Analysis of twenty-four Gal4 lines in Drosophila melanogaster. Genesis *34*, 51-57.

Insco, M.L., Leon, A., Tam, C.H., McKearin, D.M., and Fuller, M.T. (2009). Accumulation of a differentiation regulator specifies transit amplifying division number in an adult stem cell lineage. Proc Natl Acad Sci U S A *106*, 22311-22316.

Jiang, J., Benson, E., Bausek, N., Doggett, K., and White-Cooper, H. (2007). Tombola, a tesmin/TSO1-family protein, regulates transcriptional activation in the Drosophila male germline and physically interacts with always early. Development *134*, 1549-1559.

Kränzlin, M. (2008). Analysis of Kinetochore Proteins during Drosophila Male Meiosis. In Institute of Zoology (Zurich, University of Zurich).

Ma, J., and Ptashne, M. (1987). Deletion analysis of GAL4 defines two transcriptional activating segments. Cell *48*, 847-853.

Michiels, F., Gasch, A., Kaltschmidt, B., and Renkawitz-Pohl, R. (1989). A 14 bp promoter element directs the testis specificity of the Drosophila beta 2 tubulin gene. EMBO J *8*, 1559-1565.

Noguchi, T., and Miller, K.G. (2003). A role for actin dynamics in individualization during spermatogenesis in Drosophila melanogaster. Development *130*, 1805-1816.

Papagiannouli, F., and Mechler, B.M. (2009). discs large regulates somatic cyst cell survival and expansion in Drosophila testis. Cell research *19*, 1139-1149.

Rorth, P. (1998). Gal4 in the Drosophila female germline. Mech Dev *78*, 113-118.

Sadowski, I., Ma, J., Triezenberg, S., and Ptashne, M. (1988). Gal4-Vp16 Is an Unusually Potent Transcriptional Activator. Nature *335*, 563-564.

Schuh, M., Lehner, C.F., and Heidmann, S. (2007). Incorporation of Drosophila CID/CENP-A and CENP-C into centromeres during early embryonic anaphase. Curr Biol *17*, 237-243.

Soufir, N., Avril, M.F., Chompret, A., Demenais, F., Bombled, J., Spatz, A., Stoppa-Lyonnet, D., Benard, J., and Bressac-de Paillerets, B. (1998). Prevalence of p16 and CDK4 germline mutations in 48 melanoma-prone families in France. The French Familial Melanoma Study Group [published erratum appears in Hum Mol Genet 1998 May;7(5):941]. Hum Mol Genet *7*, 209-216.

Thummel, C.S., and Pirrotta, V. (1992). Technical Notes: New pCaSpeR P-element vectors. DIS *71*, 150.

Viktorinova, I., and Wimmer, E.A. (2007). Comparative analysis of binary expression systems for directed gene expression in transgenic insects. Insect Biochem Mol Biol *37*, 246-254.

White-Cooper, H. (2012). Tissue, cell type and stage-specific ectopic gene expression and RNAi induction in the Drosophila testis. Spermatogenesis *2*, 11-22.

Wright, K.J., Marr, M.T., 2nd, and Tjian, R. (2006). TAF4 nucleates a core subcomplex of TFIID and mediates activated transcription from a TATA-less promoter. Proceedings of the National Academy of Sciences of the United States of America *103*, 12347-12352.

Chapter 2

Transgenerational propagation and quantitative maintenance of paternal centromeres depends on Cid/Cenp-A presence in Drosophila sperm

Nitika Raychaudhuri, Raphaelle Dubruille, Guillermo A. Orsi, Homayoun C.

Bagheri, Benjamin Loppin, Christian F. Lehner

Plos Biology (2012) *in press*

Description of contributions

All the experimental work has been carried out by me except for the the analysis of centromere proteins in the first cycles of Drosophila embryogenesis (Figure 2 and Figure 5). These have been performed by our collaborators Raphaelle Dubruille, Guillermo A. Orsi and Benjamin Loppin. Moreover, the supporting text describing mathematical model for sex-specific differences of Cid loading on autosomes has been provided by Homayoun C. Bagheri. The manuscript has been written by Christian F. Lehner, who has also led the study, with contributions of the other authors and me.

Transgenerational propagation and quantitative maintenance of paternal centromeres depends on Cid/Cenp-A presence in Drosophila sperm

Nitika Raychaudhuri[1)], Raphaelle Dubruille[2)], Guillermo A. Orsi[2)+)], Homayoun C. Bagheri[3)], Benjamin Loppin[2)], Christian F. Lehner[1,*)]

1) Institute of Molecular Life Siences (IMLS), University of Zurich, Zurich, Switzerland

2) Centre de Génétique et de Physiologie Moléculaire et Cellulaire, Université Claude Bernard Lyon I, Villeurbanne, France

3) Institute of Evolutionary Biology and Environmental Studies (IEES), University of Zurich, Zurich, Switzerland

*) E-mail: christian.lehner@imls.uzh.ch

+) Current address: Department of Biological Chemistry and Molecular Pharmacology, Harvard Medical School, Boston, Massachusetts, United States of America

Running title: Transgenerational role of Cid/Cenp-A in sperm

Abstract

In *Drosophila melanogaster*, as in many animal and plant species, centromere identity is specified epigenetically. In proliferating cells, a centromere-specific histone H3 variant (CenH3), named Cid in Drosophila and Cenp-A in humans, is a crucial component of the epigenetic centromere mark. Hence, maintenance of the amount and chromosomal location of CenH3 during mitotic proliferation is important. Interestingly, CenH3 may have different roles during meiosis and the onset of embryogenesis. In gametes of *Caenorhabditis elegans,* and possibly in plants, centromere marking is independent of CenH3. Moreover, male gamete differentiation in animals often includes global nucleosome for protamine exchange that potentially could remove CenH3 nucleosomes. Here we demonstrate that the control of Cid loading during male meiosis is distinct from the regulation observed during the mitotic cycles of early embryogenesis. But Cid is present in mature sperm. After strong Cid depletion in sperm, paternal centromeres fail to integrate into the gonomeric spindle of the first mitosis, resulting in gynogenetic haploid embryos. Furthermore, after moderate depletion, paternal centromeres are unable to re-acquire normal Cid levels in the next generation. We conclude that Cid in sperm is an essential component of the epigenetic centromere mark on paternal chromosomes and it exerts quantitative control over centromeric Cid levels throughout development. Hence, the amount of Cid that is loaded during each cell cycle appears to be determined primarily by the pre-existing centromeric Cid, with little flexibility for compensation of accidental losses.

Introduction

Many eukaryotes, like humans and Drosophila, have chromosomes with a single regional centromere. Faithful propagation of this centromere during chromosome replication and cell proliferation is crucial. Loss of centromere function or extra centromeres cause aneuploidy. Therefore, the molecular mechanisms that control centromere replication have attracted considerable attention recently (for reviews see (Allshire and Karpen, 2008; Black and Cleveland, 2011b; Boyarchuk et al., 2011; Burrack and Berman, 2012b)). Importantly, these analyses have indicated that centromere identity in regional centromeres is specified epigenetically. Centromere-specific histone H3 variants (CenH3s) are thought to be an essential component of the corresponding epigenetic mark. In humans and Drosophila, the CenH3s have been named CENP-A and Centromere identifier (Cid) (FlyBase accession number FBgn0040477), respectively (Henikoff et al., 2000; Sullivan et al., 1994). Nucleosomes with these CenH3s instead of other histone H3 variants are stably incorporated exclusively within the centromeric region of the chromosome during unperturbed cell cycle progression. The precise structural details of these special centromeric nucleosomes may vary in different cell cycle phases and organisms (reviewed in (Black and Cleveland, 2011b)). Based on the analysis of stretched chromatin fibres, blocks of chromatin containing CenH3 alternate with blocks that lack it (Blower et al., 2002). The molecular mechanisms that control the number and size of these blocks and the centromere region overall are not understood. While the gradual depletion of CenH3 does not appear to have immediate effects (Liu et al., 2006), an enforced acute increase in centromeric Cid has been shown to result in severe chromosome missegregation during mitosis (Schittenhelm et al., 2010a).

A conceptually simple mechanism that might maintain the centromere during cell proliferation is “template-governed”. After random distribution of centromeric CenH3

nucleosomes during chromosome replication onto the two sister chromatids, these old nucleosomes may act as a template, allowing the local stoichiometric loading of new CenH3 nucleosomes during each cell cycle. Such a mechanism for maintenance of centromere position and size would lack flexibility for correction of occasional errors. In contrast, "homeostatic" mechanisms controlling the loading of new CenH3s to a target level that is set independently from the actual amount that is already present at the centromere would allow for correction of accidental fluctuations. Elegant experiments in Drosophila have provided clear evidence for template-governed CenH3 loading. Cid-GFP-LacI targeting to lac operator arrays was shown to recruit endogenous Cid that appeared to be maintained independently of Cid-GFP-LacI at least to some extent (Mendiburo et al., 2011). On the other hand, recent findings from *C. elegans* and plants have indicated that centromere maintenance during meiosis and onset of embryogenesis can be mechanistically distinct. Cenp-A nucleosomes are transiently eliminated from chromosomes in the *C. elegans* germline and not required for subsequent Cenp-A incorporation in non-transcribed regions throughout the holocentric chromosomes (Gassmann et al.; Monen et al., 2005). Although this independence on pre-existing Cenp-A in *C. elegans* might represent a derived state resulting from the evolution of the holocentric chromosomes, a similar transient absence of centromeric CenH3 has also been described in egg cells of *A. thaliana* (Ingouff et al., 2010) which has regional centromeres. In addition, de novo formation of centromeres can occasionally occur in humans and various experimental systems (Folco et al., 2008; Harrington et al., 1997; Ishii et al., 2008; Ketel et al., 2009; Marshall et al., 2008; Mejia et al., 2002; Nakashima et al., 2005). These findings emphasize that in animals, the uncharacterized role of CenH3 in regional centromeres during meiosis and fertilization might not necessarily be the same as during mitotic cell proliferation, where it is both required and

sufficient according to the evidence obtained in case of Cid (Blower et al., 2006; Blower and Karpen, 2001; Blower et al., 2002; Heun et al., 2006; Mendiburo et al., 2011).

To address significance, composition and transgenerational maintenance of epigenetic centromere marking during sexual reproduction in *D. melanogaster*, we analyzed Cid behavior during spermatogenesis and early embryogenesis. Drosophila spermatogenesis begins at the closed apical end of the testis tube (Figure 1a) (Cenci et al., 1994; Fuller, 1993). Germline stem cells located there divide asymmetrically. The resulting differentiating daughter cell, the gonioblast, progresses through four mitotic cell cycles with incomplete cytokinesis, and thereby generates a cyst with 16 interconnected spermatocytes. Premeiotic S phase is completed very soon after the last of these four mitotic divisions. Thereafter extensive spermatocyte growth occurs during an extended meiotic G2 phase before progression through the first and second meiotic division. The haploid cell nucleus of postmeiotic spermatids, which remain interconnected within each cyst, is extensively remodeled. Nucleosomes are massively replaced with sperm-specific proteins such as protamines and the genetic material is highly compacted (200-fold) into a needle-shaped sperm head (Jayaramaiah Raja and Renkawitz-Pohl, 2005). After complete elongation of the sperm tails, mature sperm is individualized and released in a motile form into the seminal vesicle at the distal end of the testis tube. After fertilization, the sperm nucleus is once more extensively remodeled (Bonnefoy et al., 2007; Loppin et al., 2005). Protamines are rapidly replaced with nucleosomes concomitant with transformation into a round male pronucleus. Thereafter progression through the first S phase occurs. In parallel, female meiosis is completed. After S phase and pronuclear migration, the female pronucleus and the closely apposed male pronucleus enter into the first mitosis by forming a gonomeric spindle (Callaini and Riparbelli, 1996). The reformation of daughter nuclei in telophase combines the two

parental genomes within the first two daughter nuclei. Subsequent progression through the rapid and synchronous cleavage cycles generates a syncytium because cytokinesis is omitted during early Drosophila embryogenesis. After cellularization of the syncytial blastoderm nuclei at the onset of gastrulation, additional cell proliferation involves progression through cell cycles including cytokinesis.

Here we show that Cid survives the radical nucleosome replacement process that accompanies spermatogenesis. Centromeric Cid in sperm also perdures during formation of the male pronucleus after fertilization. Finally, analyses after experimental changes of centromeric Cid levels in sperm demonstrate its crucial role in centromere specification and quantitative maintenance.

Results

Paternal Cid but not Cenp-C is inherited with paternal centromeres

In case of epigenetic specification of centromere identity, all essential components of the corresponding mark have to be preserved when the bulk of nucleosomes are replaced with protamines during postmeiotic spermatid differentiation. Otherwise paternal chromosomes could not be propagated after fertilization. Cid, the Drosophila CenH3, which is essential for centromere maintenance during mitotic proliferation (Blower et al., 2006; Blower and Karpen, 2001), was therefore expected to be present in mature sperm if Cid is also crucial for transgenerational centromere maintenance. In earlier attempts Cid was not detected in sperm, but technical problems with antigen accessibility during immunolabeling were suspected (Loppin et al., 2001). To avoid such problems, we analyzed testis from transgenic *cid* mutant males that expressed functional Cid-EGFP under control of the normal *cid* cis-regulatory region instead of endogenous Cid. Specific dot-like EGFP signals were clearly observed in mature *cid; cid-EGFP* sperm (Figure 1b,c), indicating that Cid is indeed present in sperm. While centromeres are strongly clustered close to the chromocenter in most somatic Drosophila interphase cells, Cid-EGFP dots were found to be predominantly unclustered in mature sperm (46%, 42% and 12% with 4, 3 and 2 signals, respectively; n = 24).

In contrast to Cid-EGFP, we were unable to detect Cenp-C-EGFP in mature sperm (Figure 1b,d). During earlier stages, Cenp-C-EGFP was readily detectable (Figure 1b,d). For comparison of Cid and Cenp-C changes during spermatogenesis, centromeric EGFP signal intensities observed in S4-6 spermatocytes were set to 1 arbitrary unit in Figure 1c and d. During the S4-6 stages, however, centromeric Cenp-C-EGFP signals were at least as strong as those observed for Cid-EGFP (data not shown). Our failure to detect Cenp-C-EGFP in mature sperm is therefore not simply a result of limited detection

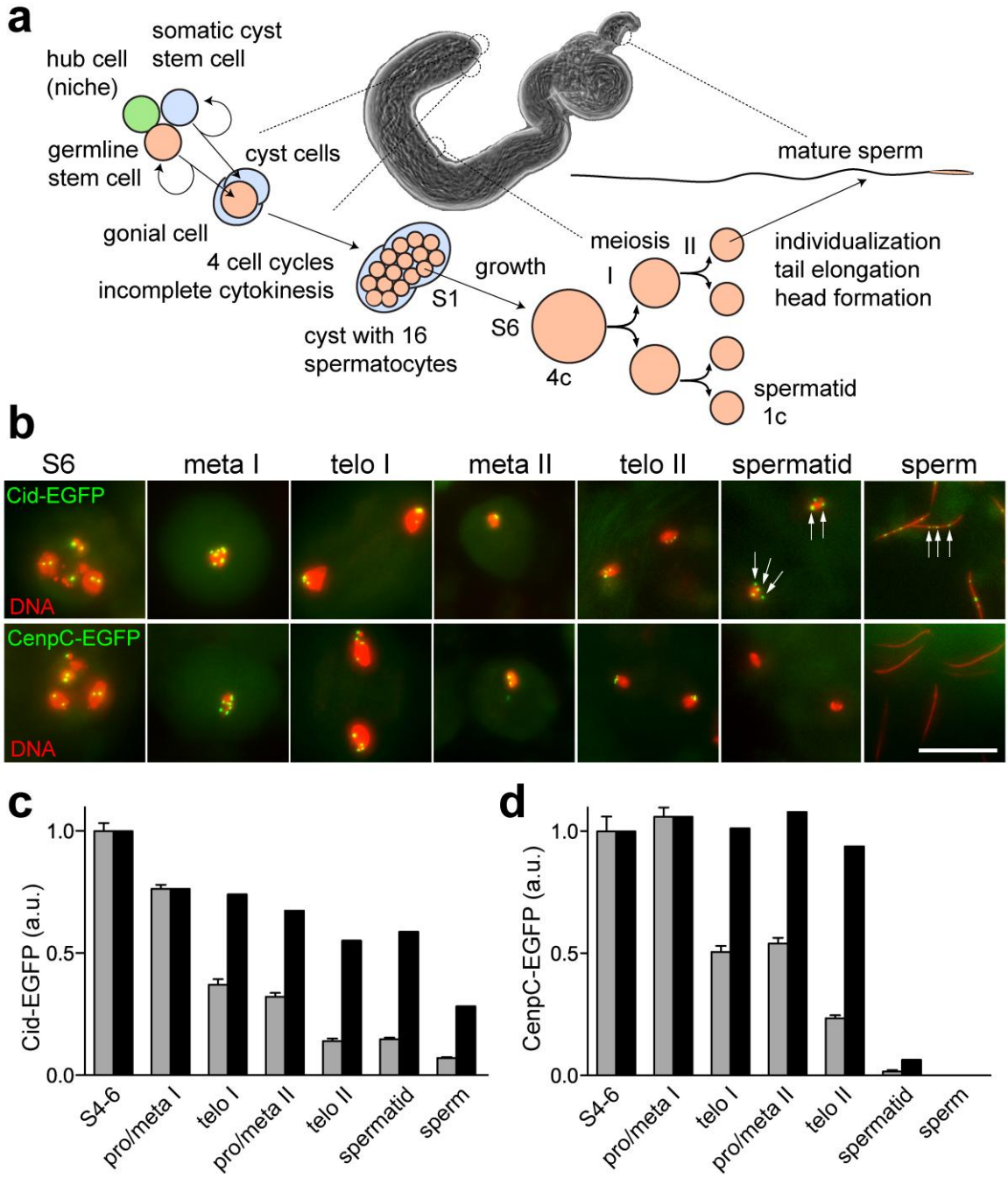

Figure 1. Centromere protein levels during Drosophila spermatogenesis. (a) Schematic overview of spermatogenesis (see also (Fuller, 1993)). Spermatocyte stages S1 to S6, as well as the meiotic stages have been described in detail by (Cenci et al., 1994) (b) Regions from DNA-stained squash preparations of testes expressing either only Cid-EGFP (upper row) or only Cenp-C-EGFP (lower row) instead of endogenous Cid and Cenp-C, respectively, illustrate the stages where EGFP signal intensities were quantified (see panel c and d). White arrows indicate Cid-EGFP signals in postmeiotic stages which lack Cenp-C-EGFP signals. Scale bar = 10 µm. (c and d) Total Cid-EGFP (c) and Cenp-C (d) signal intensity per

cell was determined, except for telophase I and II where each daughter nucleus was analyzed separately. Grey bars represent average intensity in arbitrary units (a.u.) with whiskers indicating s.d. after normalization to the spermatocyte S4-6 value. Black bars indicate centromere protein level per genome equivalent after correction of grey bars according to genome ploidy. Progression through male meiosis is not accompanied by net loading of Cid- and Cenp-C-EGFP onto centromeres, in contrast to mitosis during the syncytial blastoderm (Schuh et al., 2007). n = > 20 cells

sensitivity. We conclude that centromeric Cenp-C (FlyBase accession number FBgn0086697) is eliminated during sperm head formation. It is either absent or very low in mature sperm. Another centromere protein described in Drosophila apart from Cid and Cenp-C is Cal1 (FlyBase accession number FBgn0038478) (Goshima et al., 2007). Cal1-EGFP could also not be detected in sperm (see below). Therefore, Cenp-C and Cal1 do not appear to be essential components of the suspected epigenetic centromere mark.

To analyse the fate of paternal Cid protein after fertilization, *cid; cid-EGFP* males were crossed with wild-type females, followed by analyses during the initial cleavage cycles in the resulting embryos. Cid-EGFP signals in up to four discrete spots were readily detected during male pronucleus formation (Figure 2a-c). At metaphase of the first mitosis, Cid-EGFP was present on four pairs of sister centromeres in one of the two chromosome sets within the gonomeric metaphase plate (Figure 2d). Cid-EGFP signals in essentially all of the analyzed paternal pronuclei (11 out of 12) were also observed when males hemizygous for the *cid-EGFP* transgene were crossed to wild-type females. If Cid-EGFP signals in paternal pronuclei, however, were to reflect zygotic expression of the paternally inherited transgene after fertilization, at most 50% of the progeny of hemizygous fathers would be expected to display Cid-EGFP at paternal centromeres. We conclude that the Cid protein of mature sperm remains associated with paternal

centromeres during chromatin remodeling and male pronucleus formation, followed by equal distribution onto sister centromeres during the first S phase. During metaphase of mitosis 2, centromeric Cid-EGFP was still detectable but again on only one half of the chromosomes and with reduced intensity (data not shown). During mitosis 3, paternal Cid-EGFP was no longer detectable (Figure 2e). Progression through the cleavage stages therefore appears to be accompanied by dilution of the inherited paternal Cid-EGFP during each cell cycle by newly recruited unlabeled Cid from maternally provided stores. In contrast to Cid, but as expected from the absence of Cenp-C in mature sperm described above, we did not detect EGFP signals in early embryos after crossing *Cenp-C-EGFP, Cenp-C* males with wild-type females (Figure 2f).

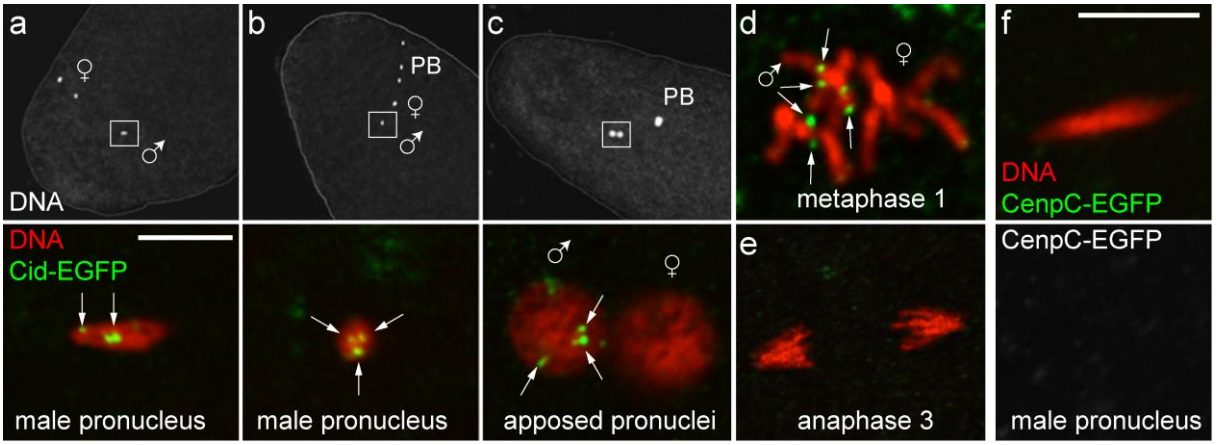

Figure 2. Transmission of paternal Cid to progeny. (a-e) eggs were collected from females without Cid-EGFP after mating with males with Cid-EGFP. Top panels (a-c) display DNA staining (DNA) at low magnification and white frames indicate the regions shown at high magnification in the bottom panels. Paternal Cid-EGFP is detected in maximally 4 spots (white arrows) in the decondensing male pronucleus during (a) and after (b) completion of female meiosis, as well as after pronuclear migration (c). 67 of 69 male pronuclei analyzed in 3 independent experiments were positive for Cid-EGFP. In the gonomeric metaphase plate of the first embryonic mitosis (d), Cid-EGFP is detected on sister centromeres of paternal but not maternal chromosomes. Cid-EGFP is no longer detectable during mitosis 3 (e). (f) In contrast to Cid-EGFP, paternal Cenp-C-EGFP is not transmitted to progeny. It cannot be detected in the decondensing male pronucleus in eggs collected from females without Cenp-C-EGFP after mating with males with Cenp-

C-EGFP. None of the analyzed male pronuclei (n = 10) and metaphase 1 figures (n = 3) displayed detectable GFP dots. PB: polar bodies. Scale bar = 10 μm.

Sperm centromere Cid is required for maintenance of paternal chromosomes after fertilization

To evaluate the functional significance of paternal Cid inherited with sperm, we applied deGradFP (Caussinus et al., 2011) for Cid protein depletion during spermatogenesis. In deGradFP, depletion of GFP fusion proteins is achieved by expression of a GFP-specific recombinant ubiquitin ligase (NSlmb-vhhGFP4) with the UAS/GAL4 system. For expression of this ubiquitin ligase specifically in late spermatocytes, we generated a *topi-GAL4-VP16* driver. Using this driver for deGradFP in *cid; cid-EGFP* males, we were able to obtain sperm in which EGFP signals were no longer above background (Figure 3a). We assume that some centromeric Cid was still present at least during the preceding meiotic divisions, as these were clearly successful. The resulting Cid-depleted sperm allowed successful fertilization, as evidenced by analyses of embryos collected from crosses of deGradFP *cid; cid-EGFP* males with control females. Around 90% of progeny developed to the syncytial blastoderm stage, when thousands of nuclei are regularly arranged just below the egg cell membrane. As fertilization is required for the initiation of embryonic development in *D. melanogaster*, we conclude that fertilization with sperm is still possible after Cid elimination.

However, careful cytological analyses of embryos derived from deGradFP *cid; cid-EGFP* fathers indicated that development after fertilization is not normal. When in control experiments *cid; cid-EGFP* males without deGradFP were crossed to *cid; cid-EGFP* females, we observed normal progeny development with centromeric Cid-EGFP signals in both chromosome sets within all of the analyzed gonomeric metaphase plates of mitosis 1 (Figure 3a; n = 10), as expected. However, when deGradFP was active in the

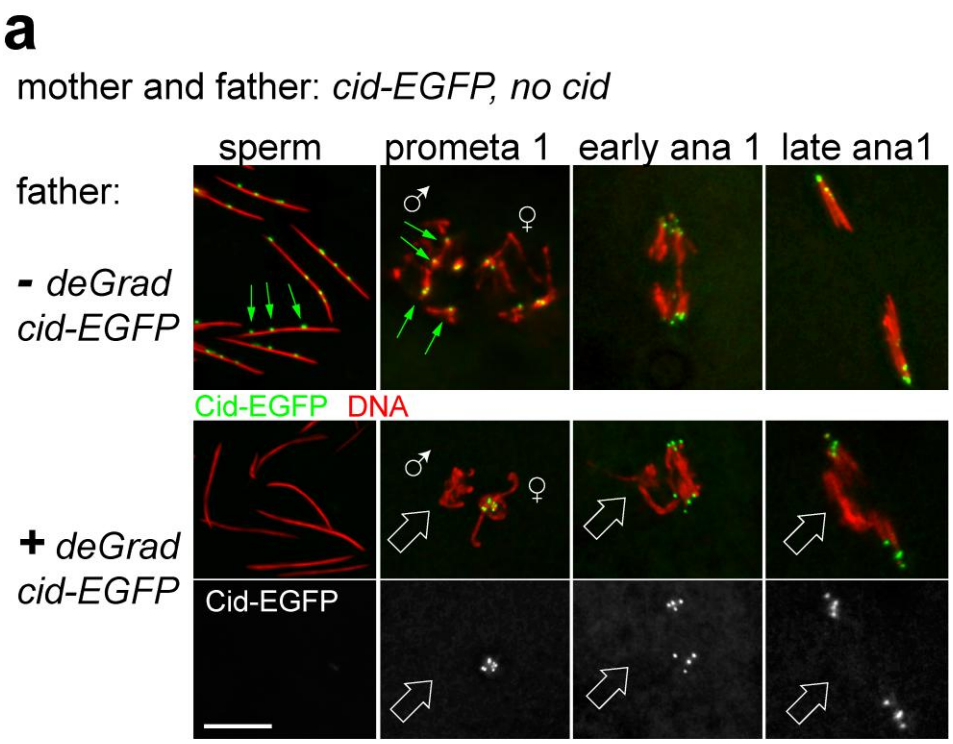

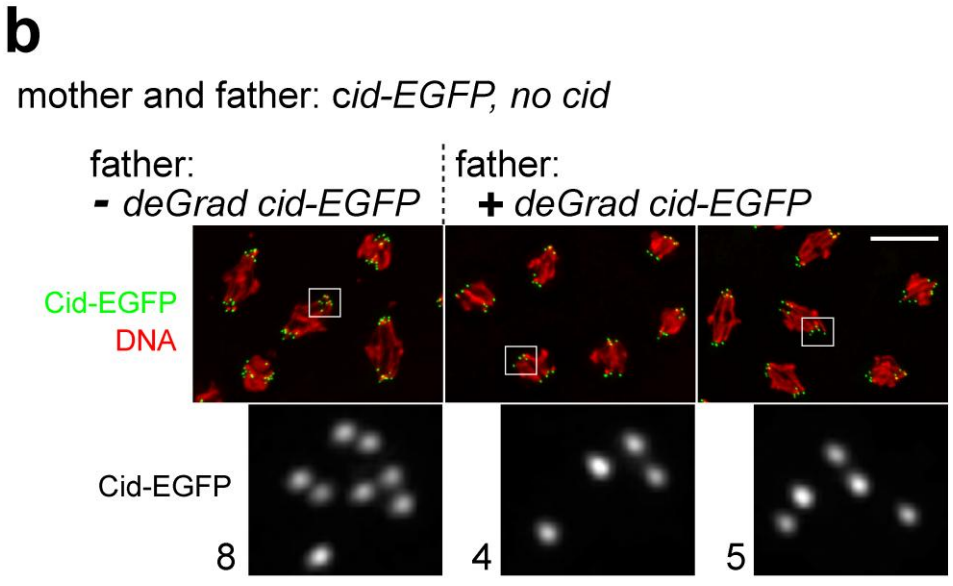

	number of embryos with: 8	4	4/5	5 Cid-EGFP spots
- *deGrad cid-EGFP*	20	0	0	0
+ *deGrad cid-EGFP*	0	80	4	2

Figure 3. Cid in sperm is required for propagation of paternal chromosomes in progeny. During spermatogenesis a GFP-specific ubiquitin ligase (Caussinus et al., 2011) was either expressed (*+ deGrad cid-EGFP*) or not expressed (*- deGrad cid-EGFP*) in males producing only Cid-EGFP instead of normal Cid. (a) Analysis of their sperm and of early embryos obtained after mating the males with Cid-EGFP females

revealed that GFP ubiquitin ligase expression resulted in effective Cid-EGFP depletion in sperm, inhibited maternal Cid-EGFP recruitment onto paternal centromeres and abolished paternal centromere function during embryonic cycle 1. Centromeric Cid-EGFP signals detectable in – but not + *deGrad cid-EGFP* samples are indicated by green arrows. Chromosomes without Cid-EGFP signals that were not segregated to the poles of mitosis 1 spindles are indicated by white block arrows. (b) Analysis of – and + *deGrad cid-EGFP* progeny during early anaphase of syncytial blastoderm mitoses revealed in each half spindle 8 sister centromeres in the former, as expected for diploid embryos, but only 4 (or rarely 5) in the latter. White frames in top panels indicate regions shown at high magnification in bottom panels.

cid; cid-EGFP males that were crossed to *cid; cid-EGFP* females, one of the two chromosome sets within all of the analyzed gonomeric metaphase plates of mitosis 1 did not display centromeric Cid-EGFP signals (Figure 3a; n = 9). This indicates that paternal centromeres cannot acquire maternally derived Cid-EGFP after degradation of Cid-EGFP during spermatogenesis. Mitotic figures in anaphase and telophase of mitosis 1 indicated that Cid-EGFP-free paternal chromosomes did not attach normally to the mitotic spindle. Only the Cid-EGFP containing chromatids were oriented towards the spindle poles in all of the analyzed late mitosis 1 figures (Figure 3a; n = 11). We conclude that Cid elimination from sperm results in the loss of paternal chromosomes during the initial syncytial cycles of early embryogenesis.

Gynogenetic haploid embryos obtained from various mutant genotypes (*mh*, *ms(3)K81*, *Hira*) all progress through 14 instead of the normal 13 syncytial blastoderm cycles before cellularization, and they eventually arrest late in embryogenesis (Edgar et al., 1986; Loppin et al., 2000). The progeny from *cid; cid-EGFP* fathers with deGradFP expressed these traits as well. First, none of the progeny obtained from these fathers reached the larval stages. We point out that expression of the GFP-specific recombinant ubiquitin ligase (NSlmb-vhhGFP4) with the *topi-GAL4-VP16* driver did not affect male fertility when *cid* function was provided by the endogenous wild-type *cid* gene instead of

the *cid-EGFP* transgene. The sterility of *cid; cid-EGFP* fathers with deGradFP therefore does not reflect a Cid-EGFP independent deGradFP effect. Second, compared to progeny derived from wild-type or *cid; cid-EGFP* fathers without deGradFP, the nuclear density during cellularization was 2-fold higher in embryos obtained from *cid; cid-EGFP* fathers with deGradFP (Figure S1).

Counting the number of Cid-EGFP dots during mitosis, revealed only 4 pairs of sister centromeres in the large majority (> 90%) of the syncytial blastoderm embryos obtained from a cross of *cid; cid-EGFP* males with deGradFP during spermatogenesis and *cid; cid-EGFP* females (Figure 3b). In contrast, the expected 8 pairs of sister centromeres characteristic for the normal diploid karyotype were detected with control fathers lacking deGradFP (Figure 3b).

Centromere counting revealed that a minority (< 10%) of progeny from *cid; cid-EGFP* fathers with deGradFP contained nuclei with 5 pairs of sister centromeres with comparable amounts of Cid-EGFP. Such nuclei were often in patches next to regions with nuclei containing 4 pairs of sister centromeres. Similarly, a minority of embryos fertilized with Cid-depleted sperm displayed a mosaic of nuclear densities during cellularization with patches of wild-type next to patches with twofold higher density (Figure S1), as characteristically observed in near-haploid embryos (Lu et al., 2009). While it is not excluded that these near-haploid embryos reflect occasional neocentromere formation or postzygotic centromere restoration by maternal Cid, we favor alternative explanations as discussed below.

Developmental regulation of Cid centromere loading during spermatogenesis and early embryogenesis

Our analysis of the consequences of Cid-EGFP degradation during spermatogenesis demonstrates that the paternally contributed Cid protein on centromeres of paternal chromosomes is required for normal function of these centromeres. Evidently, the maternally derived Cid supplies present in early embryos cannot be used for restoration of centromere function on paternal chromosomes contributed by Cid-depleted sperm, at least in the great majority of cases. This finding argues against efficient homeostatic compensation of centromeric Cid losses and supports template-governed regulation where Cid recruitment is strictly dependent on already present centromeric Cid. Therefore, the amount of old Cid nucleosomes partitioned onto the two sister chromatids during chromosome replication might determine the loading of a precisely equivalent amount of new Cid into the centromere during cell cycle progression.

Cid recruitment into the centromere occurs during exit from M phase according to our earlier analyses of the syncytial blastoderm cycles (Schuh et al., 2007). As meiosis includes progression through two consecutive M phases without an intervening S phase, meiotic Cid loading attracted our attention. If new Cid was loaded during both meiotic M phases in amounts precisely equal to the already present centromeric Cid protein, an increase of centromeric Cid levels with each generation had to occur unless compensated by periodic reduction.

To analyse meiotic Cid loading, we quantified centromeric EGFP signals during spermatogenesis in *cid; cid-EGFP* males. Interestingly, this did not reveal any net Cid loading during exit from MI and MII (Figure 1c), suggesting the possibility of compensatory loading during other developmental stages. Indeed, analysis of early spermatocytes revealed net centromeric Cid loading between stage S1 and S4 (Figure 4a), i.e. during G2 well after the premeiotic S phase (Cenci et al., 1994). The expression pattern of Cal1, a protein required for Cid loading (Erhardt et al., 2008; Schittenhelm et

al., 2010a) appeared to be entirely consistent with the observed meiotic Cid loading pattern. Cal1-EGFP expressed from a transgene under control of the normal *cal1* cis-regulatory region in a *cal1* null mutant background was detected at centromeres of spermatocytes between S1 and S3 but not during progression through the meiotic divisions (Figure 4b, S2 and data not shown). Moreover, Cal1 depletion in early spermatocytes by RNAi abolished the increase in Cid-EGFP levels that normally occurred between S1 and S4 (Figure 4c), supporting our conclusion that this Cid-EGFP increase in centromeres of early spermatocytes represents compensatory Cid loading during G2.

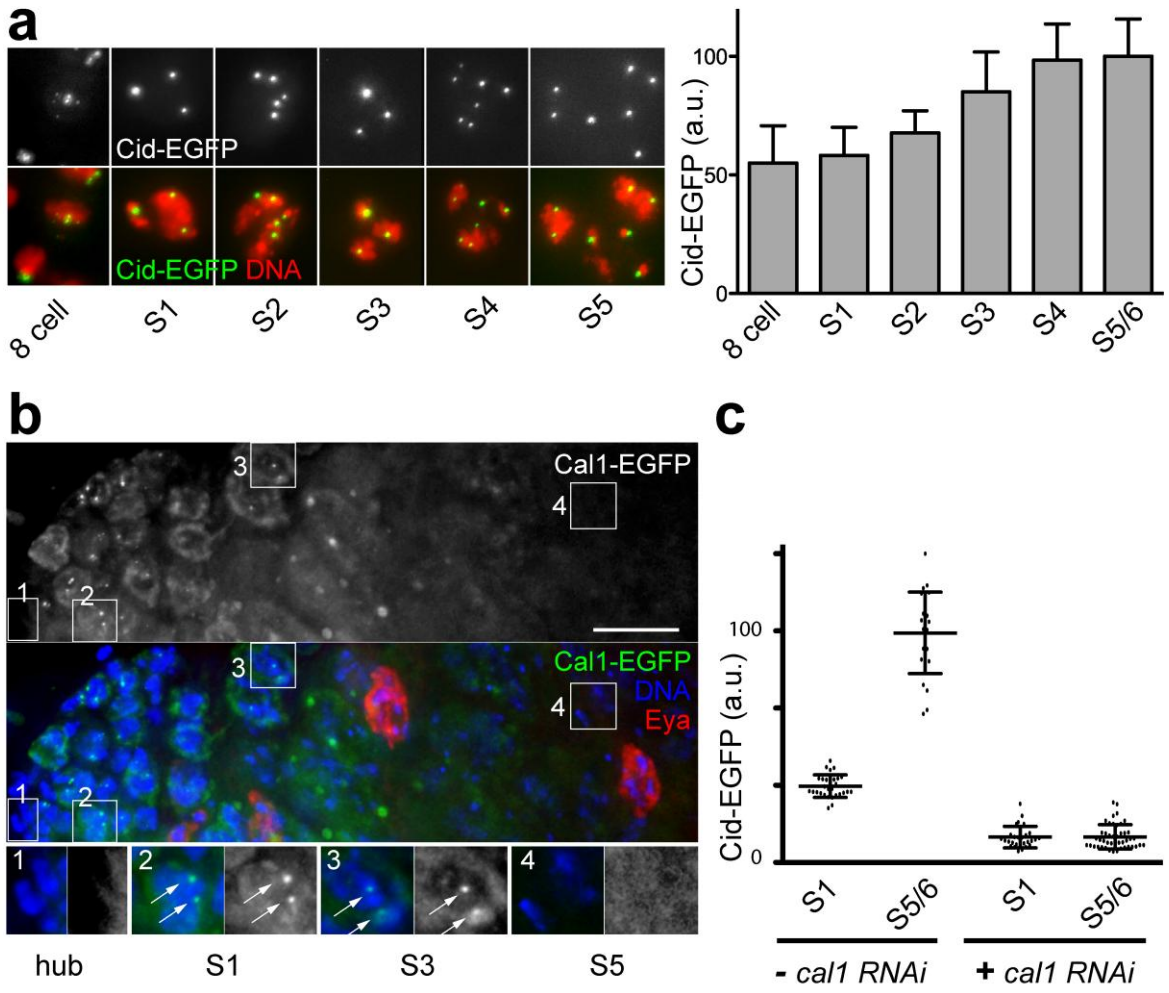

Figure 4. *cal1*-dependent loading of Cid-EGFP during early G2 in spermatocytes. (a) Quantification of EGFP signal intensity per cell revealed an increase in Cid-EGFP levels in spermatocytes between the stages

S1 and S4. Bars indicate average and whiskers for s.d.; n > 20 cells (b) Analysis of *cal1-EGFP* expression in testis whole mount preparations indicated that Cal1, which is required for Cid loading during mitotic proliferation (Erhardt et al., 2008; Schittenhelm et al., 2010a), is present during the four gonial cycles and during Cid-EGFP loading in early spermatocytes (inset 2: S1, inset 3: S3) but no longer in late spermatocytes (inset 4: S5) and subsequent stages (data not shown). Cal1-EGFP was also not detectable in postmitotic hub cells (inset 1: hub) and Eya-positive cyst cells. Scale bar = 10 µm (c) *bamP-GAL4-VP16* driven expression of a *UAS-cal1RNAi* transgene during late gonial cycles and in early spermatocytes abolished Cid-EGFP loading in early spermatocytes. Dots indicate total Cid-EGFP intensity measured in individual cells. Average intensity (long horizontal line) with s.d. (short horizontal lines) is indicated as well. n > 24 cells.

Apart from Cid loading during spermatogenesis, we also analyzed the initial phase of embryogenesis when sperm nucleus remodeling occurs concomitant with completion of female meiosis. Given that Cenp-C was found to be no longer present on centromeres of mature sperm (see above) and given that this centromere protein provides an essential link between Cid and outer kinetochore components (Przewloka et al., 2007; Schittenhelm et al., 2007), loading of maternally derived Cenp-C onto paternal centromeres during the first cell cycle following fertilization was expected. Therefore, we crossed wild-type males to *Cenp-C-EGFP*; *Cenp-C* females and analyzed progeny during early embryogenesis in order to evaluate whether centromere loading of maternally derived GFP fusion proteins onto paternal centromeres is detectable. Indeed, maternally derived Cenp-C-EGFP was observed to associate very soon after fertilization with the sperm nucleus (Figure 5a,b). Cenp-C-EGFP spots were already observed in sperm nuclei that had not yet attained a regular round shape. Cenp-C-EGFP spots were also present in the paternal pronucleus during S phase and pronuclear apposition (Figure 5c). Moreover, in the first metaphase, Cenp-C-EGFP was present in paternal centromeres just like in the maternal centromeres (Figure 5d,e).

In contrast to Cenp-C, paternal Cid is still present in mature sperm and remains stably associated with paternal centromeres after fertilization, as shown above. Therefore, rapid association of maternally derived Cid before mitosis 1 as in the case of Cenp-C was not necessarily expected. However, in analogous analyses with progeny obtained from *cid; cid-EGFP* mothers and wild-type fathers, such early association of Cid-EGFP was clearly observed (Figure 5f-j). In contrast to the Cenp-C-EGFP experiments, where signal intensities during metaphase 1 were comparable on maternal and paternal centromeres, this was not the case in the Cid-EGFP experiments. Cid-EGFP signal intensities were clearly weaker in paternal compared to maternal centromeres. While both maternal and paternal centromeres contain exclusively the EGFP-tagged version in the Cenp-C experiments, this is only true for the maternal centromeres in case of the Cid

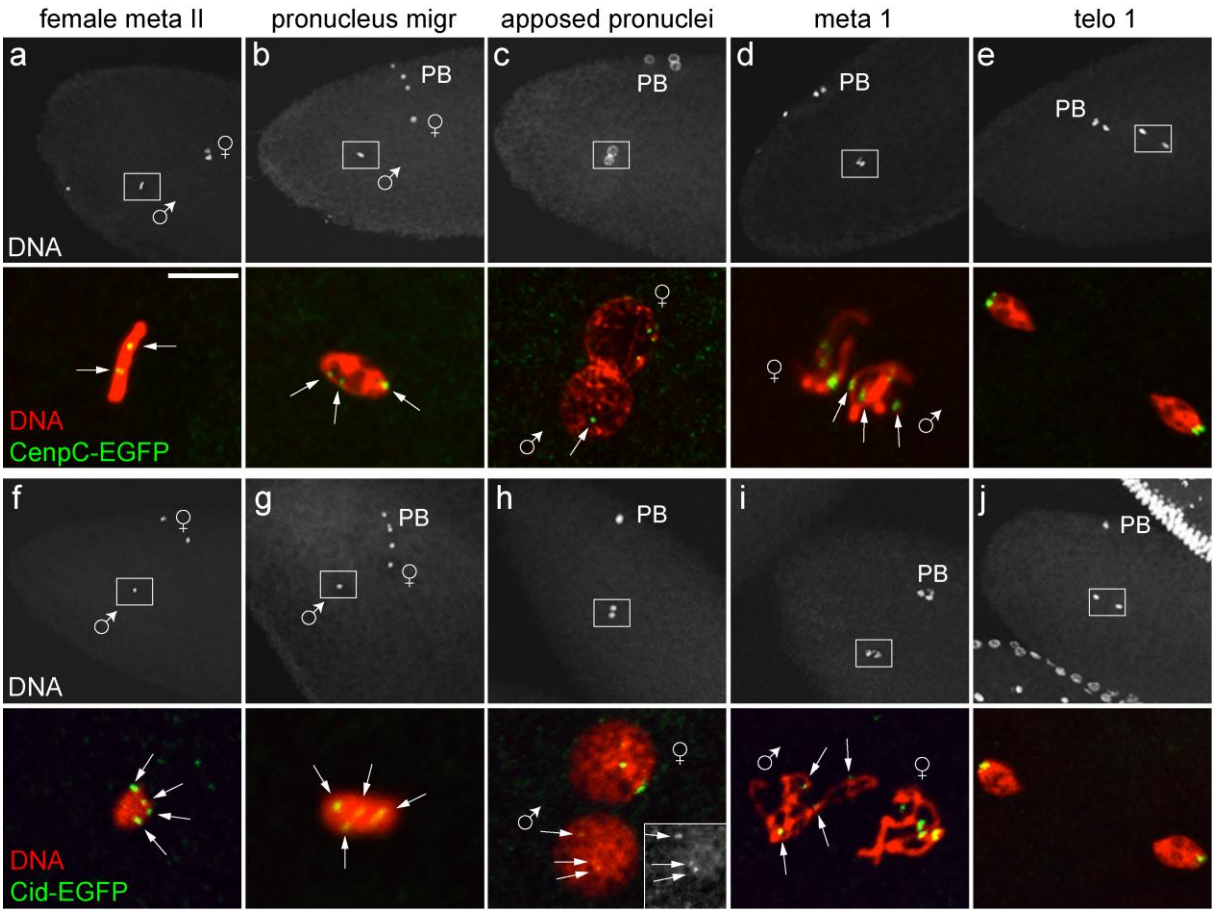

Figure 5. Incorporation of maternal Cid and Cenp-C into paternal centromeres after fertilization.

Eggs were collected from transgenic females producing only Cenp-C-EGFP (a-e) or Cid-EGFP (f-j) instead

of endogenous Cenp-C and Cid, respectively, after mating with non-transgenic males. The regions indicated by white frames in top panels are shown at high magnification in the bottom panels. (a-e) Maternally derived Cenp-C-EGFP associated with paternal centromeres (arrows) before full decondensation of the male pronucleus and was present during mitosis 1. (f-j) Maternally derived Cid-EGFP displayed a comparable association dynamics with paternal centromeres (arrows) although signals were generally weaker on paternal centromeres (see h and i). PB: polar bodies. Scale bar = 10 µm.

experiments, where the paternal centromeres also contain unlabeled wild-type Cid inherited from the father apart from newly loaded maternally derived Cid-EGFP. We conclude that in addition to the net loading of Cid in G2 spermatocytes described above, the rapid association of maternally derived Cid onto paternal centromeres soon after fertilization might provide additional compensation for the absence of Cid loading during the male meiotic divisions. However, we point out that precise quantification of total centromeric Cid-EGFP levels in early embryos is precluded by various factors (like sample thickness, high and variable autofluorescence levels). Thus, we cannot exclude the possibility that the rapid association of maternal Cid-EGFP with paternal centromeres might be balanced by loss of paternal Cid in early embryos. Similarly, we cannot exclude the occurrence of dynamic Cid-EGFP turnover at centromeres during the stages of spermatogenesis where we have not detected any net loading.

Chromosome-specific levels of centromeric Cid and kinetochore proteins

By a more detailed quantification of Cid levels during spermatogenesis we addressed yet another aspect of the control of centromeric Cid levels, i.e. chromosome-specific variation. Drosophila testis provides a unique advantage for the analysis of chromosome-specific variation of centromeric Cid because of the characteristic segregation of chromosome bivalents into discrete sub-nuclear territories in late

spermatocytes (Cenci et al., 1994). In principle, an observation of reproducible chromosome-specific differences in centromeric Cid amounts would argue in favor of template-governed control of centromeric Cid levels. Such control would readily propagate distinct chromosome-specific amounts of centromeric Cid. In contrast, homeostatic mechanisms might be expected to equalize occasional fluctuations and keep a uniform level of Cid in all of the centromeres. Therefore, to evaluate whether centromeric Cid amounts vary on different chromosomes, we quantified EGFP signals in individual centromeres of S5/6 spermatocytes in *cid; cid-EGFP* testis preparations. At the S5/6 stage, DNA staining revealed the three characteristic chromosome territories within the large spermatocyte nucleus. Two of these territories represent the bivalents of chromosome 2 and 3, respectively. Their DNA labeling is more homogenous than that of the third territory which is formed by an association of the bivalent of chromosome 4 with the X chromosome and those parts of the Y that are not involved in Y loop formation (Cenci et al., 1994). The territories with the bivalents of chromosome 2 and 3 both contained two Cid-EGFP spots (Figure 6a). Each spot is known to represent the tightly associated sister centromeres of one homolog (Vazquez et al., 2002). Double labeling with anti-ModC (Buchner et al., 2000; Thomas et al., 2005) allowed the identification of the X-Y bivalent (Figure 6a). The X-Y region was observed to be associated with two spots of obviously unequal Cid-EGFP intensity. An additional bright spot was usually observed in close association with a dot of very bright DNA staining near the X-Y region (Figure 6a). This bright Cid-EGFP spot represents the paired centromeres of the small dot-like chromosome 4 bivalent.

The characteristic unequal intensity of the two Cid-EGFP spots within the X-Y chromosome territory suggested that either the X or the Y centromere is associated with higher levels of centromeric Cid. To clarify this issue we crossed *cid-EGFP* into X/0

males. Apart from the paired centromeres of chromosome 4, the X/0 spermatocytes no longer contained a second bright Cid-EGFP spot (Figure 6b), as characteristically present in normal X/Y spermatocytes (Figure 6a). Therefore we conclude that the Y centromere contains more Cid than all the other centromeres. A quantification of the Cid-EGFP signals on the different chromosomes revealed that the Y centromere contains ~ 2-fold more Cid than the other centromeres. Analyses with Y chromosomes introgressed from different Drosophila strains into the *cid; cid-EGFP* background indicated that the increased Cid levels on the Y centromere are not strain-specific (Figure S3).

Analogous quantification of Cenp-C revealed that the level of this centromere protein was also ~ 2-fold higher on the Y centromere (Figure 6c). To evaluate whether the ~ 2 fold higher levels of the centromere proteins Cid and Cenp-C on the Y centromere were accompanied by a corresponding increase in kinetochore components, we analyzed Spc25-EGFP signals. Spc25 is a component of the Ndc80 complex which represents the major microtubule binding site of the kinetochore. Before the onset of the meiotic divisions, we did not detect dot-like Spc25-EGFP signals. However, during prometaphase of meiosis I, spermatocytes often displayed eight distinct Spc25-EGFP signals, as expected. In such prometaphase I figures, one of the eight signals was always considerably stronger than all the others (Figure 6d). In contrast, in X/0 testis, prometaphase I figures with seven distinct Spc25-EGFP signals did not include such a conspicuously stronger signal (Figure 6d), suggesting that the especially strong Spc25-EGFP signals in X/Y testis represent the Y kinetochore. As predicted by this interpretation, prometaphase II figures in X/Y testis with 4 Spc25-EGFP signals could readily be grouped into two classes: a first class with a conspicuously strong signal, and a second class without such an intensity outlier. In all likelihood, these two classes represent early spermatids that had inherited the Y and the X chromosome, respectively,

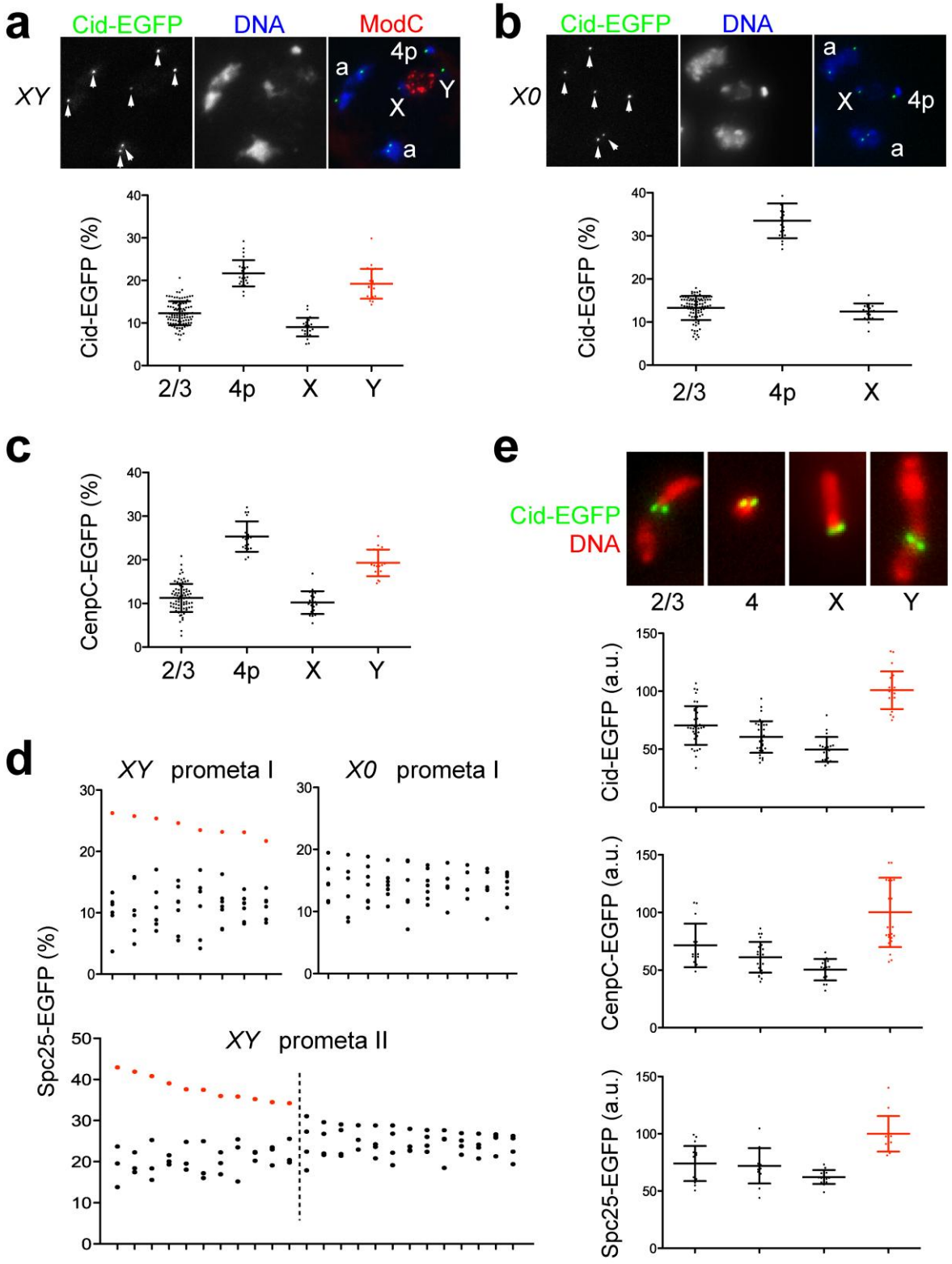

Figure 6. Chromosome-specific differences in centromere and kinetochore protein levels. (a,b) Double labeling of *X/Y*; *cid-EGFP* spermatocytes with anti-ModC (a), which marks the X-Y chromosome territory, and analysis of *X/0*; *cid-EGFP* spermatocytes (b) indicated that the Y centromere contains ~2fold higher levels of Cid-EGFP compared to the other centromeres. Dots in the diagrams below the images indicate relative intensity of individual Cid-EGFP dots in S5 stage spermatocytes representing either a

chromosome 2 or 3 centromere (2/3), the paired chromosome 4 centromeres (4p), the X centromere (X) or the Y centromere (Y). The sum of all the individually measured centromeric signals within each analyzed spermatocyte was set to 100%. Averages (long horizontal line) are given with s.d. (short horizontal lines). n > 22.

(c) Analogous analysis of *Cenp-C-EGFP* spermatocytes during stage S5 indicated that the Y centromere contains ~2fold higher levels of Cenp-C-EGFP compared to the other centromeres.

(d) In case of Spc25-EGFP, meiotic cells were analyzed because this kinetochore protein is only present at centromeres during the meiotic M phases. The diagrams display data from cells during prometaphase of meiosis I from either X/Y (XY prometa I) or X/0 (X/0 prometa I) males but only if 8 or 7 distinct EGFP signals, respectively, could be resolved. In case, of the diagram of prometaphase II in X/Y males (XY prometa II) exclusively cells with 4 distinct signals are displayed. Dots in the diagrams below the images indicate relative intensity of individual Spc25-EGFP spots after setting the sum of all the individually measured kinetochore signals within each analyzed cell to 100%. Each column of dots represents one of the analyzed cells. Red dots indicate the values proposed to correspond to the Y centromere.

(e) Spreads of mitotic chromosomes were prepared from syncytial blastoderm embryos expressing Cid-EGFP, Cenp-C-EGFP or Spc25-EGFP, and stained for DNA. As illustrated by the image panels, individual chromosomes could be identified based on chromosome size, pattern of intensely staining heterochromatin blocks and centromere position. Dots in the diagram indicate total centromeric EGFP intensity per chromosome in arbitrary units (a.u.) chosen to result in an average intensity on the Y chromosome of 100 a.u. Averages (long horizontal line) are given with s.d. (short horizontal lines). n > 15 chromosomes.

in the preceding meiosis I. Finally, a quantification of kinetochore signal intensities in mitotic chromosomes released from early syncytial embryos provided a further confirmation that the Y centromere has higher levels of Cid, Cenp-C and Spc25 (Figure 6e). Thus the increased levels of centromere and kinetochore proteins on the Y centromere are not a peculiarity of the spermatocyte stages. Moreover, these observations argue against the existence of efficient homeostatic mechanisms that enforce identical Cid amounts on all the different centromeres.

Transgenerational propagation of altered centromeric Cid levels in sperm

For a direct evaluation of the role of centromeric Cid for quantitative maintenance, we generated sperm with either moderately increased or decreased levels of Cid on centromeres and analyzed whether the altered centromeric levels were maintained during development of the next generation.

To raise centromeric Cid levels in sperm, we used the UAS/GAL4 system for targeted *cid-EGFP* overexpression during spermatogenesis. Overexpression was driven in a *cid; cid-EGFP* background that did not produce any untagged wild-type Cid. Therefore, the accurately quantifiable Cid-EGFP was the only Cid species produced. Concomitantly with *UAS-cid-EGFP*, we also expressed *UAS-cal1* because increased Cid deposition in centromeres was previously found to depend on simultaneous overexpression of *cid* and *cal1* (Schittenhelm et al., 2010a). *bam-GAL4-VP16* driven co-expression of *UAS-cid-EGFP* and *UAS-cal1* in *cid; cid-EGFP* testis resulted in a strong increase in centromeric Cid-EGFP signals in sperm compared to controls lacking the UAS transgenes (Figure 7a). Quantification revealed almost 7-fold higher Cid-EGFP levels after overexpression. Judging from the number and size of the observed Cid-EGFP spots, Cid-EGFP was still primarily confined to the centromeric region.

Males with “high Cid-EGFP” sperm as well as control males lacking the UAS transgenes were crossed with *cid; cid-EGFP*; *Cenp-C-Tomato* females and progeny was aged to the syncytial blastoderm stage before fixation and quantification of centromeric Cid-EGFP signals in prometa- and metaphase embryos. The total centromeric Cid-EGFP intensity per nucleus was found to be ~ 1.7-fold higher in embryos generated with high Cid-EGFP sperm compared to embryos generated with control sperm (Figure 7b). Centromeric Cenp-C-Tomato was increased to a comparable extent (data not shown). Considering that only one half of the centromeres in the embryo are of paternal origin, we conclude

that the increased Cid-EGFP levels on paternal centromeres appear to be maintained during progression through the early embryonic cell cycles although not quantitatively. The level of Cid-EGFP during embryogenesis might not be sufficiently high to support a complete maintenance of the paternally increased centromeric Cid-EGFP levels during postzygotic development. Results from an analysis of the effects of the zygotic *cid-EGFP* gene dose on centromeric Cid-EGFP levels in wing imaginal disc cells of third instar wandering stage larvae and in spermatocytes of adult males supported the notion that the expression level governed by the normal *cid* regulatory region is not much higher than what is required for maintenance of physiological centromeric Cid levels. In the absence of endogenous Cid, cells with only one *cid-EGFP* copy were observed to display centromeric signals that were 40% weaker than those in cells with two *cid-EGFP* copies (Figure S4).

As limiting *cid* expression might have prevented complete maintenance of increased Cid levels on paternal centromeres, we also analyzed whether decreased Cid levels on paternal centromeres in sperm are maintained during development of the next generation. Transgenic RNAi allowed a partial Cid depletion during spermatogenesis. Targeted depletion using *bam-GAL4-VP16* in combination with a *UAS-cid*^{RNAi} transgene was achieved in a *cid; cid-EGFP* background lacking untagged wild-type Cid. Quantification of centromeric signals in sperm indicated that RNAi resulted in a reduction of Cid-EGFP to about 33% of its level in controls lacking the *UAS-cid*^{RNAi} transgene (Figure 7c). In a second independent experiment, a somewhat lower reduction to about 50% was obtained, and the centromeres of X, Y and autosomes were found to be affected to comparable degree (Figure S5a, b). Males producing low Cid-EGFP sperm and control males were crossed with *cid; cid-EGFP*; *Cenp-C-Tomato* females and centromeric Cid-EGFP levels in progeny were determined at the syncytial

blastoderm stage. The total centromeric Cid-EGFP intensity per nucleus in the embryos derived from low Cid-EGFP sperm was found to be ~ 72% of the intensity observed in the controls (Figure 7d). Considering that only one half of the centromeres are of paternal origin, the reduced Cid-EGFP levels on paternal centromeres appeared to have been quantitatively maintained during progression through the early embryonic cell cycles.

To evaluate whether the reduced Cid-EGFP levels were also maintained during subsequent development, we analyzed wing imaginal discs from third instar wandering stage larvae. These measurements revealed that the reduced Cid-EGFP levels were indeed maintained beyond embryogenesis (Figure 7e and S5c, d). Finally, we measured centromeric Cid-EGFP levels in sperm of adult male progeny. As in embryos and imaginal discs, only ~ 71% of the control levels were observed in sperm of males fathered by Cid-depleted sperm (Figure 7f).

Since chromosome territory formation in spermatocytes is accompanied by conversion of chromocenter-associated centromere clusters into well separated centromeres, we were able to quantify Cid-EGFP levels in individual centromeres in this special cell type. Because the X and Y chromosomes are of maternal and paternal origin, respectively, only the Y but not the X centromere is expected to have reduced centromeric Cid-EGFP, if the reduction reflects propagation on paternal centromeres after Cid depletion during spermatogenesis in the father.

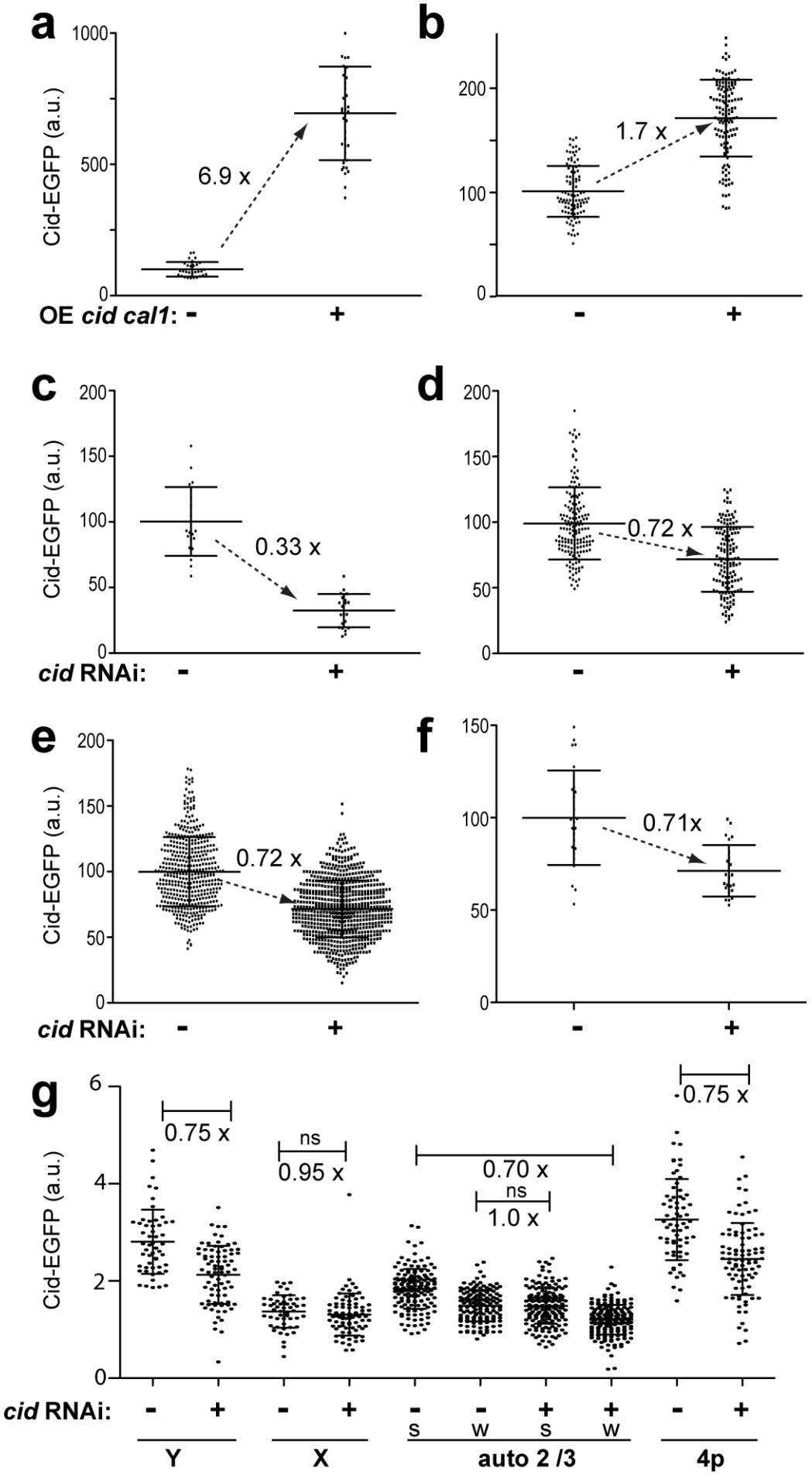
a
Cid-EGFP (a.u.)
1000
500
0
6.9 x
OE cid cal1: -
+
b
200
100
0
1.7 x
-
+
c
Cid-EGFP (a.u.)
200
150
100
50
0
0.33 x
cid RNAi: -
+
d
200
150
100
50
0
0.72 x
-
+
e
Cid-EGFP (a.u.)
200
150
100
50
0
0.72 x
cid RNAi: -
+
f
150
100
50
0
0.71x
-
+
g
Cid-EGFP (a.u.)
6
4
2
0
0.75 x
ns
0.95 x
0.70 x
ns
1.0 x
0.75 x
cid RNAi: - + - + - - + + - +
s w s w
Y
X
auto 2 /3
4p

Figure 7. Transgenerational maintenance of Cid levels. Experimentally, centromeric Cid-EGFP levels were either increased (a, b) or decreased (c-g) in sperm in a background producing only Cid-EGFP instead of endogenous Cid. Sperm with altered centromeric Cid-EGFP levels was used for progeny generation. Propagation of altered Cid-EGFP levels during progeny development was analyzed. (a) Comparison of the total amount of Cid-EGFP per sperm in males without (-) or with (+) *bamP-GAL4-VP16*-driven expression of *UAS-cid-EGFP* and *UAS-cal1*. (b) Comparison of the total amount of Cid-EGFP per nucleus in syncytial blastoderm embryos derived from males without (-) or with (+) increased Cid-EGFP in sperm as determined in (a). (c) Comparison of the total amount of Cid-EGFP per sperm in males without (-) or with (+) *bamP-GAL4-VP16*-driven expression of *UAS-Cid*^{RNAi}. (d-f) Comparison of the total amount of Cid-EGFP per nucleus in progeny derived from males without (-) or with (+) decreased Cid-EGFP in sperm as determined in (c) at different developmental stages: syncytial blastoderm (d), wing imaginal discs of third instar larvae (e), sperm of adult males (f). Dots in A-F indicate total centromeric EGFP intensity per nucleus in arbitrary units (a.u.) chosen to result in an average intensity of 100 a.u. in the controls where Cid-EGFP was neither increased nor decreased in sperm. Averages (long horizontal line) are given with s.d. (short horizontal lines). n > 22. The fold change of average Cid-EGFP levels between controls and experimental samples is indicated next to the dashed arrows. All the indicated differences were found to be highly significant ($p < 0.001$, t test).

(g) Comparison of Cid-EGFP levels in individual centromeres of Y (Y), X (X), major autosomes (2/3) and the paired chromosome 4 centromeres (4p) in S5 spermatocytes of adult progeny derived from *P{w*$^{+}$*, pUASt-mCherry-nls}III* females mated to males without (-) or with (+) decreased Cid-EGFP in sperm as determined in (c). Each major autosome territory contains two Cid-EGFP spots. The stronger (s) and weaker (w) spots, respectively, were grouped and analyzed separately. Dots indicate centromeric EGFP intensity in arbitrary units (a.u.). Averages (long horizontal line) are given with s.d. (short horizontal lines). n > 50. The fold change of average Cid-EGFP levels between controls and experimental samples is indicated below brackets. The corresponding differences of the averages are highly significant ($p < 0.001$, t test) except for two non-significant cases (ns).

Indeed reduction of Cid-EGFP in paternal sperm was found to result in a significant decrease of Cid-EGFP in the Y but not in the X centromere in two independent experiments (Figure 7g, and data not shown).

In case of chromosome 2 and 3 territories, parental origin could not be assigned to the two signals within a territory. Under the assumption that in control spermatocytes Cid amounts in maternally and paternally derived centromeres of chromosome 2 and 3 are usually equal on average, the results obtained after quantification of centromeric Cid-EGFP signal intensities in major autosome territories were not in accord with the findings concerning the X and Y centromeres. Under this assumption it is expected that the intensity difference between the stronger and weaker centromere signal within a major autosome territory should be greater after reduction in sperm and subsequent propagation of reduced Cid on paternal centromeres in comparison to control spermatocytes. However, the average intensity difference between the two signals of a major autosome territory was not increased after reduction of Cid-EGFP in paternal sperm (Figure 7g). In principle, this result might argue for chromosome-specific differences in the control of centromeric Cid levels on sex chromosomes and autosomes. However, this apparent support for chromosome-specific discrepancies is completely abolished under the following alternative assumption. If centromeric Cid levels in control spermatocytes on average are usually higher on paternal compared to maternal centromeres, our results are clearly consistent with quantitative propagation of centromeric Cid not only on the Y but on all paternal centromeres. According to this alternative assumption, the stronger of the two signals in each major autosome territory within control spermatocytes in general corresponds to the paternal and the weaker to the maternal centromere. After reduction in sperm and subsequent propagation of reduced centromeric Cid, only the paternal (i.e. the stronger) but not the maternal (i.e.

the weaker) centromere signals should be decreased. This expectation is born out by our data (Figure 7g). While statistical analyses did not favor one over the other assumption, we propose that our other findings (Figures 5 and 6) provide support for the second assumption, as discussed below.

Our comparison of spermatocytes in males with either two or only one Cid-EGFP gene copies also corroborated the second interpretation. After reduction of the zygotic Cid-EGFP gene dose, centromeric Cid-EGFP was no longer decreased exclusively on the Y centromere (as after centromeric Cid-EGFP reduction in paternal sperm), but equally on both sex chromosomes, and also on all autosomal centromeres (Figure S4C).

Based on our analysis of the consequences after reduction of centromeric Cid in sperm, we conclude that centromeric Cid-EGFP is not replenished to normal levels during development of progeny, at least in case of the Y centromere and presumably also on all other centromeres.

Discussion

Among the known Drosophila centromere proteins (Cid, Cenp-C, Cal1), only Cid survives the excessive chromatin remodeling that accompanies the compaction of the haploid genome into sperm heads. We demonstrate that this centromeric Cid in sperm is essential for the propagation of the paternal genome in the next generation. When normal oocytes are fertilized with sperm lacking centromeric Cid, paternal chromosomes fail to recruit the maternally provided Cid and cannot generate functional kinetochores during mitosis 1. As a result, gynogenetic haploid embryos develop. These findings demonstrate that a minimal amount of pre-existing centromeric Cid is required for centromere propagation during cell cycle progression. Moreover, by partial depletion of centromeric Cid in sperm, in combination with precise quantification, we establish that pre-existing centromeric Cid not only functions as a permissive factor but actually exerts quantitative control over centromeric Cid maintenance during cell proliferation. Reduced centromeric Cid levels in sperm are maintained throughout development of the next generation. They are not restored to the normal amount.

The presence of CenH3 in sperm has previously been demonstrated in mammals and Xenopus (Milks et al., 2009; Palmer et al., 1990; Zeitlin et al., 2005). Similarly, the absence of Cenp-C in sperm has been observed in Xenopus (Milks et al., 2009). A future analysis of the mechanism that selectively maintains all or at least a substantial amount of centromeric CenH3 during the radical chromatin re-organization that accompanies genome compaction into sperm heads will be of interest. The fact that CenH3 nucleosomes are not exchanged for protamines, in contrast to bulk nucleosomes, is crucial, at least in case of Drosophila sperm where centromeric Cid is an essential component of an epigenetic centromere mark for paternal chromosome maintenance in progeny. The demonstration that Cid is indispensible for epigenetic centromere marking

in sperm may appear trivial in the light of the clear evidence that Cid is required and sufficient for centromere maintenance during mitotic proliferation (Blower et al., 2006; Blower and Karpen, 2001; Mendiburo et al., 2011). However, recent findings in *C. elegans* (Gassmann et al., 2012; Monen et al., 2005) and *A. thaliana* (Ingouff et al., 2010) have indicated that functional gametes do not necessarily require centromeric CenH3.

While the large majority of progeny generated after Cid elimination in sperm are gynogenetic haploid embryos, a fraction appears to have an extra chromosome with normal centromeric Cid levels. We cannot rule out that these near-haploid embryos represent cases where normal Cid amounts have been restored postzygotically on a particular paternal chromosome at the original centromere or at an ectopic location. The successful production of human artificial chromosomes (HACs) for example is a clear case for de novo CenH3 acquisition and subsequent maintenance (Harrington et al., 1997). While the alpha-satellite arrays used in HAC production are completely CenH3-free before transfection, the centromeres in Cid-depleted sperm might have residual Cid below the level of detection in our experiments. A partial Cid depletion might also explain the apparently normal chromosome segregation during the two meiotic divisions. These meiotic divisions reduce Cid intensity per spot by a factor of at least four (Figure 1c) and thereby in our deGradFP experiments perhaps below our detection limit. Alternatively, it is not excluded that Cid depletion continues after the meiotic divisions in these deGradFP experiments. However, even if the near-haploid embryos were to result from postzygotic restoration after partial or complete Cid elimination in sperm, such centromere restorations would be rare exceptions and not the rule. Since postzygotic replenishment is not even effective after far more moderate Cid reduction in sperm by RNAi, we consider centromere restoration to be an unlikely explanation for the observed near-haploid embryos. Perhaps these embryos arise after missegregation

of maternal chromosomes during the first embryonic mitoses because occasionally the lagging paternal chromosomes might affect the function of the gonomeric spindle. Consistent with this interpretation, embryos fathered by Cid-EGFP-depleted sperm often displayed a reduced and irregular nuclear density during the syncytial stages within the anterior region where fertilization occurs (33% versus 5% in controls). Similarly, polar body morphology in this anterior region was also often abnormal (64% versus 20% in controls). It appears therefore that the lagging paternal chromosomes somehow cause local cell cycle defects in a considerable fraction of the progeny.

The fact that centromeric Cid, after moderate reduction in sperm to 33-50% of its normal level, is not restored back to normal during development of progeny with normal levels of maternal and zygotic *cid* expression, demonstrates that the pre-existing level of centromeric Cid is a major determinant for quantitative control over centromeric Cid levels during cell cycle progression. Some restoration occurs within one generation according to our data, and Cid on the Y centromere does no longer seem to be significantly reduced in spermatocytes of grandsons and great-grandsons of fathers with Cid-depleted sperm (N.R. and C.F.L., preliminary observations). However, it is clear that the efficiency of this restoration is poor. Starting from sperm, generation of F1 spermatocytes requires more than 2 weeks of development including progression through about 20 or more cell cycles. This is insufficient to replenish centromeric Cid to the normal level. Thus our data clearly supports the idea that the Cid nucleosomes, which remain after random partitioning of pre-existing centromeric Cid nucleosomes onto the two sister chromatids during chromosome replication, instruct the local loading of an equivalent amount of new CenH3 nucleosomes during each cell cycle. Accordingly, centromeric Cid nucleosomes might be licensed for loading in a first cell cycle period, followed by actual loading and concomitant license consumption during a

later cell cycle period. Overproduction of Cid and its loading factor Cal1 might by-pass the license requirement. Thus, the proposed quantitative dependence of Cid loading on pre-existing amounts is not necessarily incompatible with our finding that a centromeric Cid increase can be induced.

Apart from the fact that pre-existing centromeric Cid is critical for quantitative regulation, our over-expression experiments and the effects of *cid-GFP* transgene dose indicate that the level of *cid* expression is also a critical factor. We demonstrate that a single copy of this transgene under control of the *cid* cis-regulatory region (in a *cid* mutant background with Cid-EGFP as the only Cid source) is not sufficient for maintenance of centromeric Cid-EGFP at the level established in the presence of two copies. Therefore, the normal level of *cid* expression does not seem to be in great excess over what is required for centromere maintenance.

Our previous analyses have clearly revealed cell cycle-dependent control of centromeric Cid deposition (Schittenhelm et al., 2010a; Schuh et al., 2007). In syncytial Drosophila embryos, Cid loading occurs during and depends on exit from mitosis. Studies in vertebrates (Bernad et al., 2011; Jansen et al., 2007; Moree et al., 2011; Silva et al., 2012) have similarly suggested that Cid loading in animal cells might generally depend on exit from M phase and occur early in the cell cycle. However, here we demonstrate that cell-cycle coupling of Cid loading is subject to developmental control. Exit from M phase during the meiotic divisions in testis is not accompanied by Cid loading and expression of the loading factor Cal1. Instead, we observe Cal1-dependent loading during G2 before the onset of the meiotic divisions. Similarly, recent data has suggested that Cid loading in cultured Drosophila cells occurs already during metaphase, i.e. before exit from M phase (Mellone et al., 2011). Moreover, observations from plant and fungal cells (Dunleavy et al., 2007; Lermontova et al., 2011; Ravi et al., 2011) have

also indicated that the control of CenH3 loading during eukaryotic cell cycle progression is not governed by an invariant universal mechanism. Although presently precluded by background problems, a precise quantitative understanding of Cid loading throughout female gametogenesis would be of great interest.

The quantitative control of centromeric Cid during male and female gametogenesis might not be precisely identical and subtly subvert the quantitative control exerted by pre-existing Cid. Our quantification of centromeric Cid on Y, X and autosomes is clearly consistent with the notion that centromeres are somewhat overloaded during passage through the male germline. This might explain the fact that the Y centromere, which is transmitted exclusively through the male germline, has about twofold higher levels of centromeric Cid. Moreover, the X centromere, which is transmitted more frequently through the female germline than any other centromere, seems to have the lowest amount of centromeric Cid. A possible reason for the postulated sex-specific difference in Cid loading might be linked to the fact that paternal centromeres experience exit from meiotic M phase, not only in the testis, but also again in the egg after fertilization during completion of female meiosis. Indeed we find that maternal Cid associates with paternal centromeres very early after fertilization during completion of the meiotic divisions of the oocyte. Importantly, mathematical analysis (Text S1) demonstrates that if the extent of over- and underloading are equal in the male and female germline, respectively, then a stable difference between Cid levels on paternal and maternal autosomal centromeres is reached within only two generations. Such a difference is also required for compatibility of our quantitative measurements (Figure 7g) with the parsimonious interpretation that centromeric Cid levels on autosomes (where we cannot assign parental origin) behave in the same way as revealed by our results concerning X and Y (where parental origin is known). Our mathematical analysis also implies that

overloading in the male germline will result in a continuous increase of Y-centromeric Cid in the absence of counterbalancing mechanisms. In the case of the Y chromosome, Cid underloading in the female germline will of course not act as counterbalancing process but we speculate that the observed limited level of Cid expression might be involved. In addition, the Drosophila Y centromere contains unique telomere-related satellite repeats (Mendez-Lago et al., 2011) that may have chromosome-specific effects. Even though centromeres in animals are specified primarily in an epigenetic manner, centromeric and pericentromeric DNA sequences are unlikely to be irrelevant and they have been implicated in meiotic drive and speciation (Malik and Henikoff, 2009).

Some aspects of centromere control that we have defined in Drosophila are presumably not valid or of minor importance in case of humans. In contrast to Drosophila, the Y centromere in human cell lines appears to have the lowest level of centromeric Cenp-A, while the X has average amounts (Irvine et al., 2004). Cenp-A levels on a given chromosome might vary considerably within the human population and appear to correlate with the size of the alpha-satellite region (Sullivan et al., 2011).

While our experiments concur with the notion that limited variation in the level of centromeric Cid is not necessarily detrimental, we also demonstrate that the variation of centromeric Cid on different chromosomes correlates with the amount of recruited kinetochore proteins, as previously found in some (Burrack et al.; Castillo et al., 2007) but not all experiments (Joglekar et al., 2008) with fungi. Moreover, evidence from human cancer cells has implicated Cenp-A over-expression in chromosome mis-segregation ((Amato et al., 2009; Tomonaga et al., 2003). Further clarification of the mechanisms that control centromeric CenH3 levels can therefore be expected to provide important insights into evolution of rogue cells, as well as of new species.

Materials and Methods

Drosophila genetics

Most of the mutant alleles and transgenes used here have been characterized previously. *cid*$^{T12\text{-}1}$ and *cid*$^{T22\text{-}4}$ (Blower et al., 2006) carry premature stop codons. *cid*^{G5950} (Bloomington Drosophila Stock Center #29695) has a P element insertion within the coding sequence. Moreover also *Cenp-C*^{prl41} (Heeger et al., 2005), *cal1*^{MB04866} (Schittenhelm et al., 2010a) and *Spc25*^{c00064} (Schittenhelm et al., 2007) are known or predicted to abolish the production of gene products that can localize to centromeres. The transgenes *P{w*$^{+}$*, gcid-EGFP-cid}III.2* (Schuh et al., 2007), *P{w*$^{+}$*, giEGFP-Cenp-C}II.1* (Schittenhelm, 2009), *P{w*$^{+}$*, gi2xtdTomato-Cenp-C}II.3* and *III.1*(Althoff et al., 2012), *P{w*$^{+}$*, gcal1-EGFP}II.2* (Schittenhelm et al., 2010a) and *P{w*$^{+}$*, gSpc25-EGFP} II.1* (Schittenhelm et al., 2007) have been shown to complement recessive lethal mutations in the corresponding endogenous loci, demonstrating the functionality of the encoded fluorescently tagged centromere and kinetochore proteins. *P{w*$^{+}$*, His2Av-mRFP}II.2* (Schuh et al., 2007) and *P{w*$^{+}$*, pUASt-mCherry-nls}III* were used for genotype marking in some experiments. *P{w*$^{+}$*, pUASt-cal1}III.1* (Schittenhelm et al., 2010a) was used for ectopic *cal1* expression.

The *C(1;Y), y*^{1} *v*^{1} *f*^{1} *B*^{1}*: y*$^{+}$*/C(1)RM, y*^{2} *su(wa)*^{1} *w*^{a} stock for generation of X/0 males was kindly provided by Terry Orr-Weaver (Whitehead Institute for Biomedical Research, Cambridge, MA, USA). *P{w*$^{+}$*,bamP-GAL4-VP16}III* (Chen and McKearin, 2003b), *P{w*$^{+}$*,UASt-NSlmb-vhh-GFP4} III* (Caussinus et al., 2011) and *P{w*$^{+}$*, Cid-RNAi*^{GD4436}*}v43857* were kindly provided by D. McKearin, E. Caussinus and the Vienna Drosophila RNAi Center (VDRC), respectively.

The *P{w*$^{+}$*, gtopi-GAL4-VP16 }III* line was obtained by PhiC31-mediated germline transformation with pattB-topi-GAL4-VP16-topi. In this construct, the cis-regulatory

sequences of the spermatocyte-specific gene *matotopetli (topi)* (Perezgasga et al., 2004) control the production of a Gal4-VP16-Topi fusion protein. The *topi* cis-regulatory sequences were isolated by enzymatic DNA amplification with the primers NT15 (5´-CTTGGGATCCCTCGCAGATCGAATGTCTTG-3´) and NT16 (5´-CTTCAGATCT TTTCATGGCG CTAGTCCGAT-3´), the *GAL4-VP16* sequences with the primers NT17 (5´-CGACC AGATCT ATGAAGCTACTGTCTTCTATCG-3´) and NT19 (5´-GTTTAGCGGCCGCCCCACCGTACTCGTC AATTC-3´) from a bamP-GAL4-VP16 plasmid (kindly provided by D. McKearin), and the *topi* coding and 3'UTR sequences with NT20 (5´-AAGAGGCGGCCGCGATGAAAGTCAAAG TTTCGGG-3´) and NT21 (5´-AATTCGCGGCCGCCGCTATCTTGCCGCTTTATTT-3´)

The *UAS-Cid-EGFP* lines were obtained after germline transformation with a pUAST construct where the sequences coding for Cid with an internal EGFP insertion were inserted after enzymatic amplification using pCaSpeR4-*gcid-EGFP-cid* (Schuh et al., 2007) as a template in combination with the primers NT41 (5´-CTTTAAGCGGCCGC TTAAGCAAATACCGAAAATTTG-3´) and NT42 (5´-GCAAATCTAGAAACTAAGCCTAAACT TCTCTTT TGG-3´).

The *UAS-cal1^{RNAi}* lines were obtained after PhiC31-mediated germline transformation with a Valium20 (Ni et al.) construct with an insert generated by annealing the oligonucleotides 5'-ctagcagt ACGAGTGTAGTTGCTGCAATA tagttatattcaagcata TATTGCAG CAACTACACTCGTgcg-3' and 5'-attcgc ACGAGTGTAGTTGCTGCAATA tatgcttgaatataacta TATTGCAGCAACTACACTCGT actg-3'.

The testis squash preparations for the quantification of EGFP signals at centromeres and kinetochores were made with males of the following genotypes:

- *w*; cid$^{T12\text{-}1}$/cid$^{T22\text{-}4}$; P{w$^+$, gcid-EGFP-cid}III.2* (Figure 1b,c, Figure 4a, Figure 6a)

- *w*; P{w$^+$, giEGFP-Cenp-C}II.1; FRT82B Cenp-C^{prl41}* (Figure 1b,d, Figure 6c)

- *w*; P{w$^+$, gSpc25-EGFP}II.1; Spc25^{c00064}* (Figure 6d)

- *w*; P{w+, gcal1-EGFP}II.2; cal1^{MB04866}* (Figure 4b, Figure S2)

Males with the first two genotypes were also crossed to *w^{1118}* females for the analysis of the transmission of paternal centromere proteins in progeny embryos (Figure 2). Moreover, females with these genotypes were crossed to *w^{1118}* males for the analysis of the association of maternally derived centromere proteins with sperm DNA (Figure 5). The squash preparations for the quantification of EGFP signals at centromeres and kinetochores of mitotic chromosomes (Figure 6e) were made with 1-2 hour embryos collected from parents with the first three genotypes.

For deGrad Cid-EGFP during spermatogenesis (Figure 3) we *generated w*; cid^{T12-1}/cid^{G5950}, P{w+, gcid-EGFP-cid}II.1; P{w+, UASt-NSlmb-vhhGFP4}III/P{w+, gtopi-GAL4-VP16-topi}III, P{w+, gcid-EGFP-cid}III.2* males by standard crossing schemes. In parallel, we generated *w*; cid^{T12-1}/cid^{G5950}, P{w+, gcid-EGFP-cid}II.1; +/P{w+, gtopi-GAL4-VP16-topi}III, P{w+, gcid-EGFP-cid}III.2* males for control experiments. The males were crossed with *w*; cid^{T12-1}/cid^{T22-4}; P{w+, gcid-EGFP-cid}III.2* females for analysis of the subsequent generation.

For the analysis of X/0 spermatocytes, we used testis isolated from *v+*, *f+*, *B+* males obtained after crossing *C(1;Y), y^{1} v^{1} f^{1} B^{1}: y+* males with either *w*; cid^{T12-1}/cid^{T22-4}; P{w+, gcid-EGFP-cid}III.2* (Figure 6b) or *w*; P{w+, gSpc25-EGFP}II.1; Spc25^{c00064}* females (Figure 6d).

To increase Cid-EGFP levels on sperm centromeres (Figure 7a,b), we generated *w*; cid^{T12-1}/cid^{G5950} , P{w+, gcid-EGFP-cid}II.1; P{w+, pUASt-cal1}III .1, P{w+, pUASt-cid-EGFP-Cid} III.1/P{w+, bamP-GAL4-VP16}III, P{w+, gcid-EGFP-cid}III.2* males by standard crossing schemes. In parallel, *w*; cid^{T12-1}/cid^{G5950} , P{w+, gcid-EGFP-cid}II.1; +/P{w+, bamP-GAL4-VP16}III, P{w+, gcid-EGFP-cid}III.2* males were generated for control experiments. For analysis in the next generation (Figure 7b), the males were crossed to

w; cid^{G5950} , P{w$^+$, gcid-EGFP-cid}II.1/cid^{G5950}, P{w$^+$, gi2xtdTomato-Cenp-C}II.3; P{w$^+$, gcid-EGFP-cid} III.2/Cenp-C^{prl41}, P{w$^+$, gi2xtdTomato-Cenp-C}III.1* females.

To decrease Cid-EGFP levels on sperm centromeres (Figure 7c-g), we generated *w*; cid^{T12-1}/cid^{G5950}, P{w$^+$, gcid-EGFP-cid}II.1; P{w$^+$, cid-RNAi^{GD4436}}v43857/P{w$^+$, bamP-GAL4-VP16}III , P{w$^+$, gcid-EGFP-cid}III.2* males. In parallel, *w*; cid^{T12-1}/cid^{G5950}, P{w$^+$, gcid-EGFP-cid}II.1; +/P{w$^+$, bamP-GAL4-VP16}III, P{w$^+$, gcid-EGFP-cid}III.2* males were generated for controls experiments. For analyses during embryogenesis of the next generation (Figure 7d), the males were crossed to *w*; cid^{G5950} , P{w$^+$, gcid-EGFP-cid}II.1/cid^{G5950}, P{w$^+$, gi2xtdTomato-Cenp-C}II.3; P{w$^+$, gcid-EGFP-cid} III.2/Cenp-C^{prl41}, P{w$^+$, gi2xtdTomato-Cenp-C}III.1* females. For analyses with wing imaginal discs of the next generation (Figure 7e), the males were crossed to *w*; cid^{T12-1}, P{w$^+$, His2Av-mRFP}II.2/CyO, Dfd-EYFP* females. Wing discs of larvae with *His2Av-mRFP* expression were mounted and imaged (Schittenhelm et al., 2010a). The rest of the larvae was used for further genotype analysis by PCR using primers specific for the *bam-GAL4-VP16* transgene and the P insertion in *cid^{G5950}*, respectively. The data shown in Figure 7e is from the genotype *w*; cid^{G5950}, P{w$^+$, gcid-EGFP-cid}II.1/cid^{T12-1}, P{w$^+$, His2Av-mRFP}II.2; {w$^+$, bamP-GAL4-VP16}III, P{w$^+$, gcid-EGFP-cid}III.2/+*. We point out that this genotype, which does not include the *cid-RNAi^{GD4436}* transgene results from crosses with both the experimental and the control males. The data obtained with this genotype therefore cannot be affected by *cid-RNAi^{GD4436}* expression during zygotic development. As shown in Figure S5c,d, data from additional progeny genotypes was fully consistent with the findings made with the genotype displayed in Figure 7e. For analyses with testis of the next generation (Figure 7f,g), the males were crossed to *P{w$^+$, pUASt-mCherry-nls}III* females followed by isolation of testis from male progeny with the genotype *w*; cid^{G5950}, P{w$^+$, gcid-EGFP-cid}II.1/+; P{Cid-RNAi^{GD4436}}v43857/P{w$^+$, pUASt-mCherry-nls}III* or *w*;*

cid^{G5950}, P{w$^+$, gcid-EGFP-cid}II.1/+; +/P{w$^+$, pUASt-mCherry-nls}III in case of the control experiments. These testes were characterized by the presence of green centromeric signals and absence of red nuclear signals.

Testis preparations

Testis squash preparations were made, fixed and stained essentially as described (Gunsalus et al., 1995) with the following modifications. After dissection in testis buffer (183 mM KCl, 47 mM NaCl, 10 mM Tris-HCl, pH 6.8), testes were transferred to a 5 μl drop of phosphate buffered saline (PBS) on a poly-L-lysine-treated slide and cut open to spill the contents. The sample was squashed very gently after addition of 15 μl of 4% formaldehyde in PBS under a 22 x 22 mm siliconized cover slip. Fixation was continued for 6 minutes.

Testes whole mount immunolabeling was done as described (White-Cooper, 2003) with the following modifications. After testis dissection (see above), fixation was done in 4% formaldehyde in PBS for 10 minutes. Antibody incubations were performed in a humid chamber.

For immunolabeling rabbit antiserum against ModC (Buchner et al., 2000) was diluted 1:4000 in PBS. Affinity-purified rabbit antibodies against Cenp-C (Heeger et al., 2005) were diluted 1:5000. Hybridoma supernatant containing mouse monoclonal antibody eya10H6 (generated by S. Benzer and N.M. Bonini and kindly provided by the Developmental Studies Hybridoma Bank developed under the auspices of the NICHD and maintained by The University of Iowa, Department of Biology, Iowa City, IA 52242) or 38F3 against NopI/Fibrillarin (Abcam, ab4566) was diluted 1:100 and 1:300, respectively, Secondary antibodies were Cy5 or Alexa568-conjugated goat antibodies against rabbit or mouse IgG.

The images shown in Figure 1b, Figure 3a, Figure 4a,b, Figure S2, Figure 6a,b represent projections of image stacks assembled using Adobe Photoshop. Deconvolution was performed before maximum projection in case of Figure 3a. To reveal the weaker signals in advanced stages of spermatogenesis, increasing adjustment of brightness and contrast was applied to the progressive stages shown in Figure 1b. Therefore, the EGFP signals displayed in Figure 1b do not reflect their quantified intensities (Figure 1c,d). However, to document differences between Cid-EGFP and Cenp-C-EGFP intensities, images were treated equally at a given stage. Concerning X/0 spermatocytes, we point out that the Cid-EGFP signals of the X and the fourth chromosomes were often tightly associated in a single cluster during S5 (in 65% of the spermatocytes, n = 25). The data displayed in Figure 6b was obtained from spermatocytes with separate X and chromosome 4 signals.

Embryo preparations

For analyses during the very early embryonic stages, eggs were collected for 30 minutes at 25°C. For analyses during the syncytial blastoderm cycles, eggs were collected for 1 hour and aged for an additional hours. For analyses of nuclear densities during cellularization, the embryos were aged for an additional 1.5 hours. After dechorionation, embryos were fixed and released from the vitelline membrane by shaking in methanol. After DNA staining with Hoechst 33258 (1 μg/ml in PBS), we mounted the embryos under a cover slip in 70% glycerol, 1% n-propyl gallate and 0.05% p-phenylenediamine.

For the preparation of mitotic chromosome spreads, eggs were collected for 1 hour and aged for an additional hour. Embryos were dechorionated in 1.4% sodium hypochlorite and extensively rinsed with deionized water. After transfer into an

Eppendorf tube containing a 1:1 mixture of heptane and Schneider's tissue culture medium with 10 μM demecolcine (Sigma D7385), embryos were incubated on a rotating wheel. In case of the analysis of Cenp-EGFP and Spc25-EGFP, the incubation in demeocolcine was omitted. After 30 minutes, embryos were transferred to 75 mM KCl in a depression slide and incubated for 10 minutes. Embryos were then transferred into a 5 μl drop of polyamine buffer (Cram et al., 2002) on a glass slide and torn apart using fine tungsten needles. A drop of 5μl of 4% formaldehyde in PBS was added. After addition of a cover slip, the sample was inverted onto a filter paper and squashed for a few seconds to spread the embryos. After a 5 minute incubation, the sample was frozen in liquid nitrogen. After flipping away the cover slip, the slide was immediately placed into chilled 100% ethanol and incubated for 10 minutes at -20°C. Excess ethanol was removed by tapping the slide onto a paper towel. After washing the sample area with PBS for 5 minutes, DNA staining was performed with 0.5 μg/ml Hoechst 33258 in PBS during 10 minutes. After a 5 minute wash in PBS, the sample was mounted under a cover slip in 70% glycerol, 1% n-propyl gallate and 0.05% p-phenylenediamine.

Immunostainings of eggs and embryos shown in Figure 2 and 5 were performed as described (Dubruille et al., 2010). Briefly, embryos were dechorionated in bleach, fixed in methanol and rehydrated in 1X PBS, 0.15% Triton X-100. Embryos were then incubated overnight in the same buffer with rabbit anti-GFP antibody (Invitrogen) at a 1:200 dilution. They were then washed three times in 1X PBS, 0.15% Triton X-100 and incubated overnight in secondary antibody (AlexaFluor 488 goat anti-rabbit (Molecular Probes) at 1:1000. After an incubation step in a RNAse A solution (2 mg/ml in PBS) for 1 hour at 37°C, embryos were mounted in a mounting medium (DAKO) containing propidium iodide (5 μg/ml) to stain DNA. Male and female pronuclei at the pronuclear apposition stage and during the first prometaphase were identified based on their

position. As previously revealed by immunolabeling using an antibody against actetylated histone H4, a histone mark which is enriched in paternal chromatin, the female pronucleus (or the maternal set of chromosomes) is known to be systematically oriented towards the polar bodies (Bonnefoy et al., 2007). Accordingly, the first pronucleus encountered along the virtual line from polar bodies to the apposed pronuclei was considered to be the female pronucleus.

Microscopy and Image Analysis

Quantification of EGFP signals on centromeres and kinetochores was performed after acquiring stacks (20–28 sections, 250 nm spacing) from squashed testis preparations using a 63x/1.4 oil immersion objective on a Zeiss Cell Observer HS microscope. Stacks were converted into maximum projections using ImageJ. Signal quantification was performed essentially as described previously (Schittenhelm et al., 2010a) with the following modifications. For quantification of centromeric signal intensities during spermatogenesis, all centromeric signals within a cell were surrounded with the free hand tool followed by measurement of area (A_s) and integrated pixel intensity (I_s) of the selected regions. For subtraction of diffuse signals (background and GFP signals from any non-centromeric pools), the selected region was slightly enlarged yielding A_l and I_l. Total centromeric signal intensity per cell was then calculated as $I_s – [A_s \times (I_l - I_s) / (A_l - A_s)]$. An analogous subtraction of diffuse signals was performed for quantification of intensities of individual centromeres in spermatocytes where each centromeric spot was surrounded individually. The characteristics of the DNA staining pattern during the S5 spermatocytes stage provided the basis for an assignment of Cid-EGFP signals to different chromosomes. While the centromeres of the two chromosome 4 homologs in the large majority of all S5 spermatocytes analyzed are paired into a single Cid-EGFP

spot next to a strongly staining DNA dot, each homolog of all the other chromosomes usually displays a single Cid-EGFP dot. The X centromere Cid-EGFP signal is usually also close to a region of intense DNA labeling which however is more irregular in shape and not as intense as in case of chromosome 4. In contrast, the Y centromere is very rarely associated with a region of intense DNA staining presumably as a result of the Y loops present during the S5 stage. Finally, the territories of chromosome 2 and 3 display a far more homogenous DNA staining than the regions with chromosomes X,Y and 4. We would like to point out that quantification of centromeric signals obtained after immunofluorescent labeling with anti-Cid, anti-Cenp-C or anti-GFP resulted in far more noisy data. Moreover, comparison of GFP fluorescence signals and immunofluorescent signals after double labeling of cells expressing only Cid-EGFP or Cenp-C-EGFP with antibodies recognizing these GFP fusions indicated that immunofluorescent signal variability is likely to be caused by problems with antibody accessibility that at least in part also reflect the kinetochore attachment status. Accurate centromere signal quantification in combination with DNA fluorescent in situ hybridization (FISH) for chromosome identification was therefore not an option, also because GFP fluorescence does not survive the FISH procedure.

In case of the analyses in syncytial blastoderm embryos stack size was 16 focal planes with 250 nm spacing, in case of wing discs, 20 focal planes with 250 nm spacing. For all quantitative analyses of EGFP signals intensities, data was acquired from at least three different slides. The data displayed in Figure 7b and d is from embryos in prometaphase or metaphase of mitosis 11 and 12. As we did not observe significant intensity differences between mitosis 11 and 12, values were pooled for preparation of the s.

References

1. Black BE, Cleveland DW (2011) Epigenetic centromere propagation and the nature of CENP-a nucleosomes. Cell 144: 471-479.
2. Boyarchuk E, Montes de Oca R, Almouzni G (2011) Cell cycle dynamics of histone variants at the centromere, a model for chromosomal landmarks. Curr Opin Cell Biol 23: 266-276.
3. Burrack LS, Berman J (2012) Flexibility of centromere and kinetochore structures. Trends Genet.
4. Allshire RC, Karpen GH (2008) Epigenetic regulation of centromeric chromatin: old dogs, new tricks? Nat Rev Genet 9: 923-937.
5. Sullivan KF, Hechenberger M, Masri K (1994) Human CENP-A contains a histone H3 related histone fold domain that is required for targeting to the centromere. J Cell Biol 127: 581-592.
6. Henikoff S, Ahmad K, Platero JS, van Steensel B (2000) Heterochromatic deposition of centromeric histone H3-like proteins. Proc Natl Acad Sci U S A 97: 716-721.
7. Blower MD, Sullivan BA, Karpen GH (2002) Conserved organization of centromeric chromatin in flies and humans. Dev Cell 2: 319-330.
8. Liu ST, Rattner JB, Jablonski SA, Yen TJ (2006) Mapping the assembly pathways that specify formation of the trilaminar kinetochore plates in human cells. J Cell Biol 175: 41-53.
9. Schittenhelm RB, Althoff F, Heidmann S, Lehner CF (2010) Detrimental incorporation of excess Cenp-A/Cid and Cenp-C into Drosophila centromeres is prevented by limiting amounts of the bridging factor Cal1. J Cell Sci 123: 3768-3779.
10. Mendiburo MJ, Padeken J, Fulop S, Schepers A, Heun P (2011) Drosophila CENH3 is sufficient for centromere formation. Science 334: 686-690.
11. Monen J, Maddox PS, Hyndman F, Oegema K, Desai A (2005) Differential role of CENP-A in the segregation of holocentric C. elegans chromosomes during meiosis and mitosis. Nat Cell Biol 7: 1248-1255.
12. Gassmann R, Rechtsteiner A, Yuen KW, Muroyama A, Egelhofer T, et al. (2012) An inverse relationship to germline transcription defines centromeric chromatin in C. elegans. Nature.
13. Ingouff M, Rademacher S, Holec S, Soljic L, Xin N, et al. (2010) Zygotic resetting of the HISTONE 3 variant repertoire participates in epigenetic reprogramming in Arabidopsis. Curr Biol 20: 2137-2143.
14. Folco HD, Pidoux AL, Urano T, Allshire RC (2008) Heterochromatin and RNAi are required to establish CENP-A chromatin at centromeres. Science 319: 94-97.
15. Ishii K, Ogiyama Y, Chikashige Y, Soejima S, Masuda F, et al. (2008) Heterochromatin integrity affects chromosome reorganization after centromere dysfunction. Science 321: 1088-1091.
16. Ketel C, Wang HS, McClellan M, Bouchonville K, Selmecki A, et al. (2009) Neocentromeres form efficiently at multiple possible loci in Candida albicans. PLoS Genet 5: e1000400.
17. Mejia JE, Alazami A, Willmott A, Marschall P, Levy E, et al. (2002) Efficiency of de novo centromere formation in human artificial chromosomes. Genomics 79: 297-304.
18. Nakashima H, Nakano M, Ohnishi R, Hiraoka Y, Kaneda Y, et al. (2005) Assembly of additional heterochromatin distinct from centromere-kinetochore chromatin is

required for de novo formation of human artificial chromosome. J Cell Sci 118: 5885-5898.
19. Marshall OJ, Chueh AC, Wong LH, Choo KH (2008) Neocentromeres: new insights into centromere structure, disease development, and karyotype evolution. Am J Hum Genet 82: 261-282.
20. Harrington JJ, Vanbokkelen G, Mays RW, Gustashaw K, Willard HF (1997) Formation of de novo centromeres and construction of first- generation human artificial microchromosomes. Nat Genet 15: 345-355.
21. Blower MD, Karpen GH (2001) The role of Drosophila CID in kinetochore formation, cell-cycle progression and heterochromatin interactions. Nat Cell Biol 3: 730-739.
22. Blower MD, Daigle T, Kaufman T, Karpen GH (2006) Drosophila CENP-A mutations cause a BubR1-dependent early mitotic delay without normal localization of kinetochore components. PLoS Genet 2: e110.
23. Heun P, Erhardt S, Blower MD, Weiss S, Skora AD, et al. (2006) Mislocalization of the Drosophila centromere-specific histone CID promotes formation of functional ectopic kinetochores. Dev Cell 10: 303-315.
24. Fuller MT (1993) Spermatogenesis. In: Bate M, Martinez Arias A, editors. The development of Drosophila melanogaster. 1 ed. Cold Spring Harbor, NY: Cold Spring Harbor Laboratory Press. pp. 71-148.
25. Cenci G, Bonaccorsi S, Pisano C, Verni F, Gatti M (1994) Chromatin and microtubule organization during premeiotic, meiotic and early postmeiotic stages of Drosophila- melanogaster spermatogenesis. J Cell Sci 107: 3521-3534.
26. Jayaramaiah Raja S, Renkawitz-Pohl R (2005) Replacement by Drosophila melanogaster protamines and Mst77F of histones during chromatin condensation in late spermatids and role of sesame in the removal of these proteins from the male pronucleus. Mol Cell Biol 25: 6165-6177.
27. Bonnefoy E, Orsi GA, Couble P, Loppin B (2007) The essential role of Drosophila HIRA for de novo assembly of paternal chromatin at fertilization. PLoS Genet 3: 1991-2006.
28. Loppin B, Bonnefoy E, Anselme C, Laurencon A, Karr TL, et al. (2005) The histone H3.3 chaperone HIRA is essential for chromatin assembly in the male pronucleus. Nature 437: 1386-1390.
29. Callaini G, Riparbelli MG (1996) Fertilization in Drosophila-melanogaster - centrosome inheritance and organization of the first mitotic spindle. Developmental Biology 176: 199-208.
30. Loppin B, Berger F, Couble P (2001) The Drosophila maternal gene sesame is required for sperm chromatin remodeling at fertilization. Chromosoma 110: 430-440.
31. Goshima G, Wollman R, Goodwin SS, Zhang N, Scholey JM, et al. (2007) Genes required for mitotic spindle assembly in Drosophila S2 cells. Science 316: 417-421.
32. Caussinus E, Kanca O, Affolter M (2011) Fluorescent fusion protein knockout mediated by anti-GFP nanobody. Nat Struct Mol Biol 19: 117-121.
33. Edgar BA, Kiehle CP, Schubiger G (1986) Cell cycle control by the nucleo-cytoplasmic ratio in early Drosophila development. Cell 44: 365-371.
34. Loppin B, Docquier M, Bonneton F, Couble P (2000) The maternal effect mutation sesame affects the formation of the male pronucleus in Drosophila melanogaster. Dev Biol 222: 392-404.

35. Lu X, Li JM, Elemento O, Tavazoie S, Wieschaus EF (2009) Coupling of zygotic transcription to mitotic control at the Drosophila mid-blastula transition. Development 136: 2101-2110.
36. Schuh M, Lehner CF, Heidmann S (2007) Incorporation of Drosophila CID/CENP-A and CENP-C into centromeres during early embryonic anaphase. Curr Biol 17: 237-243.
37. Erhardt S, Mellone BG, Betts CM, Zhang W, Karpen GH, et al. (2008) Genome-wide analysis reveals a cell cycle-dependent mechanism controlling centromere propagation. J Cell Biol 183: 805-818.
38. Schittenhelm RB, Heeger S, Althoff F, Walter A, Heidmann S, et al. (2007) Spatial organization of a ubiquitous eukaryotic kinetochore protein network in Drosophila chromosomes. Chromosoma 116: 385-402.
39. Przewloka MR, Zhang W, Costa P, Archambault V, D'Avino PP, et al. (2007) Molecular analysis of core kinetochore composition and assembly in Drosophila melanogaster. PLoS ONE 2: e478.
40. Vazquez J, Belmont AS, Sedat JW (2002) The dynamics of homologous chromosome pairing during male Drosophila meiosis. Curr Biol 12: 1473-1483.
41. Buchner K, Roth P, Schotta G, Krauss V, Saumweber H, et al. (2000) Genetic and molecular complexity of the position effect variegation modifier mod(mdg4) in Drosophila. Genetics 155: 141-157.
42. Thomas SE, Soltani-Bejnood M, Roth P, Dorn R, Logsdon JM, Jr., et al. (2005) Identification of two proteins required for conjunction and regular segregation of achiasmate homologs in Drosophila male meiosis. Cell 123: 555-568.
43. Palmer DK, O'Day K, Margolis RL (1990) The centromere specific histone CENP-A is selectively retained in discrete foci in mammalian sperm nuclei. Chromosoma 100: 32-36.
44. Zeitlin SG, Patel S, Kavli B, Slupphaug G (2005) Xenopus CENP-A assembly into chromatin requires base excision repair proteins. DNA Repair (Amst) 4: 760-772.
45. Milks KJ, Moree B, Straight AF (2009) Dissection of CENP-C-directed centromere and kinetochore assembly. Mol Biol Cell 20: 4246-4255.
46. Jansen LE, Black BE, Foltz DR, Cleveland DW (2007) Propagation of centromeric chromatin requires exit from mitosis. J Cell Biol 176: 795-805.
47. Silva MC, Bodor DL, Stellfox ME, Martins NM, Hochegger H, et al. (2012) Cdk activity couples epigenetic centromere inheritance to cell cycle progression. Dev Cell 22: 52-63.
48. Bernad R, Sanchez P, Rivera T, Rodriguez-Corsino M, Boyarchuk E, et al. (2011) Xenopus HJURP and condensin II are required for CENP-A assembly. J Cell Biol 192: 569-582.
49. Moree B, Meyer CB, Fuller CJ, Straight AF (2011) CENP-C recruits M18BP1 to centromeres to promote CENP-A chromatin assembly. J Cell Biol 194: 855-871.
50. Mellone BG, Grive KJ, Shteyn V, Bowers SR, Oderberg I, et al. (2011) Assembly of Drosophila centromeric chromatin proteins during mitosis. PLoS Genet 7: e1002068.
51. Lermontova I, Rutten T, Schubert I (2011) Deposition, turnover, and release of CENH3 at Arabidopsis centromeres. Chromosoma 120: 633-640.
52. Ravi M, Shibata F, Ramahi JS, Nagaki K, Chen C, et al. (2011) Meiosis-specific loading of the centromere-specific histone CENH3 in Arabidopsis thaliana. PLoS Genet 7: e1002121.

53. Dunleavy EM, Pidoux AL, Monet M, Bonilla C, Richardson W, et al. (2007) A NASP (N1/N2)-related protein, Sim3, binds CENP-A and is required for its deposition at fission yeast centromeres. Mol Cell 28: 1029-1044.
54. Mendez-Lago M, Bergman CM, de Pablos B, Tracey A, Whitehead SL, et al. (2011) A large palindrome with interchromosomal gene duplications in the pericentromeric region of the D. melanogaster Y chromosome. Mol Biol Evol 28: 1967-1971.
55. Malik HS, Henikoff S (2009) Major evolutionary transitions in centromere complexity. Cell 138: 1067-1082.
56. Irvine DV, Amor DJ, Perry J, Sirvent N, Pedeutour F, et al. (2004) Chromosome size and origin as determinants of the level of CENP-A incorporation into human centromeres. Chromosome Res 12: 805-815.
57. Sullivan LL, Boivin CD, Mravinac B, Song IY, Sullivan BA (2011) Genomic size of CENP-A domain is proportional to total alpha satellite array size at human centromeres and expands in cancer cells. Chromosome Res 19: 457-470.
58. Burrack LS, Applen SE, Berman J (2011) The requirement for the Dam1 complex is dependent upon the number of kinetochore proteins and microtubules. Curr Biol 21: 889-896.
59. Castillo AG, Mellone BG, Partridge JF, Richardson W, Hamilton GL, et al. (2007) Plasticity of fission yeast CENP-A chromatin driven by relative levels of histone H3 and H4. PLoS Genet 3: e121.
60. Joglekar AP, Bouck D, Finley K, Liu X, Wan Y, et al. (2008) Molecular architecture of the kinetochore-microtubule attachment site is conserved between point and regional centromeres. J Cell Biol 181: 587-594.
61. Tomonaga T, Matsushita K, Yamaguchi S, Oohashi T, Shimada H, et al. (2003) Overexpression and mistargeting of centromere protein-A in human primary colorectal cancer. Cancer Res 63: 3511-3516.
62. Amato A, Schillaci T, Lentini L, Di Leonardo A (2009) CENPA overexpression promotes genome instability in pRb-depleted human cells. Mol Cancer 8: 119.
63. Heeger S, Leismann O, Schittenhelm R, Schraidt O, Heidmann S, et al. (2005) Genetic inteactions of Separase regulatory subunits reveal the diverged Drosophila Cenp-C homolog. Genes Dev 19: 2041-2053.
64. Schittenhelm RB, Chaleckis R, Lehner CF (2009) Essential functional domains and intrakinetochore localization of Drosophila Spc105. EMBO J 28: 2374-2386.
65. Althoff F, Karess RE, Lehner CF (2012) Spindle checkpoint-independent inhibition of mitotic chromosome segregation by Drosophila Mps1. Mol Biol Cell 23: 2275-2291
66. Chen D, McKearin D (2003) Dpp signaling silences bam transcription directly to establish asymmetric divisions of germline stem cells. Curr Biol 13: 1786-1791.
67. Perezgasga L, Jiang J, Bolival B, Jr., Hiller M, Benson E, et al. (2004) Regulation of transcription of meiotic cell cycle and terminal differentiation genes by the testis-specific Zn-finger protein matotopetli. Development 131: 1691-1702.
68. Ni JQ, Zhou R, Czech B, Liu LP, Holderbaum L, et al. (2011) A genome-scale shRNA resource for transgenic RNAi in Drosophila. Nat Methods 8: 405-407.
69. Gunsalus KC, Bonaccorsi S, Williams E, Verni F, Gatti M, et al. (1995) Mutations in twinstar, a Drosophila gene encoding a cofilin adf homolog, result in defects in centrosome migration and cytokinesis. J Cell Biol 131: 1243-1259.
70. White-Cooper H (2003) Drosophila Cytogenetics Protocols. Methods in Molecular Biology Spermatogenesis: Analysis of Meiosis and Morphogenesis.

71. Cram LS, Bell CS, Fawcett JJ (2002) Chromosome sorting and genomics. Methods Cell Sci 24: 27-35.
72. Dubruille R, Orsi GA, Delabaere L, Cortier E, Couble P, et al. (2010) Specialization of a Drosophila capping protein essential for the protection of sperm telomeres. Curr Biol 20: 2090-2099.

Acknowledgements:

We thank E. Caussinus and M. Affolter for deGradFP strains and communication of unpublished results, D. McKearin, T. Orr-Weaver, G. Reuter for additional fly strains, R. Dorn for anti-ModC antibodies, F. Althoff, P. Lidsky for the construction of various strains with recombinant chromosomes and M. Robinson for help with statistical analyses.

Abbreviations: Cal1, chromosome alignment 1 protein; CenH3, centromere-specific histone H3 variant; Cenp-A, centromere protein A; Cenp-C, centromere protein C; Cid, centromere identifier; EGFP, enhanced green fluorescent protein

Supporting Information:

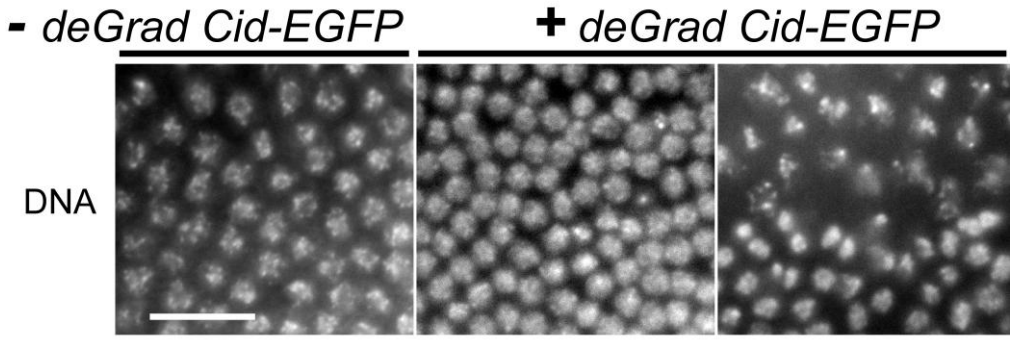

	number of embryos with: 10-12	20-24	10-12/20-24	nuclei / 20 µm²
- *deGrad Cid-EGFP*	15	0	0	
+ *deGrad Cid-EGFP*	0	19	3	

Figure S1. Gynogenetic embryos resulting from Cid depletion in sperm progress through an additional syncytial cycle before cellularization. During spermatogenesis, a GFP-specific ubiquitin ligase (Caussinus et al., 2011) was either expressed (*+ deGrad cid-EGFP*) or not expressed (*- deGrad cid-EGFP*) in males producing only Cid-EGFP instead of normal Cid. Males were crossed with wild-type females and progeny was fixed at the stage of cellularization. Comparison of the nuclear density in – and *+ deGrad cid-EGFP* progeny during cellularization revealed a twofold higher value (or rarely a mosaic of regions with normal and twofold higher values) in the latter. Scale bar = 5 µm

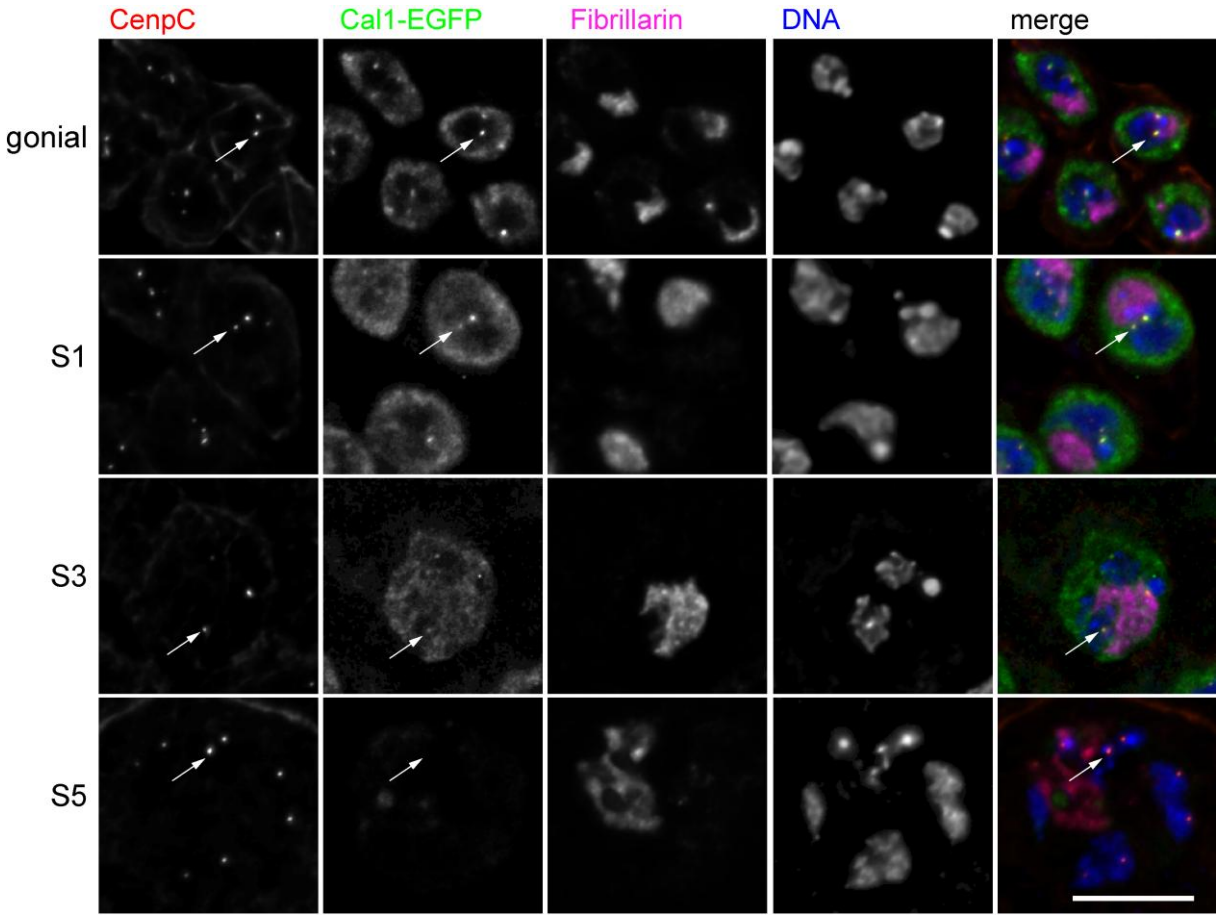

Figure S2. *cal1-EGFP* expression during spermatogenesis. Squash preparation of testis producing only Cal1-EGFP instead of endogenous Cal1 were stained for DNA and double labeled with antibodies against Cenp-C (CenpC) and Fibrillarin (Fibrillarin) to mark centromeres and nucleolus, respectively. Stacks of representative cells during the gonial division cycles (gonial) and during the spermatocyte stages S1 (S1), S3 (S3) and S5 (S5) were deconvolved and maximum projected. Cal1-EGFP dots co-localizing with Cenp-C were detected up to the S3 stage but not later. Cal1-EGFP signals could not be detected in the nucleolus, in contrast to the findings in embryonic and cultured Drosophila cells (Erhardt et al., 2008; Schittenhelm et al., 2010a). Scale bar = 10 µm.

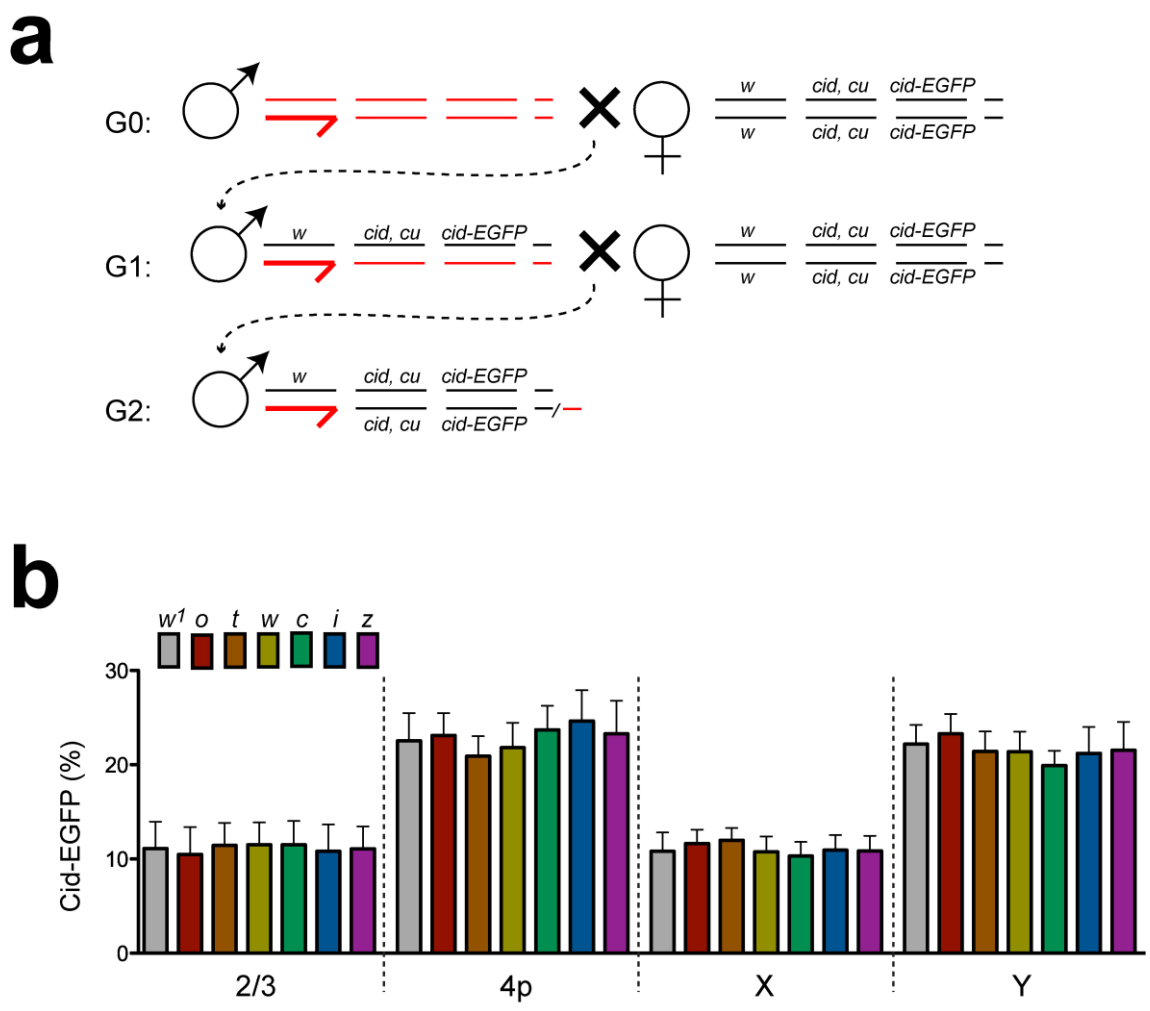

Figure S3. Comparison of Cid levels in different Y centromeres. (a) Crossing scheme for the introgression of different Y chromosomes into the *cid; cid-EGFP* background. The mini-w^+ gene of *P{w+, gcid-EGFP-cid}III.2* and the recessive mutation *curled* (*cu*) were used as marker mutations. (b) Squash preparation of testis with introgressed Y chromosome from strains w^1 (w^1), *Oregon R* (*o*), *Thurgau 1* (*t*), *Winterthur 1* (w), *Congo* (*c*), *India* (*i*), or *Zimbabwe* (*z*). Cid-EGFP levels on individual centromeres were measured, indicating that all the different Y centromeres have similarly increased Cid levels in comparison to the other centromeres. The intensity of individual Cid-EGFP dots in S5 stage spermatocytes

representing either a chromosome 2 or 3 centromere (2/3), the paired chromosome 4 centromeres (4p), the X centromere (X) or the Y centromere (Y) was measured, and the sum of all the individually measured centromeric signals within each analyzed spermatocyte was set to 100%. Bars indicate average relative intensity; s.d. is indicated by whiskers. n > 25.

The isofemale strains *Thurgau 1* and *Winterthur 1* were established from single females isolated from the wild at different locations in Switzerland in spring 2010 (P. Radermacher, L. Baumann and C.F.L., unpublished). The strains *Congo* (*c*), *India* (*i*) and *Zimbabwe* (*z*) were kindly provided by G. Reuter (University of Halle, Halle, Germany).

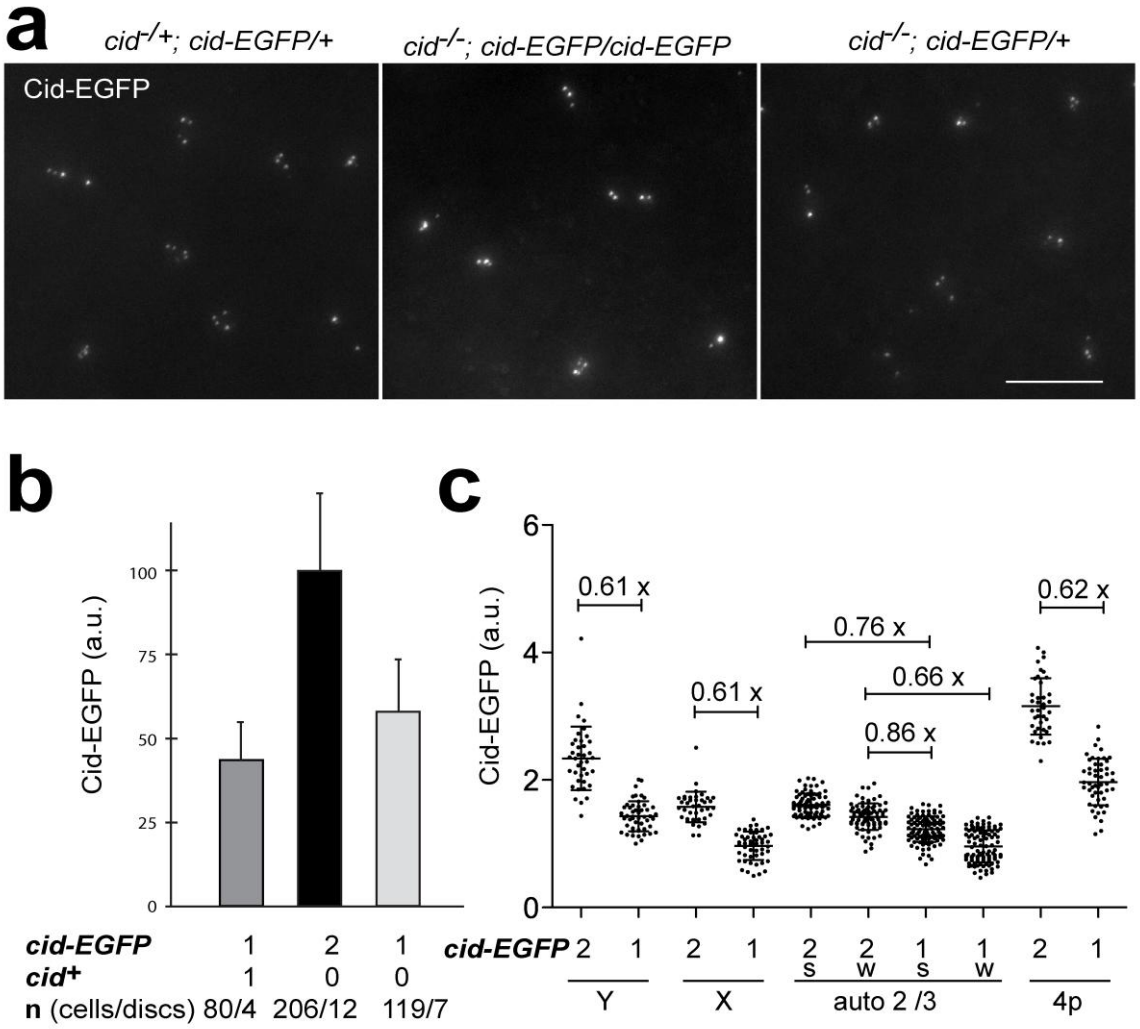

Figure S4. Effect of gene dose on centromeric Cid-EGFP levels. (a) Wing imaginal discs expressing *cid-EGFP* were isolated from wandering third instar larvae and imaged (Schittenhelm et al., 2010a). The larvae had either one endogenous *cid*$^{+}$ gene copy and one *cid-EGFP* transgene copy (*cid*$^{-/+}$*; cid-EGFP*), or no

endogenous *cid*$^{+}$ gene copy and either two (*cid*$^{-/-}$*; cid-EGFP/cid-EGFP*) or one (*cid*$^{-/-}$*; cid-EGFP/+*) transgene copy. Scale bar = 10 μm (b) Total Cid-EGFP signal intensity per nucleus was measured in cells of the peripodial membrane of wing imaginal discs from the different genotypes (as in a). Bars represent average intensity in arbitrary units (a.u.) with whiskers indicating s.d. A similar number of cells was analyzed in each disc. The total number of cells and imaginal discs analyzed is given below the bars (n). According to t test, differences between the analyzed genotypes were highly significant ($p < 0.0001$). (c) Comparison of Cid-EGFP levels in individual centromeres of Y (Y), X (X), major autosomes (2/3), and the paired chromosome 4 centromeres (4p) in spermatocytes of *cid* males with 2 or 1 copy of *cid-EGFP*, as indicated. Major autosome territories contain two spots. The stronger (s) and weaker (w) spots, respectively, were grouped and analyzed separately. Dots indicate centromeric EGFP intensity in arbitrary units (a.u.). Averages (long horizontal line) are given with s.d. (short horizontal lines). $n > 45$. The fold change of average Cid-EGFP levels between samples with 2 or 1 cid-EGFP copy is indicated. All the indicated differences were highly significant according to t-test ($p < 0.0001$).

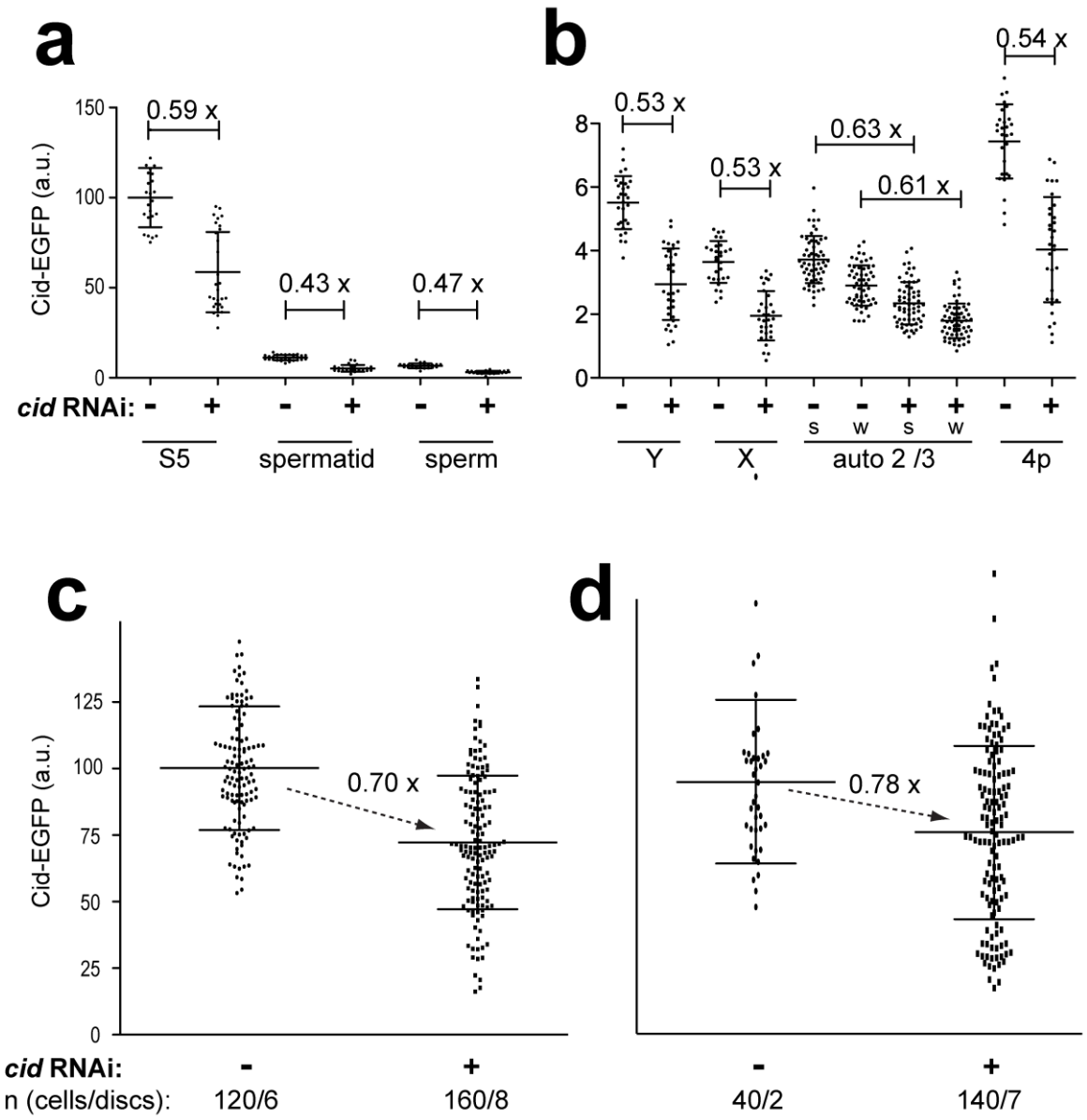

Figure S5. Transgenerational maintenance after Cid-EGFP reduction in sperm. (a, b) Analysis of the extent of Cid-EGFP knock down during spermatogenesis. Centromeric Cid-EGFP signals were quantified in males without (-) or with (+) *bamP-GAL4-VP16*-driven expression of *UAS-Cid*^{RNAi} in a background producing only Cid-EGFP instead of endogenous Cid. (a) Centromeric Cid-EGFP levels per nucleus were quantified in S5 spermatocytes, spermatids and sperm. The extent of average reduction of centromeric Cid-EGFP resulting from RNAi is indicated above the brackets and was found to be highly significant in all cases ($p < 0.0001$, t-test). At least 25 cells from at least five different testes were analyzed for each stage and genotype. (b) Centromeric Cid-EGFP levels in individual centromeres of Y (Y), X (X), major autosomes (2/3) and the paired chromosome 4 centromeres (4p) were quantified in S5 spermatocytes. Each major

autosome territory contains two Cid-EGFP spots. The stronger (s) and weaker (w) spots, respectively, were grouped and analyzed separately. The extent of average reduction of centromeric Cid-EGFP resulting from RNAi is indicated above the brackets and was found to be highly significant in all cases ($p < 0.0001$, t-test). At least 35 centromeres from at least five different testes were analyzed for each case. (c, d) Analysis of propagation of reduced centromeric Cid-EGFP levels in the next generation. Centromeric Cid-EGFP per nucleus in progeny derived from males without (-) or with (+) RNAi-mediated Cid-EGFP reduction in sperm (as determined in Figure 7c and Figure S5, a and b) was compared. In peripodial cells of wing imaginal discs of third instar larvae centromeric Cid-EGFP levels were measured before genotype assignment by PCR. While data from the genotype *w*; cid^{G5950}, P{w+, gcid-EGFP-cid}II.1/cid^{T12-1}, P{w+, His2Av-mRFP}II.2; {w+, bamP-GAL4-VP16}III, P{w+, gcid-EGFP-cid}III.2/+* is displayed in Figure 7e, further corroborating data from the genotypes *w*; cid^{T12-1}/cid^{T12-1}, P{w+, His2Av-mRFP}II.2; {w+, bamP-GAL4-VP16}III, P{w+, gcid-EGFP-cid}III.2/+* (c) and *w*; cid^{G5950}, P{w+, gcid-EGFP-cid}II.1/cid^{T12-1}, P{w+, His2Av-mRFP}II.2; P{w+, cid-RNAi^{GD4436}}v4385* or *+/+* (d) is shown here. The fold change of average Cid-EGFP levels between controls and experimental samples is indicated next to the dashed arrows. Statistical significance of the changes according to t-test: $p < 0.001$ (d) and *** $p < 0.0001$ (c). The total number (n) of analyzed cells and imaginal discs analyzed is given below the bars. Dots indicate centromeric EGFP intensity per nucleus (a, c, d) or in individual centromeres (b) in arbitrary units (a.u.) chosen to result in an average intensity of 100 a.u. in control spermatocytes in a, c and d. Averages (long horizontal line) are given with s.d. (short horizontal lines).

Supporting Text: A deterministic model for sex-specific differences of Cid loading on autosomal levels

We formulate a simple deterministic model of differential Cid loading onto autosomes in the male and female germline. We then test the consequences of the model assumptions on the expected mean Cid content of chromosomes in a population at equilibrium.

Assuming non overlapping generations and a 1:1 sex ratio, for any generation one can envisage a population chromosome pool that can be subdivided into four categories as described below. For each category, we assign a mean Cid level designated by the variables:

M_m : mean Cid level on chromosomes of maternal origin in males,

M_p : mean Cid level on chromosomes of paternal origin in males,

F_m : mean Cid level on chromosomes of maternal origin in females,

F_p : mean Cid level on chromosomes of paternal origin in females.

Consider M_m and M_p at time *t*. If one makes the simplifying assumption that for the next generation at *t+1*, the Cid level on chromosomes of paternal origin will increase by a proportion *d*, and the Cid level on chromosomes of maternal origin will decrease by *d*, then one can formulate a set of difference equations where

$$M_m(t+1) = \tfrac{1}{2}(1-d)\,F_m(t) + \tfrac{1}{2}(1-d)\,F_p(t) = \tfrac{1}{2}(1-d)\,(F_m(t) + F_p(t)) \quad \text{(eq. 1)}$$

$M_p(t+1) = \frac{1}{2}(1+d) M_m(t) + \frac{1}{2}(1+d) M_p(t) = \frac{1}{2}(1+d)(M_m(t) + M_p(t))$. (eq. 2)

Similarly,

$F_m(t+1) = \frac{1}{2}(1-d)(F_m(t) + F_p(t))$ (eq. 3)

$F_p(t+1) = \frac{1}{2}(1+d)(M_m(t) + M_p(t))$. (eq. 4)

Given the above system (eqs. 1 to 4), one sees that regardless of initial conditions, for any time t, after one generation we have

$M_m(t+1) = F_m(t+1)$ (eq. 5)

$M_p(t+1) = F_p(t+1)$. (eq. 6)

Given eqs. 1,2,5 and 6, in generation $t+2$ we have

$M_m(t+2) = \frac{1}{2}(1-d)(F_m(t+1) + F_p(t+1)) = \frac{1}{2}(1-d)(M_m(t+1) + M_p(t+1))$ (eq. 7)

$M_p(t+2) = \frac{1}{2}(1+d)(M_m(t+1) + M_p(t+1))$. (eq. 8)

Using eqs. 5 and 6, we also know that $F_m(t+2) = M_m(t+2)$ and $F_P(t+2) = M_P(t+2)$. Hence, using the values in eqs. 7 and 8, and the recursion from eq. 1, the expression for M_m at generation $t+3$ is

$M_m(t+3) = \frac{1}{2}(1-d)(F_m(t+2) + F_p(t+2)) = \frac{1}{2}(1-d)(M_m(t+2) + M_p(t+2))$

$= \frac{1}{2}(1-d)(\frac{1}{2}(1-d)(M_m(t+1) + M_p(t+1)) + \frac{1}{2}(1+d)(M_m(t+1) + M_p(t+1)))$

$= \frac{1}{2}(1-d)(M_m(t+1) + M_p(t+1)).$ (eq. 9)

Similarly,

$M_p(t+3) = \frac{1}{2}(1+d)(M_m(t+2) + M_p(t+2))$

$= \frac{1}{2}(1+d)(M_m(t+1) + M_p(t+1)).$ (eq. 10)

Examining equations 7 to 10, we see the notable result that $M_m(t+3) = M_m(t+2)$ and $M_p(t+3) = M_p(t+2)$. Hence, regardless of initial conditions, the system will reach an equilibrium after 2 generations. For any $n>2$, the equilibrium Cid contents are given by

$M_m(t+n) = \frac{1}{2}(1-d)(M_m(t+1) + M_p(t+1))$

$= \frac{1}{4}(1-d)((1-d)(F_m(t) + F_p(t)) + (1+d)(M_m(t) + M_p(t)))$ (eq. 11)

and

$M_p(t+n) = \frac{1}{2}(1+d)(M_m(t+1) + M_p(t+1))$

$= \frac{1}{4}(1+d)((1-d)(F_m(t) + F_p(t)) + (1+d)(M_m(t) + M_p(t)))$ (eq. 12)

Given that $M_m(t+n)=F_m(t+n)$ and $M_p(t+n)=F_p(t+n)$, we hence have expressions for

the equilibrium Cid content of all male and female chromosome categories. Note that when at the starting conditions the Cid content of all categories have the same value *x*, such that $F_m(t) = F_p(t) = M_m(t) = M_p(t) = x$, then eqs. 11 and 12 reduce to

$$M_m(t+n) = (1-d)\,x \qquad \text{(eq. 13)}$$

and

$$M_p(t+n) = (1+d)\,x. \qquad \text{(eq. 14)}$$

The results expressed in equations 11 to 14 show that if one assumes a symmetrical overloading/underloading proportion *d*, then after two generations the population will reach an equilibrium where the ratio of maternal to paternal Cid levels is given by

$$\frac{Mm(t+n)}{Mp(t+n)} = \frac{1-d}{1+d}. \qquad \text{(eq. 15)}$$

The same ratio is also valid for the female autosomal chromosomes.

The interpretation of eq. 15 is that after two generations, the system will maintain a constant underload of Cid on maternally derived chromosomes, and a constant overload on the paternally derived chromosomes.

Definining *f* as the ratio between maternal and paternal Cid levels in eq. 15, we have

$$f = (1-d) / (1+d)$$

and

$d = (1 – f) / (1 + f)$.

If the average of the weaker and stronger Cid-EGFP signal in each autosome territory in control spermatocytes as determined (Figure 7g) were to correspond to Mm and Mp, respectively, f would amount to about 0.8. Accordingly, under- and overloading in the female and male germline, respectively, would be predicted to change Cid-EGFP levels by 11% in each generation ($d = 0.11$).

Appendix I

Centromeric Cid levels inducing meiotic drive

Introduction

Meiotic Drive

After regular meiosis homologous maternal and paternal alleles will be present in precisely 50 percent of the meiotic products. However, female meiosis is asymmetric in higher plants and animals. Only one of the four haploid products is transmitted to the next generation while three products are discarded as polar bodies. Hence, any mechanism causing preferential segregation of one of the two parental alleles into the female pronucleus will result in meiotic drive (Buckler et al., 1999) where one of the two parental alleles is consistently found in more than half of the offspring.

Female meiotic drive is at the heart of a recent proposal explaning the very rapid evolutionary divergence of centromeric DNA sequences and associated CenH3 (Malik and Bayes, 2006). According to this 'Centromere-drive' model, female asymmetric meiosis will favor selfish centromeres that can successfully compete with homologs for inclusion into the pronucleus. In Drosophila female meiosis, for example, the interior and usually posterior facing centromere within a bivalent with bi-polar orientation within the meiosis I spindle that has an axis perpendicular to the oocyte surface will be included in the pronucleus of the oocyte (King, 1970). As the meiotic spindle is acentrosomal and nucleated by the chromatin, it is readily conceivable that certain centromere variants might favor their reproducible asymmetric orientation within the meiosis I spindle.

A non-random segregation during the asymmetric female meiosis has been reported in cases where more centromeres or pseudocentromeres are present in a meiotic chromosome complex than the usual two homologous centromeres in a

bivalent (Peacock et al., 1981; Rhoades and Vilkomerson, 1942). In heterozygous carriers of Robertsonian translocations for example the single centromere within the fused compound chromosomes on the one hand and the two centromeres of the paired unfused homologs on the other hand appear to have usually a strongly biased non-random orientation within the meiosis I spindle (Pardo-Manuel de Villena and Sapienza, 2001a, 2001b). An other well-studied example is the preferential segregation of knob containing chromosomes in maize. Knobs are blocks of heterochromatic satellite DNA that are always found distally from the centromere. They act as pseudocentromeres and can bind microtubules (Buckler et al., 1999; Dawe and Cande, 1996). These examples are consistent with the idea that stronger centromeres result in a preferential segregation and spreading of this strong centromeres and the linked chromosomal regions within the population.

Under the 'Centromere-drive' model, a first step might consist in a satellite expansion that might lead to a centromere with enhanced microtubule nucleating and binding abilities, which in turn might result in a transmission advantage during the asymmetric female meiosis (Figure 1). The expanded centromeric satellites are thought to gain this transmission advantage by more efficient recruitment of kinetochore proteins and consequential effects on organization of the polarized meiosis I spindle and also on positioning within this spindle (Lohe and Brutlag, 1987).

However, according to the 'Centromere-drive' model, the spread of a strong centromere within a population is thought to be accompanied by various detrimental effects for example on male fertility or on sex ratio (Haaf and

Willard, 1997; Lohe and Brutlag, 1987; Samonte et al., 1997). Such detrimental effects are postulated to drive the selection of adaptive mutations in genes encoding centromere proteins like CENH3 or CENP-C that specifically decrease the ability of the proteins to interact productively with the evolved stronger centromere sequences and thereby suppress the centromere drive (Nagaki et al., 2004).

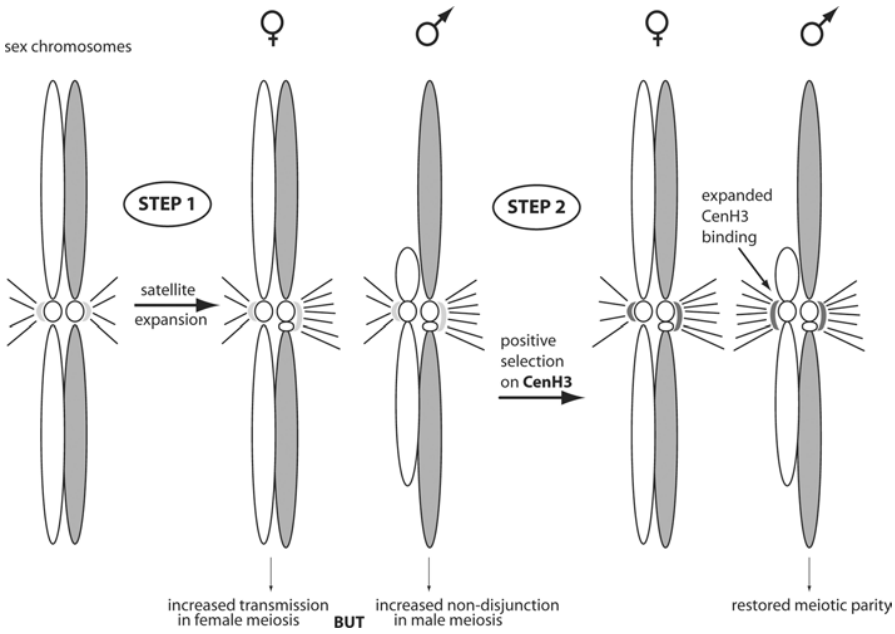

Figure 1. Centromere drive and its suppression.
The two steps of the centromere-drive model using the X–Y chromosomes as an example. In the first stage, a satellite expansion leads to a centromere with enhanced microtubule binding abilities, which can result in a transmission advantage in female meiosis. This can lead to deleterious effects, including enhanced non-disjunction between the X–Y chromosomes in male meiosis. In the second stage, a suppressor allele in CenH3 (or any other satellite-binding protein) that can restore meiotic parity will be selectively favored because it alleviates the deleterious effects of centromere-drive. This can be done in two ways: either (i) by expanding CenH3 binding and increasing microtubule attachments on the Y centromere (as shown) or (ii) by restricting CenH3 binding and reducing microtubule binding by the driving X centromere expansion (not shown). Repeated episodes of centromere-drive followed by the fixation of suppressing CenH3 alleles will lead to rapid expansions of centromeric satellites and the rapid fixation of non-synonymous nucleotide substitutions in genes encoding CenH3s (referred to as positive selection)(Malik and Bayes, 2006).

In the previous chapter, it has been shown that lower centromeric Cid levels are present when only one functional *cid* gene copy is present (Chapter 2, Fig. S3). Moreover, Cid levels were shown to be correlated with the levels of kinetochore proteins (Chapter 2 Fig. 6). In the context of the centromere drive model, it appeared of great interest to evaluate how centromeres with supposedly lower Cid levels compete during the asymmetric female meiosis with centromeres with normal Cid levels. My observations made in initial experiments are described in this appendix.

Results and Discussion

Centromere-drive affecting propagation of centromeres with reduced Cid levels, in next generation

The expression levels of Cid from two functional gene copies does not appear to be much higher than what is required for maintenance of normal centromeric Cid levels. A reduction of the *cid-EGFP* gene dose from 2 to 1 in a *cid* null mutant background was found to result in lower centromeric Cid-EGFP levels. Accordingly, the centromeres in a stock with only one functional *cid* copy as in $cid^{T12\text{-}1}/CyO$ are also expected to have reduced centromeric Cid levels. Since the accuracy of quantification of centromeric Cid levels after antibody stainings was found to be far lower than centromeric Cid-EGFP quantification (data not shown), an actual confirmation of the presence of reduced amounts of centromeric Cid in *cid* null heterozygotes compared to cid^{+} homozygotes has not yet been attempted. If these lower centromeric Cid levels are indeed present in $cid^{T12\text{-}1}/CyO$ males, these reduced levels are predicted to be maintained on paternal centromeres during development of the next generation according to my findings with Cid-EGFP (Chapter 2, Fig. 7). Accordingly, after crossing $cid^{T12\text{-}1}/CyO$ males with cid^{+} homozygous females, half of the F1 progeny is predicted to be cid^{+} homozygous with reduced centromeric Cid levels on the paternally derived centromeres and normal levels on the maternally derived centromeres. With appropriate markers it should then be feasible to follow the segregation of the paternally and maternally derived centromeres respectively during both male and female meiosis in the F1 progeny to evaluate whether meiotic drive occurs. $cid^{T12\text{-}1}/CyO$ males were therefore crossed to females homozygous for an attP element insertion marked with 3xP3-RFP near the centromere of chromosome II (Fig. 2a). The 3xP3-RFP marker is expressed in eyes and ocelli of adult

flies. This expression was therefore used to score the presence of the linked centromere. Female F1 progeny from that cross with curly wings (i.e. *attP-3xP3-RFP/CyO*) has two functional *cid*$^{+}$ copies and is expected to maintain reduced levels of centromeric Cid on paternally derived unmarked centromeres at least partially. To test for meiotic drive, these F1 females (test females) were crossed to *w1* males. Similarly, it was also tested whether meiotic drive might occur during male meiosis by crossing F1 males (test males) to *w1* females. For control experiments, a stock carrying the *CyO* balancer in a background with two functional *cid*$^{+}$ copies (*Gla/CyO*) was crossed (instead of *cid*$^{T12\text{-}1}$*/CyO*) to *attP-3xP3-RFP* before resulting F1 females and males were also crossed to *w1*.

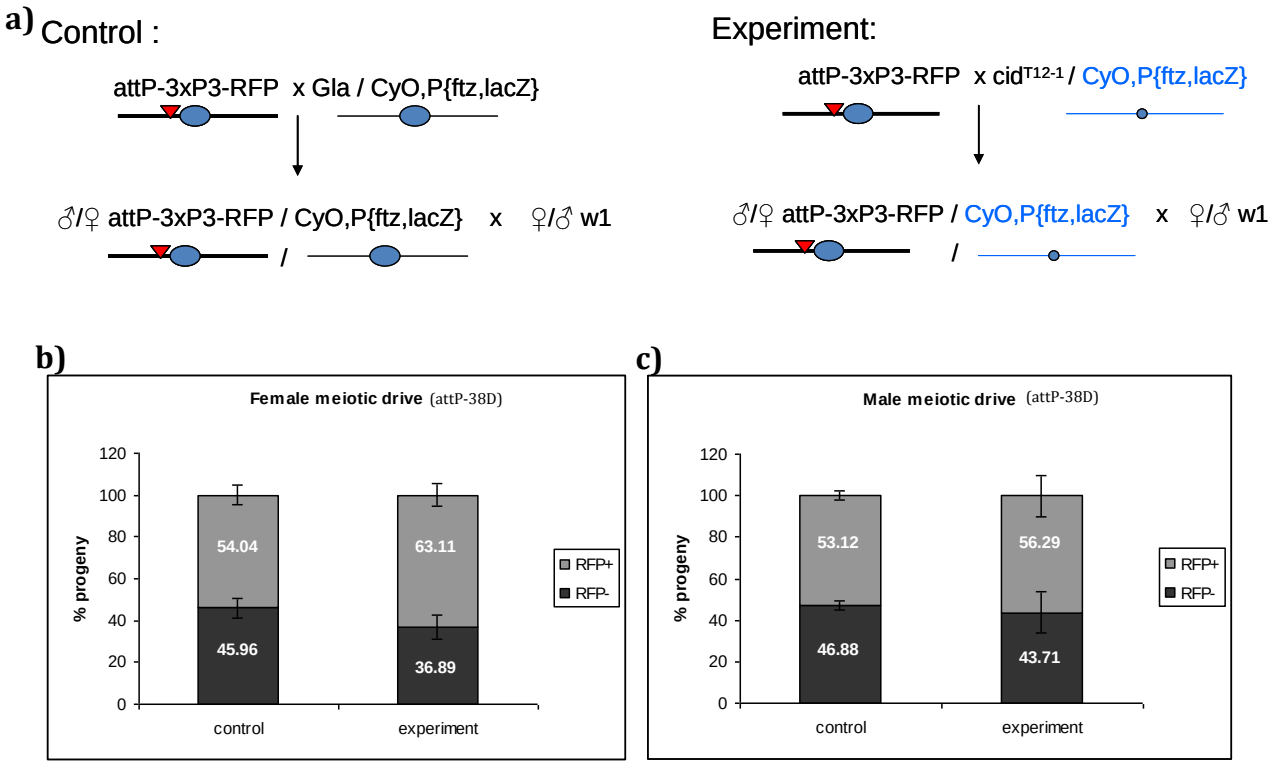

Figure 2. Preferential segregation of normal centromere over smaller centromere during female meiosis.
a) Schematics of crossing scheme. ⬭ represents the centromere, ▼ represents the *attP-3xP3-RFP* insertion, thin line represents the balancer chromosome, color coding of the CyO chromosome in the experiment represents its different origin than of the control CyO chromosome. b) The graph depicts female meiotic drive by plotting the percentage of RFP^{+} and RFP^{-} progeny obtained after crossing of females with genotype *attP-38D-3xP3-RFP/CyO* to males of *w1*. c) The graph depicts male meiotic drive by plotting the percentage of RFP+ and RFP- progeny obtained after crossing of males with the genotype *attP-38D-3xP3-RFP/CyO* to *w1* females (n = ~200 progeny counted on average from 2 parallel experiments).

In these F1 animals, the centromeric Cid levels are expected to be the identical on both paternally and maternally derived centromeres. In the F2 derived from such control F1 females, the RFP$^+$ marker was found to be present at almost the frequency predicted by Mendel's law (in 54%). Interestingly, in the experiment with F1 test females, the RFP$^+$ marker was found to be overrepresented in the F2 generation (in 63%) (Fig. 2b). In contrast, the frequency of the RFP$^+$ marker in the F2 was far more close to the predicted Mendelian ratio in the experiments with both test and control F1 males. These observation support the notion that centromeres with reduced centromeric Cid levels cannot compete effectively with normal centromeres during the asymmetric female meiosis.

In these first experiments, the *CyO* chromosome in the test and control F1 animals was not identical. One originated from the *cid$^{T12\text{-}1}$/CyO* stock and the other from control *Gla/CyO* stock To further exclude potential background effects, the *CyO* chromosome from the *Gla/CyO* stock was introgressed in the *cid$^{T12\text{-}1}$* background. Thereafter the experiments were repeated. Again the test F1 females were found to segregate the RFP$^+$ marker more frequently than predicted by Mendel (into 62% of the F2). In these experiments also the F1 test males appeared to display some meiotic dive, while control F1 animals had segregation rates closer to the expected Mendelian values (Fig. 3c).

To exclude the possibility that the observed departure from Mendelian frequencies was caused by potential selective advantages of alleles in the background of the particular *attP-3xP3-RFP* chromosome used in the initial experiments, the experiments were repeated with an independent *attP-3xP3-RFP* insertion. Also with this marker chromosome, the F1 test females were found to segregate the RFP$^+$ marker more frequently into adult F2 than predicted by Mendel (Fig. 3d).

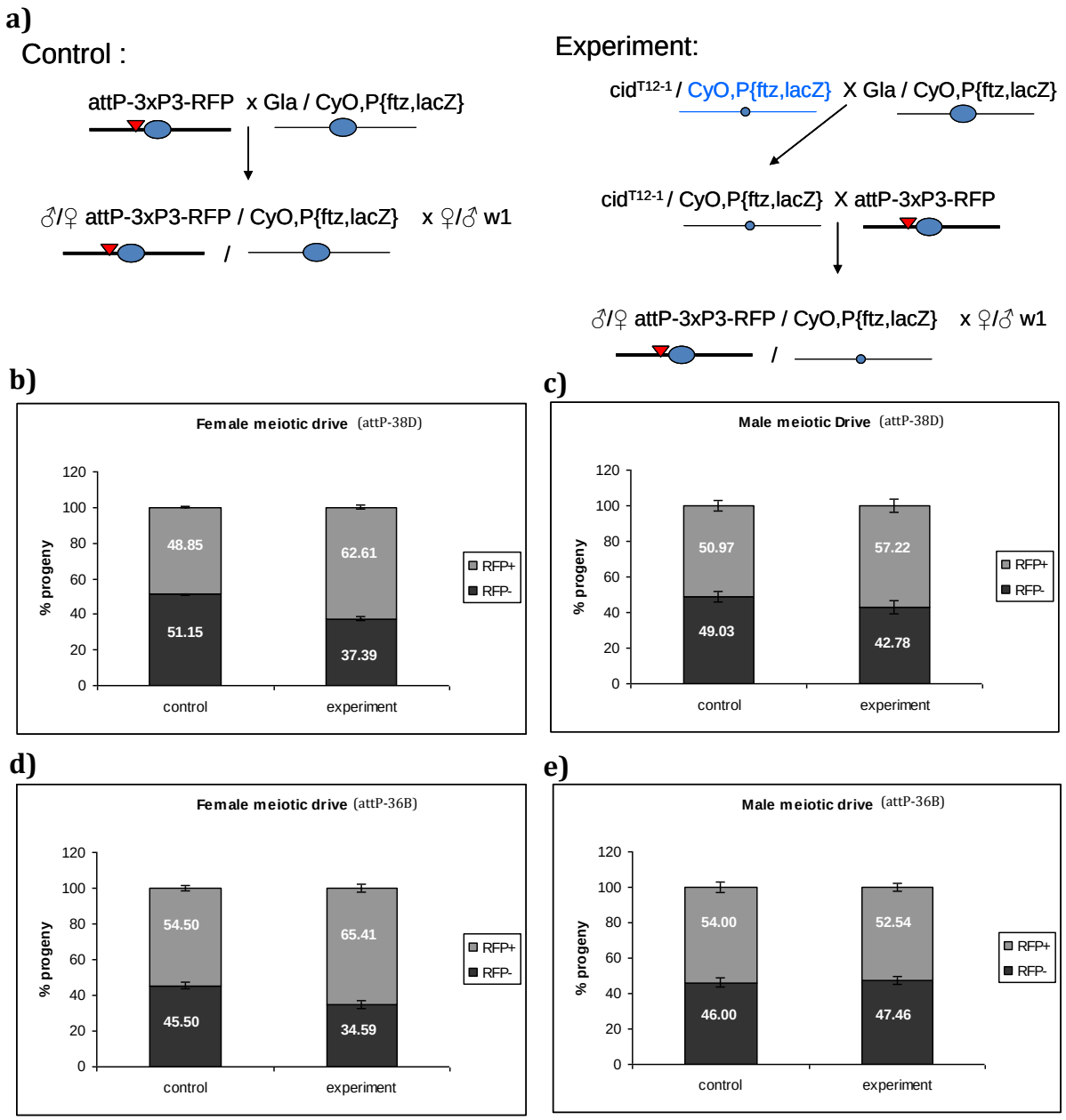

Figure 3. Preferential segregation of normal centromere over smaller centromere during female meiosis. a) Schematics of crossing scheme. ● represents the centromere, ▼ represents *attP-3xP3-RFP* insertion, the thin line represents the balancer chromosome, color coding of the CyO chromosome in the experiment represents its different origin than of the control CyO chromosome. b) The graph depicts the female meiotic drive by plotting the percentage of RFP$^+$ and RFP$^-$ progeny obtained after crossing of females with the genotype *attP-38D-3xP3-RFP/CyO* to males of *w1*. c) The graph depicts the male meiotic drive by plotting the percentage of RFP$^+$ and RFP$^-$ progeny obtained after crossing of males with the genotype *attP-38D-3xP3-RFP/CyO* to *w1* females. d) The graph depicts the female meiotic drive by plotting the percentage of RFP$^+$ and RFP$^-$ progeny obtained after crossing of females with the genotype *attP-36B-3xP3-RFP/CyO* to males of *w1*. e) The graph depicts the male meiotic drive by plotting the percentage of RFP+ and RFP- progeny obtained after crossing of males with the genotype *attP-36B-3xP3-RFP/CyO* to *w1* females (n = ~200 progenies counted on average from 2 parallel experiments).

In all the previous experiments, an RFP$^+$ chromosome was competing with a *CyO* balancer chromosome during meiosis in the analyzed F1. However, the RFP$^+$ chromosome will not undergo crossing over with the *CyO* balancer during female meiosis. These achiasmate chromosomes will therefore be handled by the distributive system and not by the chiasmate system of meiotic chromosome segregation. The sex, second, and third chromosomes typically recombine during wild-type female meiosis in Drosophila. The corresponding recombination events lead to the formation of chiasmata that hold homologous chromosomes together until anaphase I, thus ensuring proper segregation (Nicklas, 1974 #6431). However, achiasmate chromosomes are segregated using one of two separate systems: one segregates chromosomes based on homology (the homologous system), while the other system segregates chromosomes based on chromosome availability and shape (the heterologous system).

To test whether biased segregation might also occur during competition of chiasmate chromosomes with potentially unequal levels of centromeric Cid on paternally and maternally derived centromeres, respectively, *cid$^{T12\text{-}1}$/CyO* males were crossed to females homozygous for an *attP-3xP3-RFP* insertion on chromosome III (Fig. 4a). In contrast to the findings before, the segregation frequency of the RFP$^+$ chromosome was found to be comparable to that of the control chromosome in all of the analyzed F1 test and control males and females (Fig. 4b, 4c).

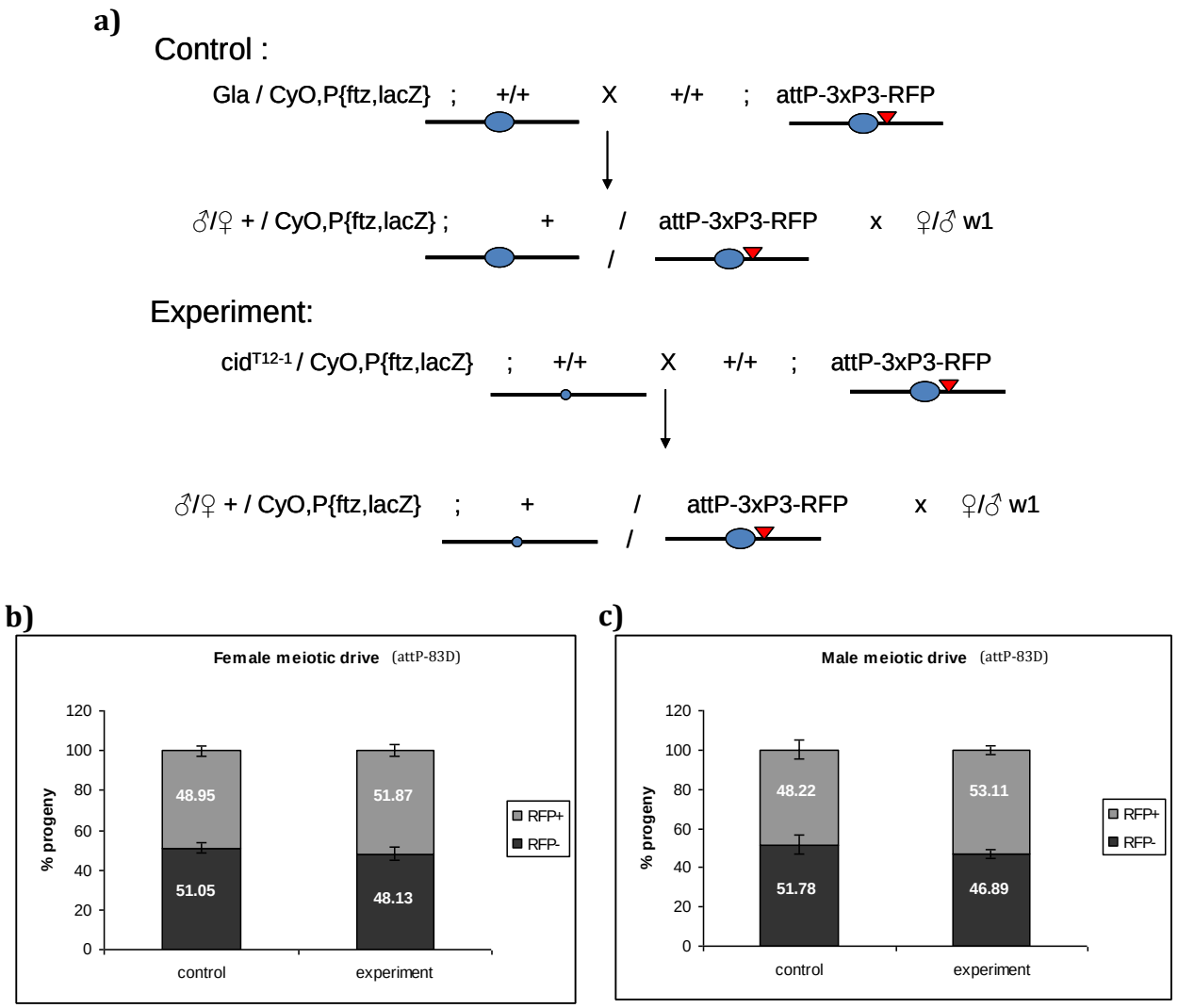

Figure 4. No preferential segregation of normal centromere over smaller centromere in case of chiasmate chromosomes during female meiosis.
a) Schematics of crossing scheme. ⬭ represents the centromere, ▼ represents the *attP-3xP3-RFP* insertion. b) The graph depicts the female meiotic drive by plotting the percentage of RFP$^+$ and RFP$^-$ progeny obtained after crossing of females with the genotype + / *CyO* ; + / *attP-83D-3xP3-RFP* to males of *w1*. c) The graph depicts the male meiotic drive by plotting the percentage of RFP$^+$ and RFP$^-$ progeny obtained after crossing of males with the genotype + / *CyO* ; + / *attP-83D-3xP3-RFP* to w1 females (n = ~200 progenies counted on average from 2 parallel experiments).

Overall, all these results are compatible with the notion that centromeric Cid levels might bias segregation via the achiasmate pathway of female meiosis but not via the chiasmate pathway. It should be emphasized that apart from biased segregation during meiosis, the observed results might also reflect selection of progeny during development to the adult stage at which the RFP$^+$ marker was scored. Experimental approaches

allowing an analysis of chromosome segregation already in early embryos would therefore be desirable.

.

Materials & Methods

Drosophila Genetics

cid$^{T12\text{-}1}$ (Blower et al., 2006) carries a premature stop codon. *attP-3xP3-RFP* lines with site-specific integrated P element insertions at 36B, 38D and 83D cytological band position, near the centromere region on the 2nd or 3rd chromosome, respectively, were kindly provided by J. Bischof, University of Zurich.

Frequency of chromosome segregation

8-10 males/females with desired genotype (*attP-3xP3-RFP / CyO*) were crossed with 8-10 females/males of *w1*. After one day the flies were transferred to a new vial. The first vial was discarded. The flies were transferred from vial (2) to vial (3) after 4 days. The percentage of F1 progeny with RFP^{+} / RFP^{-} eyes was calculated from vial (2) till the 8th day of hatching of progenies.

References

Blower, M.D., Daigle, T., Kaufman, T., and Karpen, G.H. (2006). Drosophila CENP-A mutations cause a BubR1-dependent early mitotic delay without normal localization of kinetochore components. PLoS Genet *2*, e110.

Buckler, E.S.t., Phelps-Durr, T.L., Buckler, C.S., Dawe, R.K., Doebley, J.F., and Holtsford, T.P. (1999). Meiotic drive of chromosomal knobs reshaped the maize genome. Genetics *153*, 415-426.

Dawe, R.K., and Cande, W.Z. (1996). Induction of centromeric activity in maize by suppressor of meiotic drive 1. Proceedings of the National Academy of Sciences of the United States of America *93*, 8512-8517.

Haaf, T., and Willard, H.F. (1997). Chromosome-specific alpha-satellite DNA from the centromere of chimpanzee chromosome 4. Chromosoma *106*, 226-232.

King, R.C. (1970). The meiotic behavior of the Drosophila oocyte. International review of cytology *28*, 125-168.

Lohe, A.R., and Brutlag, D.L. (1987). Identical satellite DNA sequences in sibling species of Drosophila. Journal of molecular biology *194*, 161-170.

Malik, H.S., and Bayes, J.J. (2006). Genetic conflicts during meiosis and the evolutionary origins of centromere complexity. Biochemical Society transactions *34*, 569-573.

Nagaki, K., Cheng, Z., Ouyang, S., Talbert, P.B., Kim, M., Jones, K.M., Henikoff, S., Buell, C.R., and Jiang, J. (2004). Sequencing of a rice centromere uncovers active genes. Nature genetics *36*, 138-145.

Pardo-Manuel de Villena, F., and Sapienza, C. (2001). Transmission ratio distortion in offspring of heterozygous female carriers of Robertsonian translocations. Hum Genet *108*, 31-36.

Pardo-Manuel de Villena, F., and Sapienza, C. (2001a). Female meiosis drives karyotypic evolution in mammals. Genetics *159*, 1179-1189.

Peacock, W.J., Dennis, E.S., Rhoades, M.M., and Pryor, A.J. (1981). Highly Repeated DNA-Sequence Limited to Knob Heterochromatin in Maize. Proceedings of the National Academy of Sciences of the United States of America-Biological Sciences *78*, 4490-4494.

Rhoades, M.M., and Vilkomerson, H. (1942). On the Anaphase Movement of Chromosomes. Proceedings of the National Academy of Sciences of the United States of America *28*, 433-436.

Samonte, R.V., Ramesh, K.H., and Verma, R.S. (1997). Comparative mapping of human alphoid satellite DNA repeat sequences in the great apes. Genetica *101*, 97-104.

Wright, K.J., Marr, M.T., 2nd, and Tjian, R. (2006). TAF4 nucleates a core subcomplex of TFIID and mediates activated transcription from a TATA-less promoter. Proceedings of the National Academy of Sciences of the United States of America *103*, 12347-12352.

Appendix II

Role of centromeres beyond chromosome segregation during male meiosis

Introduction

The well-established function of centromeres in spindle attachment on a chromosome ensures the segregation of chromosomes during cell division. Recently other roles of centromeres during meiosis have come to light in budding yeast and Drosophila oocytes. One of those novel functions seems to contribute to homolog pairing.

Before the meiotic divisions, cells have to identify and pair homologous chromosomes. This is followed by establishment of the synaptonemal complex (SC), an elaborate proteinaceous structure that holds homologs close together along their lengths (for review, see (Page and Hawley, 2004)).

In most organisms, including fungi, plants, mice and humans, homolog pairing initiates with telomeres clustering at the nuclear envelope. This chromosomal configuration is known as “bouquet” which is an assembly of telomeres into a structure that looks like the stems of a floral bouquet with the rest of the chromosome representing the flowers (Scherthan, 2007). The bouquet appears to facilitate homologous recognition and alignment by concentrating chromosomes within a limited region of the nuclear volume, thus enabling chromosome movements that promote the identification of homologs, perhaps by the DNA DSB repair process (Harper et al., 2004; Hiraoka, 1998; Scherthan, 2001). Clustering of telomeres are facilitated by the attachment of telomeres to nuclear envelope proteins that contain Sad1 and Unc-84 (SUN) and Klarsicht, ANC-1 and Syne-1 homology (KASH) domains. The SUN–KASH bridge interacts with specific elements of the cytoskeleton, such as dynein and kinesin and provides a connection to cytoskeletal forces for moving chromosomes (Fridkin et al., 2009). An extreme example is observed in *Schizosaccharomyces pombe* in which a tight bouquet forms near the spindle pole body in early prophase I, which drags the whole nucleus back and forth several times within the cell, forming elongated horsetail nuclei (Chikashige et al., 1994; Scherthan et

al., 1994). Similarly in worms, the tethering of special telomere-proximal chromosomal regions near the nuclear envelope assists the pairing of homologues and SC formation (Bhalla and Dernburg, 2008).

In contrast to most other organisms, no bouquet stage is observed in Drosophila. Interestingly, Drosophila telomere biology consists of some distinct features. Instead of a telomere bouquet Drosophila oocytes form another structure at the corresponding stage in meiosis called the chromocenter. The chromocenter is composed of clustered centromeres (Carpenter, 1975; Nokkala and Puro, 1976). According to recent publications, centromere clustering seems to be involved in initiating synapsis (Takeo et al., 2011; Tanneti et al., 2011). The Drosophila chromocenter therefore might be functionally similar to the bouquet. These studies have been done in females where SC is thought to mediate homolog pairing. But in male Drosophila, no SC and no homologous recombination (HR) exist (Baker, 1976). Thus, it would be interesting to investigate if clustering of centromeres takes place in Drosophila spermatocytes and/or if the role of centromere clustering is different than in oocytes.

Results & Discussion

The dynamics of centromere clustering during spermatocyte development

A germline stem cell, located in the tip of testis, undergoes an asymmetric division and the resulting gonialblast progresses through four mitotic divisions with incomplete cytokinesis and thereby generates a cyst of 16 interconnected spermatocytes. As soon as a spermatogonial cell exists from the gonial division program, it switches to a growth program, entering a very long G2 interphase (approximately lasts 3.5 days in *D. melanogaster*) (Lindsley and Tokuyasu, 1980), that can be considered as a meiotic prophase. (Cenci et al., 1994) has divided this G2 phase further into six stages on the basis of chromatin morphology and cell size.

Here, I have analyzed the behavior of centromeres as Cid-EGFP signals in *cid*$^{-}$ *; cid-EGFP* males by scoring the number of centromeres in spermatocyte stages in squashed testis preparations. The analysis of Cid-EGFP transgenic lines revealed unexpected and dynamic patterns of centromere behavior during spermatocyte development. Centromeres seem to gather to a small region beneath the nuclear membrane or cluster together in the spermatogonial nuclei at the end of gonial mitotic division (Fig.1a). This structure can be correlated with the bouquet of telomeres present during early meiotic prophase of most other eukaryotic organisms. After a rapid pre-meiotic S phase, cells enter early G2 where the chromatin appears as a compact mass and centromeres are still clustered majorly in 1-3 groups near to one focal point of the nucleus. This clustering in principle might assist in facilitating the alignment of homologous chromosomes and promote their pairing.

Later during spermatocyte development, chromatin starts to subdivide into two large and dense clumps that remain closely apposed to the inner nuclear envelope. Also, a compact, faint third clump exists in the vicinity of one of the large clump. The two large clumps are believed to correspond to the autosomes 2 and 3 whereas the third clump is composed of X, Y and tiny 4th chromosome (Cooper, 1965). The Cid-EGFP signals per clump are reduced to mainly one, which are probably coupled centromeres of the bivalents of the respective chromosome (Fig. 1, S2). Interestingly, as nuclear growth continues, the space between these clumps increases. However, the mechanism behind this is not clear. The centromeres of the paired homologs in each clump starts to separate but remain within their respective chromatin clump, this increases the number of Cid-EGFP signals to 6 per cell or 2 per territory (Fig. 1, S3). Each signal is known to represent the tightly associated sister centromere of one homolog (Vazquez et al., 2002). Unpairing of homologous centromeres therefore appears to take place just after the formation of chromosome territories in stage S3. As growth continues, the late G2 cells becomes 25 times larger in volume than early spermatogonia, territories appear to move with the nuclear membrane outwards and increase the space between each other.

Intriguing observations have been made in mouse and human spermatocytes where during prophase I centromeres were found to be associated with the nuclear envelope before the telomere clustering or bouquet formation starts on the nuclear envelope (Scherthan et al., 1996). Therefore, it would be interesting to know if such associations of centromeres with the nuclear envelope also occur in *Drosophila* spermatocytes. In S5/6 cells, two homologous centromeres were

always separated and appeared to be on the tip of territories suggesting local unpairing of homologous chromosomes (Fig. 1a S5/6). Contrary to the observation made by (Vazquez et al., 2002), my study revealed that S5/6 cells majorly show 7 Cid-EGFP signals rather than the expected 8 signals (Fig. 1). It has been shown in chapter 2, (Fig. 6a, 6d) that the bivalent of 4th chromosome remains paired till the spermatocyte enters meiosis I.

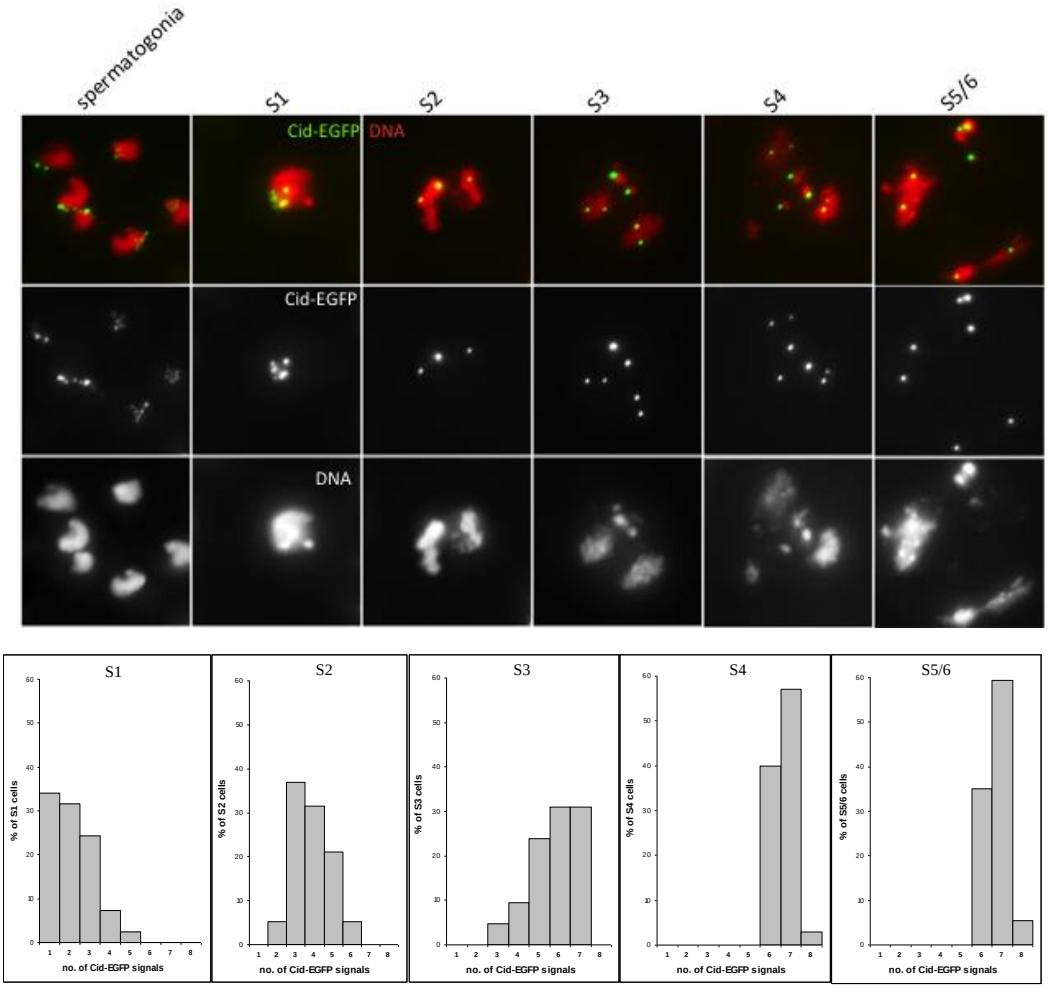

Figure 1. Number of Cid-EGFP signals during G2. Centromeric signals shows clustering from the last gonial mitotic division to early G2. A specific pattern can be seen between the chromatin morphology and centromeric signals. Note the increase in number of Cid-EGFP signals from early G2 to late G2 along with the formation of territories. Sisters are generally paired until the last stage of G2 and represent one centromere per homolog. n>30 cells.

Expression and level of SC proteins in spermatocytes

The behavior of centromeres suggests that chromosomes find their partner and pair very early during spermatocyte development, possibly during or shortly after the last gonial mitotic division. The centromere clustering analogous to telomere clustering in other eukaryotic organisms seems to play the parallel function in Drosophila spermatocytes. Recently, according to two studies in Drosophila oocytes showed that SC proteins like C(3)G and Cona are essential for centromere clustering (Takeo et al., 2011; Tanneti et al., 2011). However, in *cid^{-} ; cid-EGFP* spermatocytes after staining with anti-C(3)G or anti-Cona, no specific staining on centromeres could be seen. Also, the null mutant males of respective proteins are perfectly fertile. However, the redundancy between the two cannot be excluded and needs to be tested.

Strong depletion of Cid in early spermatocytes abolishes the territory formation and growth of cell.

In mouse and human spermatocyte centromeres have been shown to interact with the nuclear envelope during meiotic prophase (Scherthan et al., 1996). But the functional significance of this interaction is not known. Therefore, to investigate the role of centromeres during G2 or meiotic prophase, Cid protein was depleted from the centromeres of early spermatocytes of Drosophila by applying the deGradFP (Caussinus et al., 2012) approach. In deGradFP, depletion of GFP fusion proteins is achieved by expression of a GFP-specific recombinant ubiquitin ligase (NSlmb-vhhGFP4) with the UAS/GAL4 system. For expression of this ubiquitin ligase specifically in early spermatocytes, a *bam-GAL4-VP16* driver

was used. The males expressing deGradFP in their spermatocytes were found to produce significantly smaller testes with approximately half the size of control (-deGradFP) testes (Fig. 2a). However, except the size of the testes, the morphology of the testis structures like the tip region and seminal vesicle was found to be normal.

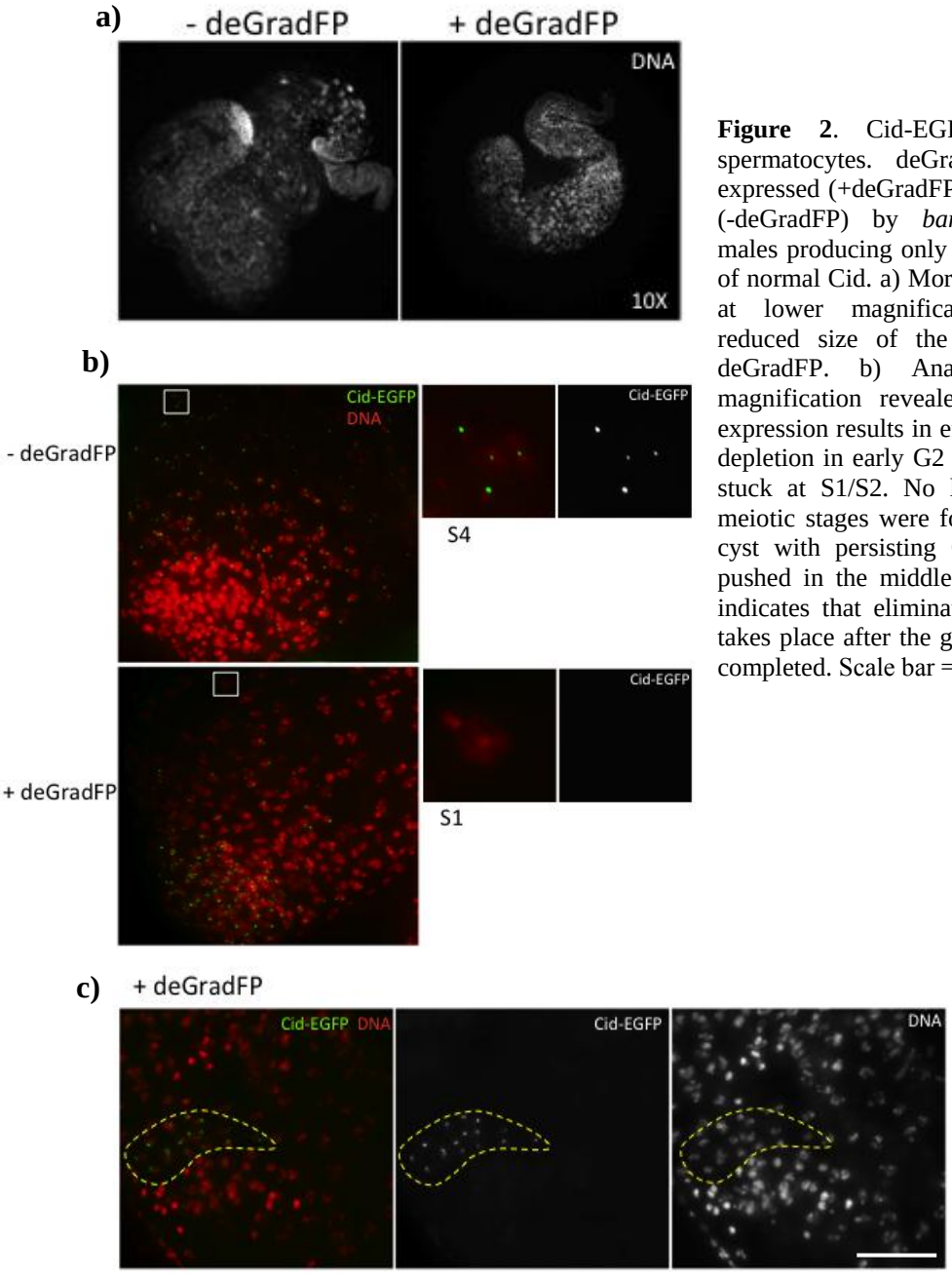

Figure 2. Cid-EGFP depletion in spermatocytes. deGradFP was either expressed (+deGradFP) or not expressed (-deGradFP) by *bam-GAL4-VP16* in males producing only Cid-EGFP instead of normal Cid. a) Morphology of a testis at lower magnification shows the reduced size of the testis expressing deGradFP. b) Analysis at higher magnification revealed that deGradFP expression results in effective Cid-EGFP depletion in early G2 and the cells were stuck at S1/S2. No late G2 stages or meiotic stages were found. c) A 16-cell cyst with persisting Cid-EGFP signals pushed in the middle part the of testis indicates that elimination of Cid-EGFP takes place after the gonial divisions are completed. Scale bar = 10µm.

Careful cytological studies at higher magnification revealed that a +deGradFP testis was largely devoid of late spermatocyte and post-meiotic stages. This could be a possible reason for the reduced size of the testis. However, some brightly Hoechst stained nuclei were found which could possibly be apoptotic nuclei.

Centromeric Cid-EGFP signals were still present in gonial mitotic cells and in some of the early spermatocyte S1 stage cells but completely undetectable in S2 stage cells. S3/4 stage cells were found very rarely (2-3 S3 cells in 2 testes out of 14, S4 cells in 1 testis out of 14) in testes. Firstly, this suggests that chromosomes devoid of centromere were unable to segregate into territories. Secondly, the growth of cell stopped at the S2/S3 stage. Based on these observations, it can be hypothesized that centromeres might interact with some cytoplasmic microtubules, which further helps in pulling of chromosome territories outwards. Alternatively, hypothetical intranuclear microtubules interact with the centromeres and push the chromosome territories outwards. Studies in budding yeast indicate the possibility of interaction between cytoplasmic/intranculear microtubules with centromeres during interphase (Jin et al., 2000). But in contrast to budding yeast, no intranuclear microtubules have been reported in animals so far.

Usually the spermatocyte stages are present in form of cyst but in deGradFP testes most of the S2 cells were found to be randomly floating which indicates that the cyst was broken. It is possible that since these cells are unable to undergo further growth, the cyst starts to undergo apoptosis. Also, defects due to degradation of Cid-EGFP in somatic cyst cells are unlikely since it has been

shown in Chapter 1 (Fig. 8a)s that Bam-GAL4-VP16 does not drive expressesion in cyst cells.

Expression of Bam starts in the last gonial mitotic division and its expression reaches a peak in spermatocytes. In order to reduce the expression as much as possible in gonial mitotic cells, the cross of deGradFP was also set up at 18 °C. The males emerged from this cross were constantly kept at 18 °C till the testis preparations were done. Testis preparation from these males gave consistently the same result as before. Spermatocytes were stuck at the S2 stage. Also to exclude the expression of deGradFP during gonial mitotic divisions, 16-cell cyst were counted with clear Cid-EGFP signals persisting on their centromeres Fig. 2c (9 testes showed clear 16-cell cysts with Cid-EGFP signals out of 14 testes). Therefore, this indicates that most of the elimination of Cid-EGFP took place only after the gonial mitotic divisions.

This study indicates possible roles of centromere other than recruiting kinetochore and segregation of chromosomes during cell division.

Materials & Methods

Drosophila Genetics

cid$^{T12\text{-}1}$ and *cid*$^{T22\text{-}4}$ (Blower et al., 2006) carry premature stop codons. *cid*^{G5950} (Bloomington Drosophila Stock Center #29695) has a P element insertion within the coding sequence. The transgene *P(w*$^{+}$*, gcid-EGFP-cid)III.2* (Schuh et al., 2007), has been shown to complement recessive lethal mutations in the corresponding endogenous loci, demonstrating the functionality of the encoded fluorescently tagged centromere.

P(w^{+}*,UASt-NSlmb-vhh-GFP4) III* (Caussinus et al., 2012), *P(w*$^{+}$*,bamP-GAL4-VP16)III* (Chen and McKearin, 2003) were kindly provided by E. Caussinus and D. McKearin.

For DeGrad Cid-EGFP during early G2 (Fig. 2) males were generated with genotype, *w*; cid*$^{T12\text{-}1}$*/cid*^{G5950}*, P(w*$^{+}$*, gcid-EGFP-cid)II.1; P(w*$^{+}$*, UASt-NSlmb-vhhGFP4)III/P(w*$^{+}$*, bam-GAL4-VP16)III , P(w*$^{+}$*, gcid-EGFP-cid)III.2* by standard crossing schemes. In parallel, males for control experiments were generated with genotype, *w*; cidT12-1/cid*^{G5950}*, P(w*$^{+}$*, gcid-EGFP-cid)II.1; +/P(w*$^{+}$*, bam-GAL4-VP16)III, P(w*$^{+}$*, gcid-EGFP-cid)III.2*.

Whole mount testis preparation

Flies were anesthetized and dissected under the binocular with two forceps in a testis buffer (183 mM KCl, 47 mM NaCl, 10 mM Tris-HCl, pH 6.8). Testes were isolated by cutting posterior to the seminal vesicle with a hypodermic needle (Terumo Neolus 27G, 0.4x20 mm). Testes were then separated from the accessory glands. 5-10 flies were dissected in a droplet of testis buffer and testes were then transferred to a droplet of 4% paraformaldehyde (in phosphate buffered saline (PBS) on a depression slide for fixation. After 10 min of fixation at room temperature, the fixative was carefully removed with a syringe under the binocular. A droplet of Hoechst staining solution (1 µg/ml Hoechst 33258 in 1x PBS) was added for 10 min (protected from light). The staining solution was then removed with a syringe and testes were washed in a droplet of PBS. Testes were finally transferred into a droplet of mounting media (Vectashield H-1000, Vector

Laboratories, Inc.) on a new slide and carefully (to avoid strong squashing of the testes) covered with a coverslip.

Squashed Testis Preparation

Testis squash preparations were made, fixed and stained essentially as described (Gunsalus and Goldberg, 1995) with the following modifications. After dissection in testis buffer (183 mM KCl, 47 mM NaCl, 10 mM Tris-HCl, pH 6.8), testes were transferred to a 5 µl drop of phosphate buffered saline (PBS) on a poly-L-lysine-treated slide and cut open to spill the contents. The sample was squashed very gently after addition of 15 µl of 4% formaldehyde in PBS under a 22 x 22 mm siliconized cover slip. Fixation was continued for 6 minutes.

References

Baker, B.a.H., J. (1976). Meiotic mutants: genetic control of meiotic recombination and chromosome segregation. The Genetics and Biology of Drosophila, 351-434.

Bhalla, N., and Dernburg, A.F. (2008). Prelude to a division. Annu Rev Cell Dev Biol *24*, 397-424.

Blower, M.D., Daigle, T., Kaufman, T., and Karpen, G.H. (2006). Drosophila CENP-A mutations cause a BubR1-dependent early mitotic delay without normal localization of kinetochore components. PLoS Genet *2*, e110.

Carpenter, A.T. (1975). Electron microscopy of meiosis in Drosophila melanogaster females. I. Structure, arrangement, and temporal change of the synaptonemal complex in wild-type. Chromosoma *51*, 157-182.

Caussinus, E., Kanca, O., and Affolter, M. (2012). Fluorescent fusion protein knockout mediated by anti-GFP nanobody. Nature structural & molecular biology *19*, 117-121.

Cenci, G., Bonaccorsi, S., Pisano, C., Verni, F., and Gatti, M. (1994). Chromatin and microtubule organization during premeiotic, meiotic and early postmeiotic stages of Drosophila- melanogaster spermatogenesis. J Cell Sci *107*, 3521-3534.

Chen, D., and McKearin, D.M. (2003). A discrete transcriptional silencer in the bam gene determines asymmetric division of the Drosophila germline stem cell. Development *130*, 1159-1170.

Chikashige, Y., Ding, D.Q., Funabiki, H., Haraguchi, T., Mashiko, S., Yanagida, M., and Hiraoka, Y. (1994). Telomere-led premeiotic chromosome movement in fission yeast. Science *264*, 270-273.

Cooper, K.W. (1965). Normal spermatogenesis in Drosophila. In Biology of Drosophila (ed M Demerec), 1-61.

Fridkin, A., Penkner, A., Jantsch, V., and Gruenbaum, Y. (2009). SUN-domain and KASH-domain proteins during development, meiosis and disease. Cellular and molecular life sciences : CMLS *66*, 1518-1533.

Gunsalus, K., and Goldberg, M. (1995). Drosophila cofilin is required during embryogenesis and oogenesis. Mol Biol Cell *6*, 135.

Harper, L., Golubovskaya, I., and Cande, W.Z. (2004). A bouquet of chromosomes. Journal of Cell Science *117*, 4025-4032.

Hiraoka, Y. (1998). Meiotic telomeres: a matchmaker for homologous chromosomes. Genes to cells : devoted to molecular & cellular mechanisms *3*, 405-413.

Jin, Q.W., Fuchs, J., and Loidl, J. (2000). Centromere clustering is a major determinant of yeast interphase nuclear organization. Journal of Cell Science *113*, 1903-1912.

Lindsley, D., and Tokuyasu, K.T. (1980). Spermatogenesis. In Genetics and Biology of Drosophila, M. Ashburner, and T.R. Wright, eds. (New York, Academic Press), pp. 225-294.

Nokkala, S., and Puro, J. (1976). Cytological evidence for a chromocenter in Drosophila melanogaster oocytes. Hereditas *83*, 265-268.

Page, S.L., and Hawley, R.S. (2004). The genetics and molecular biology of the synaptonemal complex. Annu Rev Cell Dev Biol *20*, 525-558.

Scherthan, H. (2001). A bouquet makes ends meet. Nature reviews Molecular cell biology *2*, 621-627.

Scherthan, H. (2007). Telomere attachment and clustering during meiosis. Cellular and molecular life sciences : CMLS *64*, 117-124.

Scherthan, H., Bahler, J., and Kohli, J. (1994). Dynamics of chromosome organization and pairing during meiotic prophase in fission yeast. The Journal of cell biology *127*, 273-285.

Scherthan, H., Weich, S., Schwegler, H., Heyting, C., Harle, M., and Cremer, T. (1996). Centromere and telomere movements during early meiotic prophase of mouse and man are associated with the onset of chromosome pairing. Journal of Cell Biology *134*, 1109-1125.

Schuh, M., Lehner, C.F., and Heidmann, S. (2007). Incorporation of Drosophila CID/CENP-A and CENP-C into centromeres during early embryonic anaphase. Curr Biol *17*, 237-243.

Takeo, S., Lake, C.M., Morais-de-Sa, E., Sunkel, C.E., and Hawley, R.S. (2011). Synaptonemal complex-dependent centromeric clustering and the initiation of synapsis in Drosophila oocytes. Current biology : CB *21*, 1845-1851.

Tanneti, N.S., Landy, K., Joyce, E.F., and McKim, K.S. (2011). A pathway for synapsis initiation during zygotene in Drosophila oocytes. Current biology : CB *21*, 1852-1857.

Vazquez, J., Belmont, A.S., and Sedat, J.W. (2002). The dynamics of homologous chromosome pairing during male Drosophila meiosis. Curr Biol *12*, 1473-1483.

CURRICULUM VITAE

Personal Information

Surname: **TANEJA RAYCHAUDHURI**

Name: **Nitika**

Date of birth: **27.01.1985**

Place of birth: **Delhi**

Nationality: **Indian**

Education

10th grade: Central Board of Secondary Education (CBSE). Govt. Higher Secondary School, Delhi, India. 2000

12th grade: Central Board of Secondary Education (CBSE). Prabhu Dayal Public School, Delhi, India. 2002

Bachelor of Science: (Botany, Chemistry, Zoology). Daulat Ram College, Delhi University, Delhi, India. 2003-2006

Master of Science: M.Sc. in Biotechnology. School of Biotechnology, Jawaharlal Nehru University, Delhi, India. 2006-2008

Master thesis: "Identification, characterization & study of regulatory role of a GTP sensing novel Transcription regulator CodY in *B. anthracis* on the toxin genes responsible for causing Anthrax" & "Induction of sporulation in *B. anthracis* in nutrient rich media"

PhD: Genetics. Institute of Molecular Life Sciences, University of Zürich, Switzerland.

Project: "Epigenetic control of centromeric Cid/Cenp-A levels during spermatogenesis and development"
since Dec 2008-present.

Publications

Nitika Raychaudhuri, Raphaelle Dubruille, Guillermo A. Orsi, Benjamin Loppin, Christian F. Lehner. Transgenerational propagation and quantitative maintenance of paternal centromeres depends on Cid/Cenp-A presence in Drosophila sperm.
Plos Biology 2012 (in press).